(2)

GRANT NUMBER AFSOR- 87 0243

MICROSTRUCTURE OF THIN FILMS

E. Pelletier
Ecole Nationale Supérieure de Physique de Marseille
Laboratoire d'Optique des Surfaces et des Couches Minces
Domaine Universitaire de St Jérôme
13397 Marseille Cedex 13, France

Tel: (33) 91 28 83 28

and

H.A. Macleod
Optical Sciences Center
University of Arizona
Tucson, AZ 85721, USA

Tel: (1) 602 621 2449

Final report: 1 June, 1987 - 1 June 1988

**Approved for public release;
distribution unlimited**

Prepared for

**EUROPEAN OFFICE OF AEROSPACE RESEARCH AND DEVELOPMENT
223/231 Old Marylebone Road
London, NW1 5TH, UK**

SECURITY CLASSIFICATION OF THIS PAGE

REPORT DOCUMENTATION PAGE

1a. REPORT SECURITY CLASSIFICATION: Unclassified	1b. RESTRICTIVE MARKINGS
2a. SECURITY CLASSIFICATION AUTHORITY	3. DISTRIBUTION/AVAILABILITY OF REPORT: Approved for public release ; Distribution unlimited
2b. DECLASSIFICATION/DOWNGRADING SCHEDULE	
4. PERFORMING ORGANIZATION REPORT NUMBER(S)	5. MONITORING ORGANIZATION REPORT NUMBER(S): EOARD-TR-89 01
6a. NAME OF PERFORMING ORGANIZATION: E.N.S.P.M. / 6b. OFFICE SYMBOL (If applicable)	7a. NAME OF MONITORING ORGANIZATION: European Office of Aerospace Research Development
6c. ADDRESS (City, State and ZIP Code): Domaine Universitaire de Saint-Jerome 13397 Marseille Cedex 13 France	7b. ADDRESS (City, State and ZIP Code): Box 14 FPO New York 09510-0200
8a. NAME OF FUNDING/SPONSORING ORGANIZATION: European Office of Aerospace Research & Development / 8b. OFFICE SYMBOL (If applicable): LRP	9. PROCUREMENT INSTRUMENT IDENTIFICATION NUMBER
8c. ADDRESS (City, State and ZIP Code): Box 14 FPO New York 09510-0200	10. SOURCE OF FUNDING NOS. — PROGRAM ELEMENT NO. / PROJECT NO. / TASK NO. / WORK UNIT NO.
11. TITLE (Include Security Classification): Microsture of thin films	
12. PERSONAL AUTHOR(S): Dr. Emile PELLETIER and Pr. H.A. MACLEOD	
13a. TYPE OF REPORT: Final Scientific / 13b. TIME COVERED: FROM 1jun 87 TO 1 jun 88	14. DATE OF REPORT (Yr., Mo., Day): 15 sept 88 / 15. PAGE COUNT
16. SUPPLEMENTARY NOTATION	
17. COSATI CODES — FIELD / GROUP / SUB. GR.	18. SUBJECT TERMS (Continue on reverse if necessary and identify by block number): Optical Surface Measurements, Optical Anisotropy, Optical Surface Scattering, Optical Coatings, Thin Film Measurements, Optical constants for TiO_2, Ta_2O_5, LaF_3, Al. Titanium Oxides, Lanthanum Fluoride, Aluminum

19. ABSTRACT (Continue on reverse if necessary and identify by block number)

The techniques of determination of refractive indices in air are presented. In Tucson, the surface plasmon resonance method is used for the study of silver layers produced by different techniques. In Marseille, the guided wave technique is used for the determination of anisotropy and indices of several dielectric materials. The problem of the uniformity of the thickness and of the index of a layer deposited on a large surface is especially analyzed in the case of the Ion Assisted deposition technique.

An overview of the last results obtained in Marseille and concerning the study of the scattering is given. The theoretical development performed for the interpretation of the scattering diagram leads to information concerning the grain size of the materials.

The theoretical atomistic modelling of the growth process pursued in Tucson would be a complementary tool to help in the understanding of the microstructure of deposited films.

A survey of the results concerning OSA titania films study obtained in Marseille is given.

20. DISTRIBUTION/AVAILABILITY OF ABSTRACT: UNCLASSIFIED/UNLIMITED ☒ SAME AS RPT. ☐ DTIC USERS ☐	21. ABSTRACT SECURITY CLASSIFICATION: Unclassified
22a. NAME OF RESPONSIBLE INDIVIDUAL: LARELL R SMITH - CHESTER J DYMEK	22b. TELEPHONE NUMBER (Include Area Code): 44 1 409 4505 / 22c. OFFICE SYMBOL: LRP

DD FORM 1473, 83 APR — EDITION OF 1 JAN 73 IS OBSOLETE.

GRANT NUMBER AFSOR- 87 0243

MICROSTRUCTURE OF THIN FILMS

E. Pelletier
Ecole Nationale Supérieure de Physique de Marseille
Laboratoire d'Optique des Surfaces et des Couches MInces
Domaine Universitaire de St Jérôme
13397 Marseille Cedex 13, France

Tel: (33) 91 28 83 28

and

H.A. Macleod
Optical Sciences Center
University of Arizona
Tucson, AZ 85721, USA

Tel: (1) 602 621 2449

Final report: 1 June, 1987 - 1 June 1988

Approved for public release;
distribution unlimited

Prepared for

EUROPEAN OFFICE OF AEROSPACE RESEARCH AND DEVELOPMENT
223/231 Old Marylebone Road
London, NW1 5TH, UK

Abstract

The techniques of determination of refractive indices in air are presented. In Tucson, the surface plasmon resonance method is used for the study of silver layers produced by different techniques. In Marseille, the guided wave technique is used for the determination of anisotropy and indices of several dielectric materials. The problem of the uniformity of the thickness and of the index of a layer deposited on a large surface is especially analyzed in the case of the Ion Assisted deposition technique.

An overview of the last results obtained in Marseille and concerning the study of the scattering is given. The theoretical development performed for the interpretation of the scattering diagram leads to information concerning the grain size of the materials.

The theoretical atomistic modelling of the growth process pursued in Tucson would be a complementary tool to help in the understanding of the microstructure of deposited films.

A survey of the results concerning OSA titania films study obtained in Marseille is given.

Introduction

The principal objective of the research under this contract was the continuation of the collaborative research between the Ecole Nationale Supérieure de Physique in Marseille and the Thin Films Group of the Optical Sciences Center, University of Arizona. As was the case with previous contracts of this kind, the research itself was funded from other sources. The support under the contract was purely for travel between the two institutions that was necessary to further the collaboration. The order of presentation in the report corresponds to the order of the items in the statement of work in the original contract proposal.

Refractive indices in air

Work on measurements of refractive indices in air has continued. In the Optical Sciences Center much use has been made of a method depending on the measurement of a surface plasmon resonance in the determination of the optical constants of metals. There are great difficulties in the precise measurement of the optical constants of metals especially in the multiplicity of solutions. Although ellipsometry has been used successfully, the ellipsometric measurement of the optical constants is complicated and there is considerable opportunity for making errors in the determination of the constants. The surface plasmon resonance method avoids many of the difficulties, the principal remaining ones being simply that there are two possible solutions.

The technique involves the coating of the base of a prism with the correct thickness of metal and the subsequent measurement of the resonance that appears as a sharp dip in the p-polarised reflectance beyond the critical angle (fig.1). The position, width and depth of the dip yield the thickness and the constants n and k of the metal layer (fig. 2 and 3). The two possible solutions differ principally in the thickness and the real part of refractive index, the extinction coefficient remaining reasonably constant. The thicker solution is accompanied by a higher

value of n. The difference between the two solutions decreases with decreasing residual reflectance and disappears if the minimum reflectance at the resonance is zero. Thus there is actually an advantage in choosing a thickness that does not lead to the theoretically best result of zero reflectance. This particular coupling arrangement is known by the name of Kretschmann. There is an alternative coupling arrangement, the Otto configuration, involving the deposition of a thick metal layer on a separater plane substrate and the coupling into it by means of an uncoated prism placed over it. Experiments have actually been carried out in Arizona using both arrangements with the Kretschmann configuration, although involving a more restricted range of metal thicknesses, proving definitely superior.

We have been interested in the effect of ion-assisted deposition on metals and in particular silver. With dielectrics, the effects of ion-assisted deposition are almost entirely beneficial. Packing density is increased to the point where bulk-like values are obtained. Anisotropy due to form birefringence is reduced and the refractive indices increased. Some qualitative experiments at the Optical Sciences Center suggested that the effects with metal layers might not be so completely beneficial and so a series of quantitative experiments was undertaken.

The results of argon bombardment of silver during deposition are shown in figures (fig. 4 to 8). In brief the changes in the silver can be correlated with the rate of transfer of momentum relative to the rate of deposition of the layers. The parameters measured were the optical constants n and k, (fig. 4 and 5) the degree of incorporation of argon in the layers, determined by Rutherford Backscattering, and the lattice constant measured by x-ray diffraction. The optical constants systematically changed so that n increased and k decreased, increasing the loss and reducing the optical quality of the layers. The degree of incorporation of argon increased. The lattice constant of the silver increased over a narrow range of bombardment from a value somewhat less than the lattice constant of bulk silver to a value somewhat higher.

FIGURES 1. THRU 8.
FOLLOW

Surface plasmon resonance

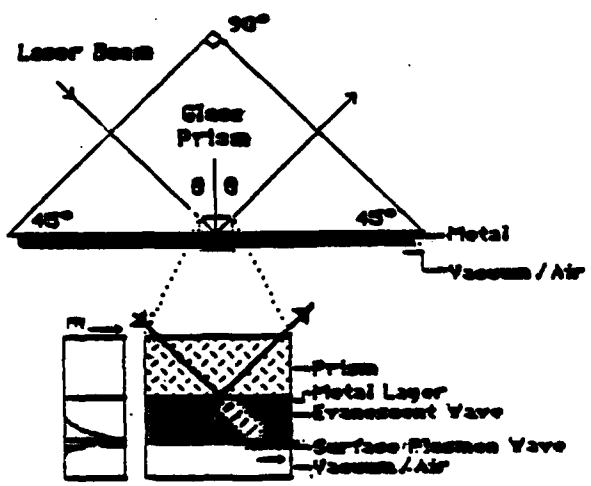

Figure 1. The configuration of metal film and prism used for the surface plasmon measurement in p-polarized light.

Surface plasmon resonance

- wavelength 632.8 nm
- about 50 nm thickness

experimental R

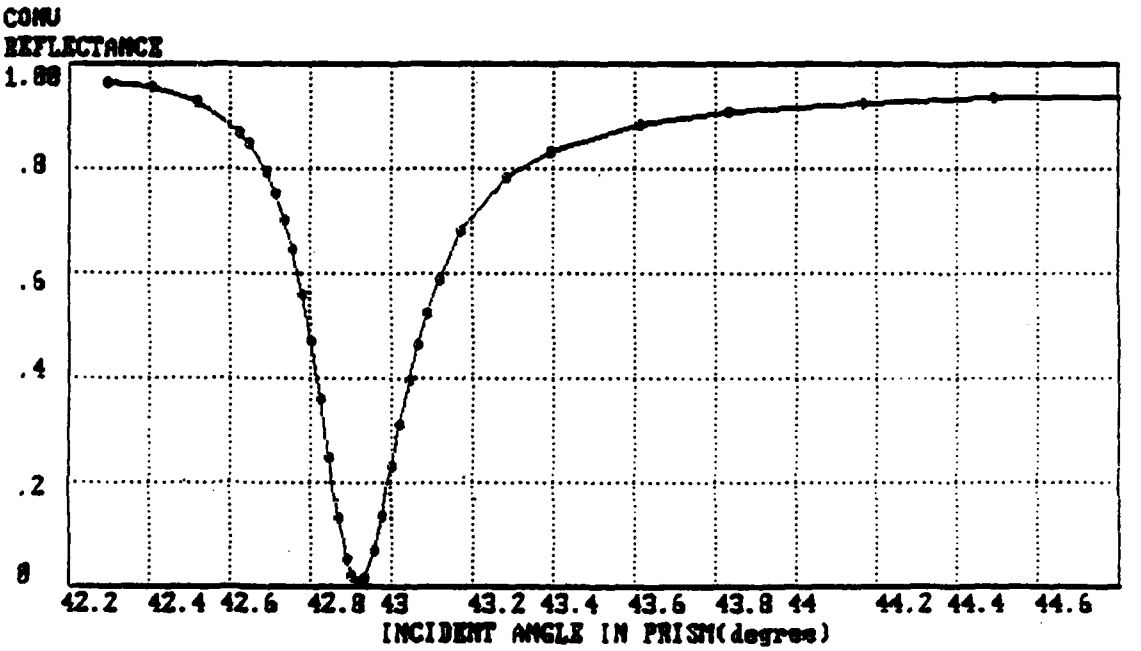

Figure 2. An experimental resonance curve for a silver film measured at 632.8 nm.

The optical constants and thickness were calculated using the nonlinear least square method.

n=.0723 k=4.142 d=50.1 nm
calculated R

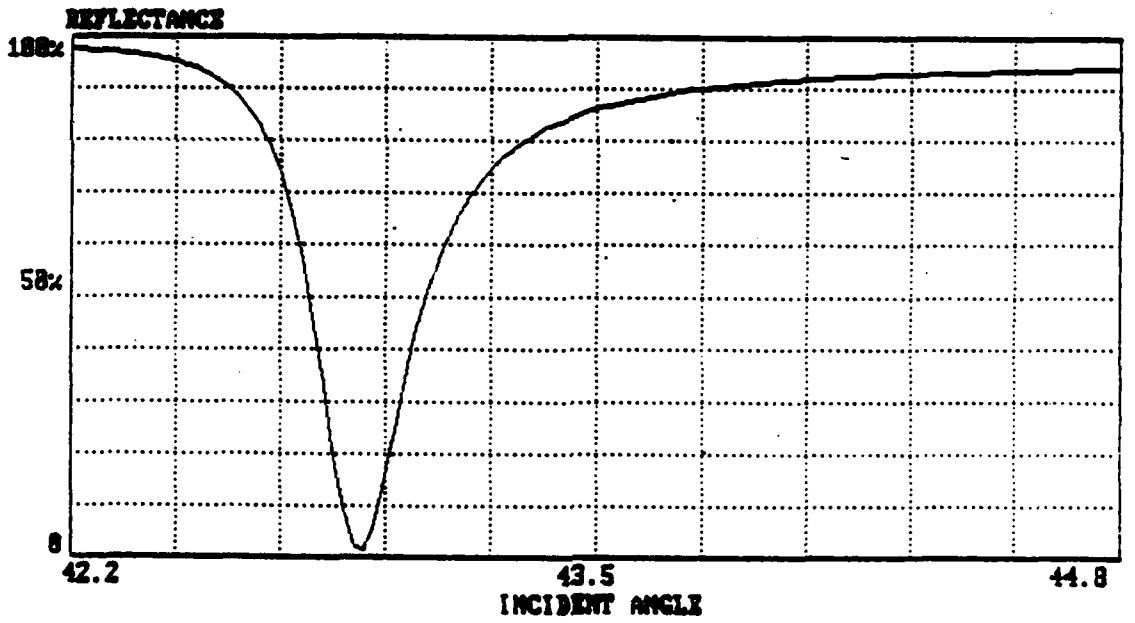

Figure 3. The optical constants and thicknesses of the silver film together with the calculated resonance fitting closely the data in Figure 2.

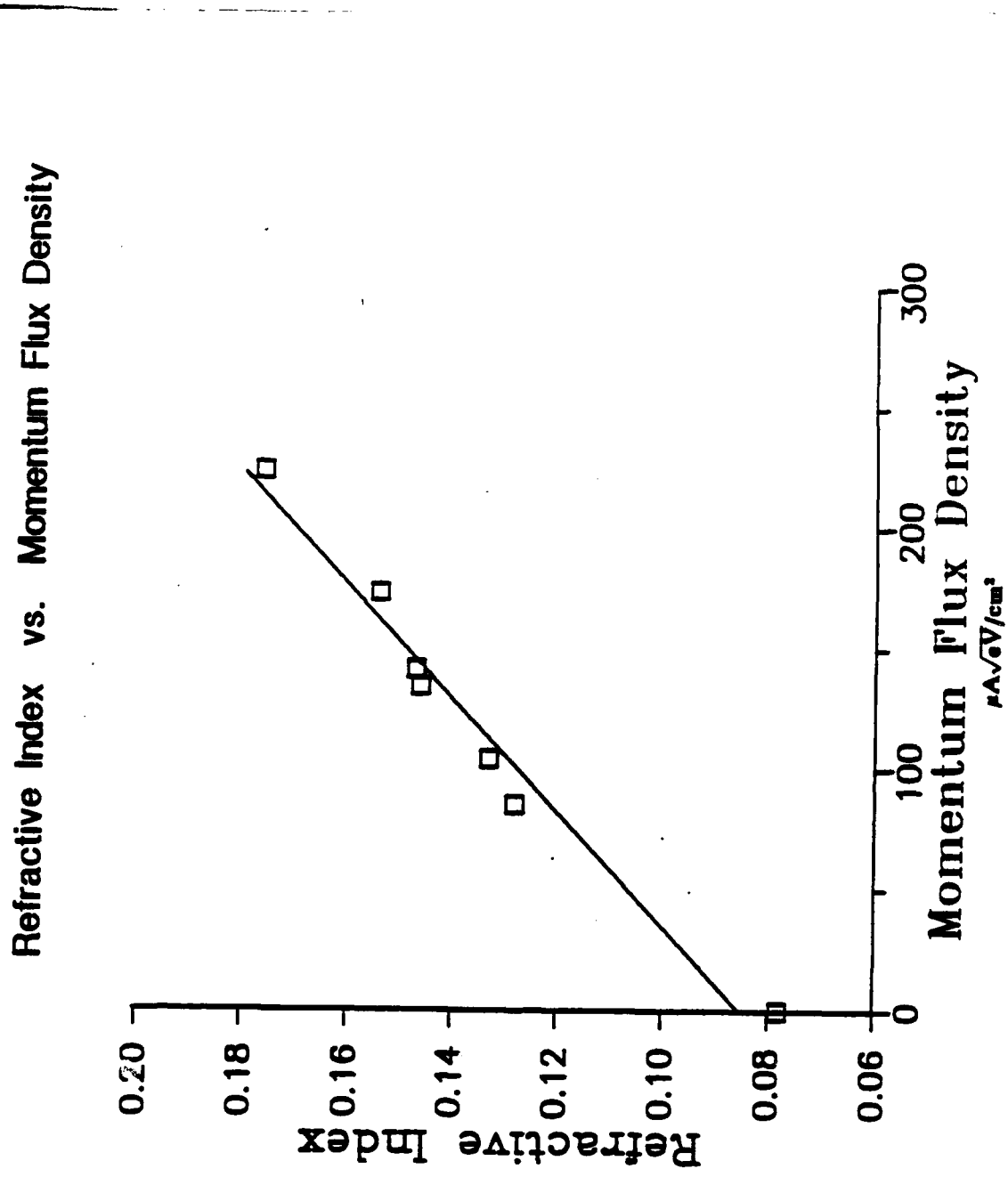

Figure 4. Experimental refractive index of IAD silver films [argon ion bombardment] as a function of momentum flux density.

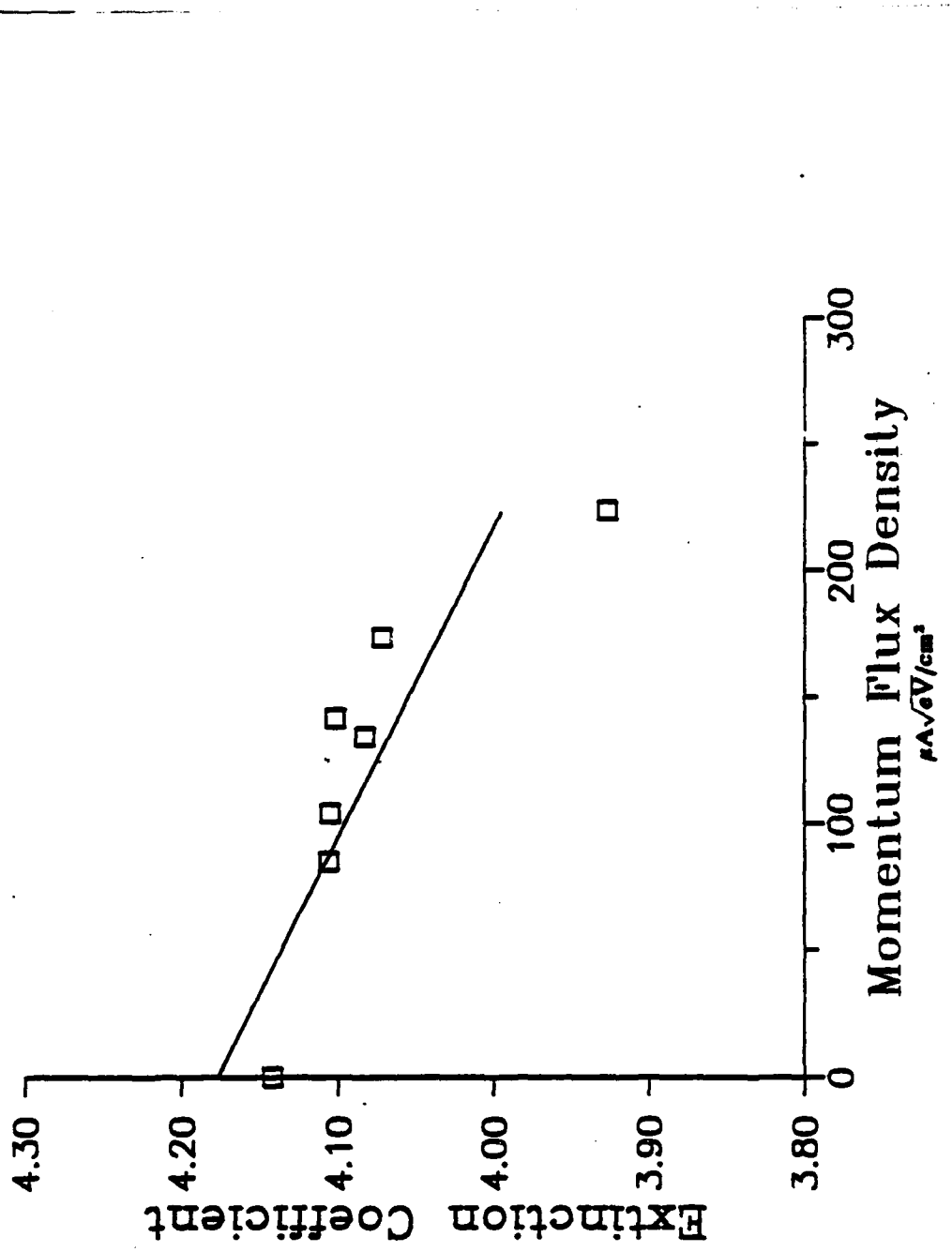

Figure 5. Experimental extinction coefficient of IAD silver films [argon ion bombardment] as a function of momentum flux density.

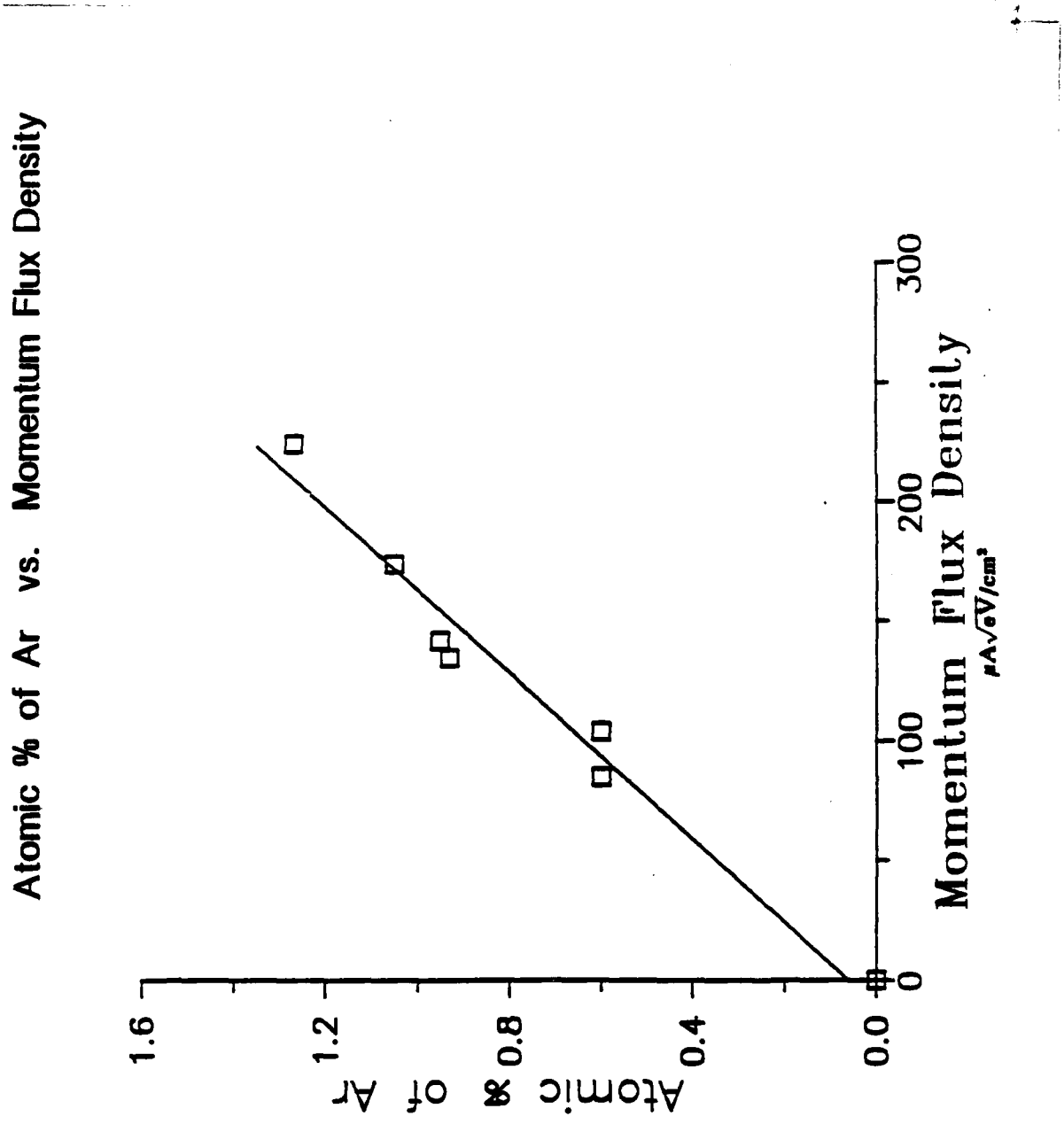

Figure 6. Atomic % of argon included in the films as a function of momentum flux density.

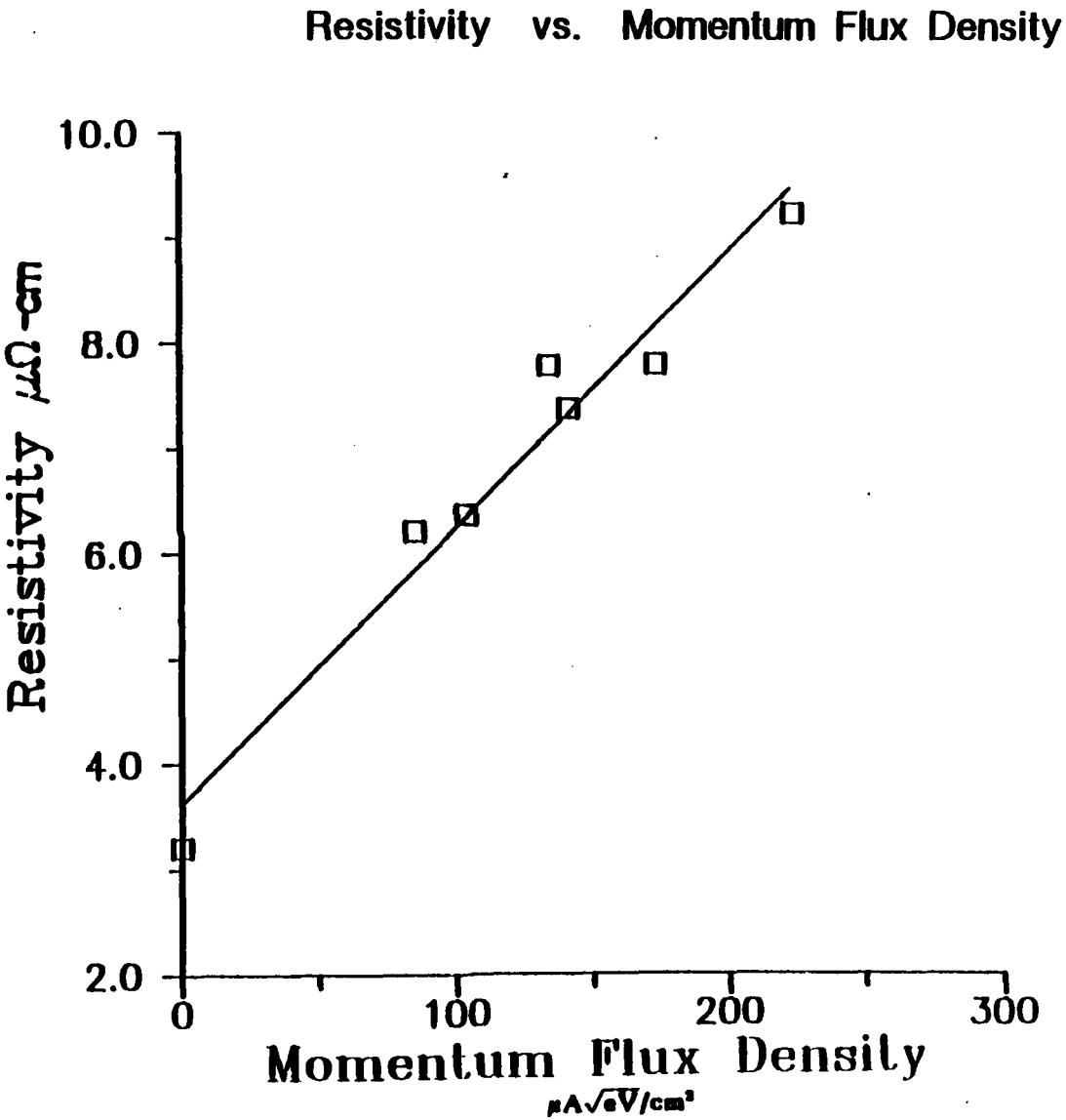

Figure 7. DC resistivity, measured by 4-point probe, of the silver films as a function of momentum flux density. Note the similarity between Figures 3, 5 and 6.

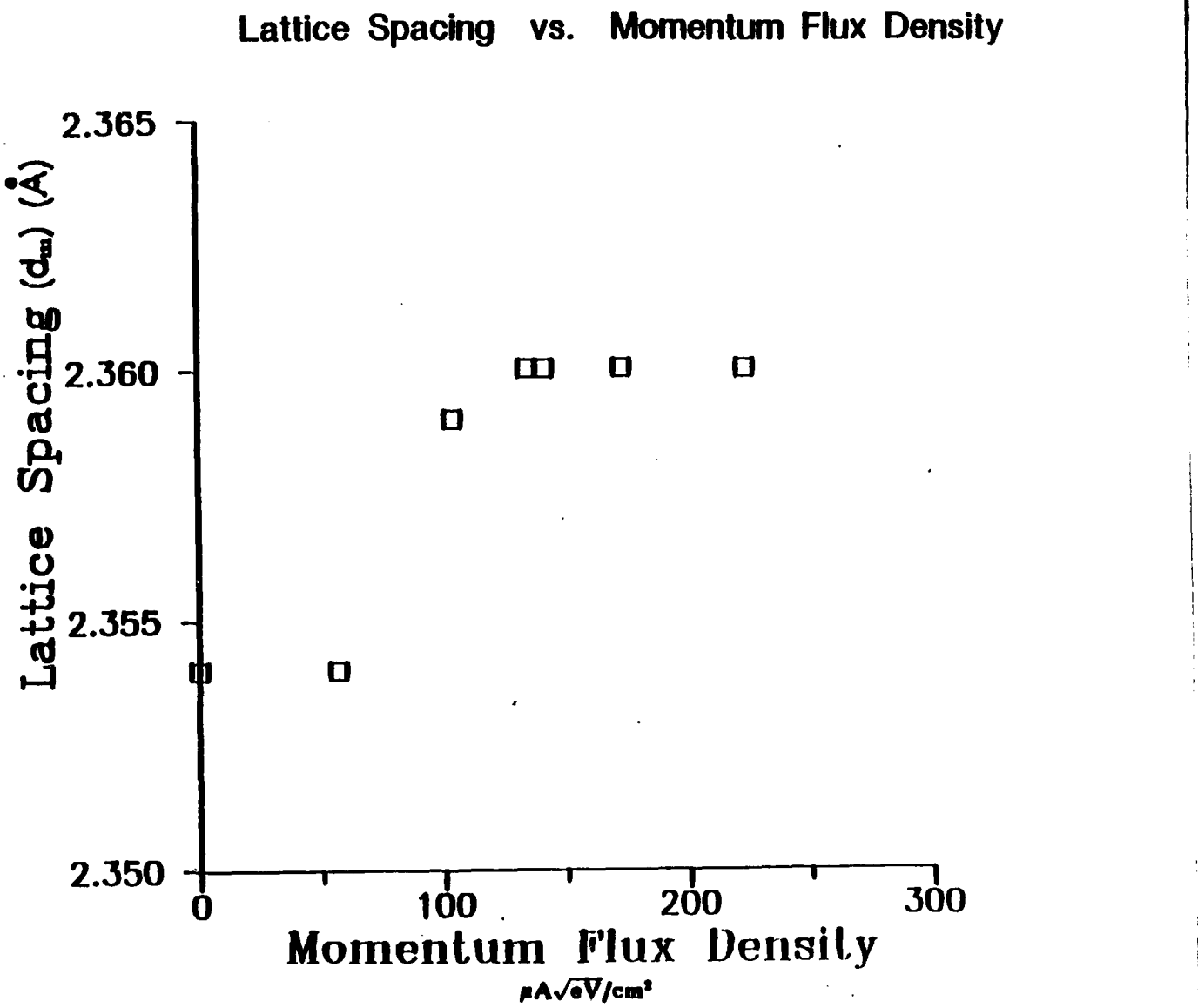

Figure 8. Lattice constant of the silver films as a function of momentum flux density. The change in the lattice constant probably indicates a shift with bombardment from tensile to compressive stress.

This suggests a change in the stress from tensile to compressive with bombardment, which might be expected. A broadening of the x-ray peaks suggests at the same time a decrease in the grain size.
Further experiments will be performed.

Concerning index measurements in air made, we give a brief reveiw of the methods used in Marseilles before presenting the most recent applications which are under development for the study of dielectric materials.

The first method is based on the utilization of layer reflectance and transmittance measurements over a wide spectral range, from which the complex refractive index and the thickness of the layer can be calculated. By using a particular model (index gradient) we can also take account of homogeneity defects [1].

The second method is, to some extent, similar to that developed in the Optical Sciences Center, but applied to dielectrics. This waveguide technique invelves coupling the light into the layer under study with a prism. It is possible to calculate the optical constants and the thickness of the layer from the coupling angles. This second method has been developed in Marseilles. For practical reasons, it effectively works with a single wavelength (λ = 632.8 nm, wavelength of the He-Ne laser). In spite of this limitation, as compared with the spectrophotometric method, it has several advantages :

- the accuracy obtained on the index values is greater;
- we can easily detect any trace of anisotropy in a layer by comparing results obtained for the two polarizations
- finally, provided some rather plausible assumptions, this characterization method can apply to multilayer systems.

In the preceding report for the US Air Force (15 Dec. 86), we described the principle of the measurements; we will present some of the more significant results obtained here. for emphasizing subjects of common interest for laboratories studying thin layers in the USA (Tucson in particular) and in the Ecole Nationale Supérieure de Physique in Marseille.

First, we recall in Table I a typical example of results obtained with guided waves on 4 layers. They concern 3 materials: TiO_2, ZnS and Ta_2O_5. For Ta_2O_5 we can compare the indices obtained on the layer produced by classical evaporation with those obtained on a layer produced by ion assisted deposition. We have used the model of Horowitz and Macleod [2] to display the anisotropy; n_1, n_2 and n_3 (which corresponds to the direction of columnar growth) are the principal indices. The measured thickness is d and $\Delta 31 = n_3 - n_1$; $\Delta 32 = n_3 - n_2$; $\Delta 21 = n_2 - n_1$.

All the experiments clearly show that anisotropy is completely correlated with the columnar microstructure of the materials. This anisotropy $\Delta 31$ $\Delta 32$ clearly depends on the deposition conditions and particularly on the incidence angle of the material flux on the substrate. Let us recall that a rotation of the substrate during deposition notably modifies the values $\Delta 31$, ... In the case of a non-rotating substrate, the columns are oriented in a well determined direction. Even if we have no information on the geometrical conditions of deposition, it is sufficient to study the conditions of guided wave propagation in different directions along the surface to locate the particular incidence plane containing the columnar growth direction.

Another important aspect illustrated in Table I concerns the layers produced by IAD: for optimal deposition conditions, anisotropy is extremely weak. This can certainly be explained by the fact that the layer is relatively more compact than a layer obtained by classical evaporation. We will see later that this is a very good test of the technique of Ion assisted Deposition.

And finally we emphasize that the measurement accuracy is such that this technique allows us to study index (and thickness) variations of coatings. In this way we have a characterization technique well suited for studying uniformity in an evaporating chamber. We will present here the results concerning IAD. However, it is interesting to show how guided wave optics can be applied to multilayer systems characterization.

	TiO_2	ZnS	Ta_2O_5	Ta_2O_5 (IAD)
n_1	2.320	2.349	2.119	2.151
n_2	2.321	2.351	2.115	2.151
n_3	2.357	2.356	2.127	2.155
d(nm)	422.4	506.9	429.9	269.4
Δ_{31}	0.037	0.007	0.008	0.004
Δ_{32}	0.036	0.005	0.012	0.004
Δ_{21}	0.001	0.002	-0.004	0.000

Table I

Refractive index anisotropy measured by guided wave technique of three materials: TiO_2, ZnS and Ta_2O_5. The Ta_2O_5 layer produced by ion assisted deposition leads to a noticeable reduction of anisotropy.

Multilayer systems

We attempt to answer the following questions:

- Compared with a single layer, is the structure of a layer modified when it is sandwiched in a stack?
- What are the consequences on the values of index, inhomogeneity rate and anisotropy?

With materials such as oxides, experiments are very critical. Due to the dependence of layer refractive index on the deposition conditions, it is not possible to start from the results of measurements concerning successive evaporations of single layers and of multilayer stacks. So we have developed a technique using a mask to simultaneously deposit TiO_2 onto different substrates. For example, on some substrates we will have a single layer; on other substrates the layer will be inserted between other layers of a different material (SiO_2). Our main conclusions are as follows (Table II) for TiO_2:

When a 6H layer is under a L layer in the stack, n_1 and n_2 increase slightly.

$$\delta n_1 = \delta n_2 = 0.010$$

On the other hand, index n_3 (in the columnar direction) is not modified by the "sandwich effect". In these conditions, speaking in terms of anisotropy Δ_{31} and Δ_{32} are slightly reduced by the "sandwich effect". With the couple Zinc Sulfide and Cryolite, this effect has not been observed (see USAF 86).

With these results in mind, we tried to develope this characterization technique to directly study complex systems of layers, such as triple half wave Fabry-Perot filters. The problem becomes very complex; one can find some information on our preliminary conclusions in [3] one of our papers given in Tucson.

Application of the methods of index characterization

Our measurement methods are available for the enhancement of international cooperation. Let us recall here the TiO_2 investigation

stack	indices and thicknesses	anisotropy
glass L 6H	$n_1 = 2.238$ $n_2 = 2.246$ $n_3 = 2.300$ d = 444.4 nm	$\Delta_{31} = 0.062$ $\Delta_{32} = 0.054$ $\Delta_{21} = 0.008$
glass 6H	$n_1 = 2.233$ $n_2 = 2.245$ $n_3 = 2.302$ d = 448.7 nm	$\Delta_{31} = 0.069$ $\Delta_{32} = 0.057$ $\Delta_{21} = 0.012$
glass 6H L	$n_1 = 2.246$ $n_2 = 2.252$ $n_3 = 2.301$ d = 447.1 nm	$\Delta_{31} = 0.055$ $\Delta_{32} = 0.049$ $\Delta_{21} = 0.006$
glass L 6H L	$n_1 = 2.247$ $n_2 = 2.256$ $n_3 = 2.302$ d = 445.2 nm	$\Delta_{31} = 0.055$ $\Delta_{32} = 0.046$ $\Delta_{21} = 0.009$

Table II

Comparison of the anisotropy of TiO_2 layers sandwiched in different multilayers.

prompted by the Optical Material and Thin Film group of the Optical Society of America. The first results were discussed at the OSA Annual Meeting in Seattle, October 1986. A complete review on this subject is now available under the form of a paper written by Jean Bennett et al. [4] which combines the results of different teams including ours. It is an important compilation work and we are indebted to Jean Bennett for having coordinated all these efforts with great attention.

Extinction coefficient

It is possible to use classical spectrophotometric methods to have access not only to the real part of index but also to the imaginary part, the extinction coefficient k. However, on this subject, we have some problems with accuracy. The values of $k(\lambda)$ are generally very low, on the order of 10^{-4}. We have studied, in detail, this problem of precision. In particular scattering losses can be of the same order of magnitude of the absorption losses. In these conditions, the values of $k(\lambda)$ extracted from spectrophotometric measurements are unreliable. The form of dependence of k on wavelength can give interesting information for better utilization of our results. An article written by Borgogno et al deals with this subject [5]; it was presented at the last conference in Tucson and submitted to Applied Optics.

In-situ optical constants

In-situ measurements of optical constants have continued at Marseille. As will be discussed in the next section, the ion-assisted process has succeeded in removing much of the sensitivity of the optical constants to process conditions and so in situ measurements of the optical constants have been less necessary. A principal use of the system has been in the comparison of the behaviour of the films before and after venting.

Differences between measurements in-situ and in air

Inhomogeneities in, and differences in, indices have always made it difficult to construct precise coatings from materials such as the refractory oxides. These materials have long been used for hard durable coatings but for precise optical properties it has been necessary to make use of the less durable but better optically behaved zinc sulphide and cryolite. For coatings to be used exposed to the atmosphere these materials have been of little use and they have always had cover slips cemented over them. For applications such as multiplexing and demultiplexing beam splitters, for example, titanium dioxide and silicon oxide have been proposed because of their durability, but they have not been acceptable because of their poor stability. Experiments in the construction of narrow band filters, by ion-assisted deposition of these materials have been carried out at Marseille.

An example of the results obtained is shown in **figure 9**. This is a triple cavity filter of design:
glass HL HL 2H LH LH L HL HL 2H LH LH L HL HL 2H LH LH L air
The vacuum-air shift has been completely suppressed [6].

Deposition processes

Work on ion-assisted deposition in both establiishments has continued. In Arizona, the principal materials under study have been the fluorides and some metals, particularly silver. The IAD of silver was carried out by C.K. Hwangbo and of lanthanum fluoride by J.D. Targrove, both of the Thin Film Group at the Optical Sciences Center.

The reduction in moisture sensitivity due to IAD is also illustrated by the results obtained from magnesium fluoride-lanthanum fluoride multilayers constructed for the near ultraviolet and reported in the paper 'Ion-assisted deposition of lanthanum fluoride thin films" attached as appendix II.

In Marseille the principal activity has been concentrated on TiO_2 and SiO_2 multilayers. The principal results in Arizona beyond what has

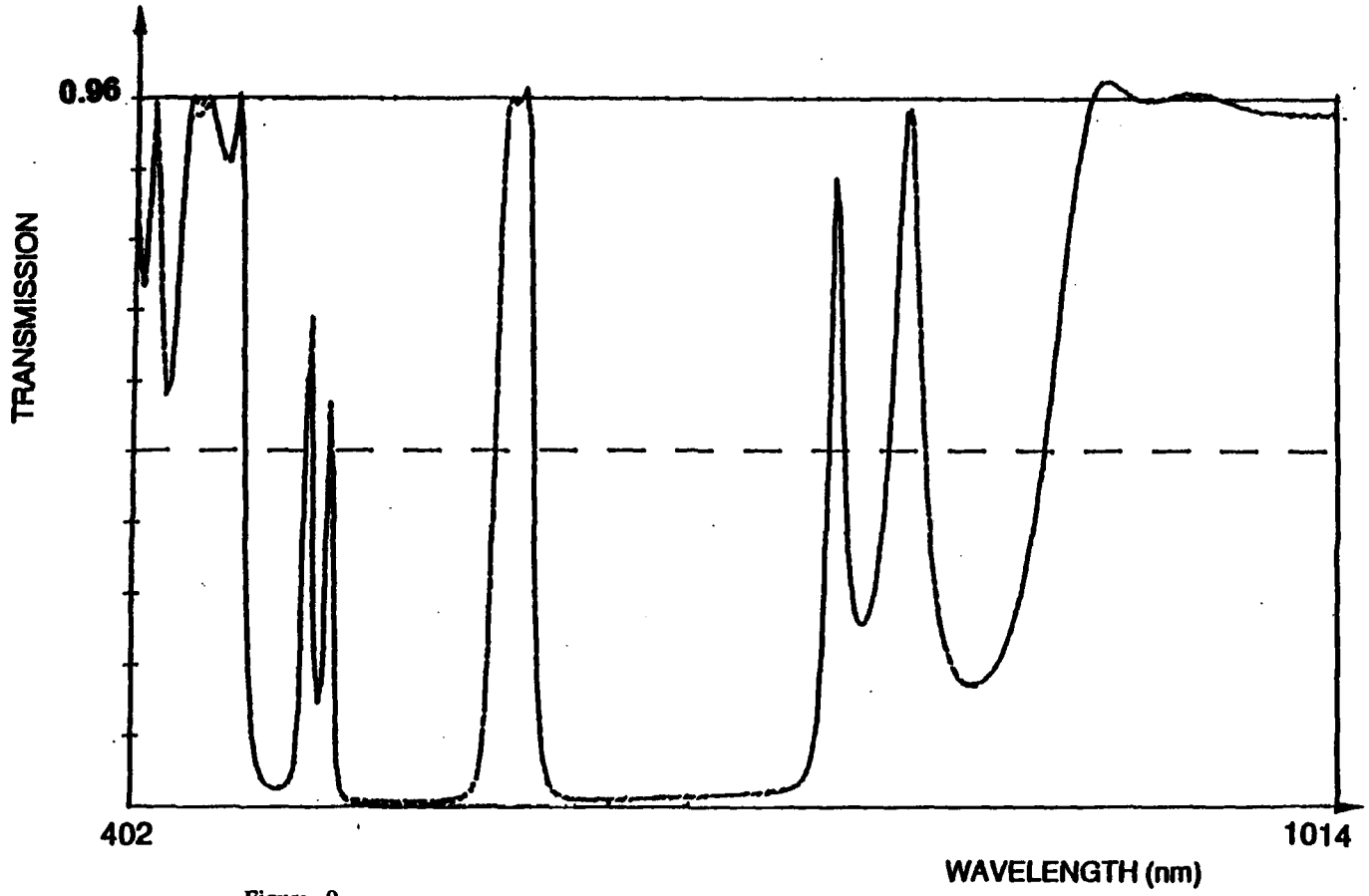

84

Figure 9

Triple Half Wave Fabry-Perot filter produced by Ion Assisted Production.
Design:
Glass HL HL 2H LH LH L HL HL 2H HL HL L HL HL 2H LH LH L .
with H: quarterwave layer of TiO_2
L: quarterwave layer of SiO_2
The measured transmittance in situ and in air are superposed; the vacuum-air shift is completely suppressed.

been reported last time, has been first of all in the silver results, reported on in section 2 above, and in the correlation with changes both in dielectric and in metallic layers with total momentum rather than energy transferred to the layers. Different energies and masses of bombarding species have been used and the correlation with momentum has been good while that with energy has been poor. Figures 10, 11 and 12 summarize the results obtained at Tucson on lanthanum fluoride films.

In Marseille, we have given particular attention on the problem of uniformity of deposits on coated surfaces of more than 20 cm in diameter.

Even with classical evaporation, we have very important problems of uniformity as soon as we want to make multiple cavity Fabry-Perot filters with a relatively narrow passband ($\Delta\lambda$ = 20 nm). The tolerances for realization of these filters are very strict. Owing to the optical control monitoring technique used, we have the advantage of an automatic error compensation *during manufacture* and thus, on the control glass, we can realize well centered filters. But for the other substrates (or for other points of the substrate holder), it is almost impossible to be sure of a correct position of the centering wavelength. Also, we would like to realize simultaneously a set of identical filters, all centered on the same wavelength as the filter obtained on the control substrate.

This necessitates carefully positioning the different elements (source, substrates, ...) in the evaporating chamber to meet very strict geometrical conditions.

In general, we consider the uniformity U(z) defined as the ratio between the optical thicknesses of a layer in two distinct points of the coated surface: $U(z) = E(z)/E_0$ where E_0 is related to the center of the substrate holder (the control glass) and E(z) to the point of abscissa z. To obtain a good uniformity, the condition U(z) = 1 must be fulfilled for all z. This condition implies uniformity on the index value and on the geometrical thickness. Obviously, we will have to consider the possible local variations of microstructure of the deposited material, with all the

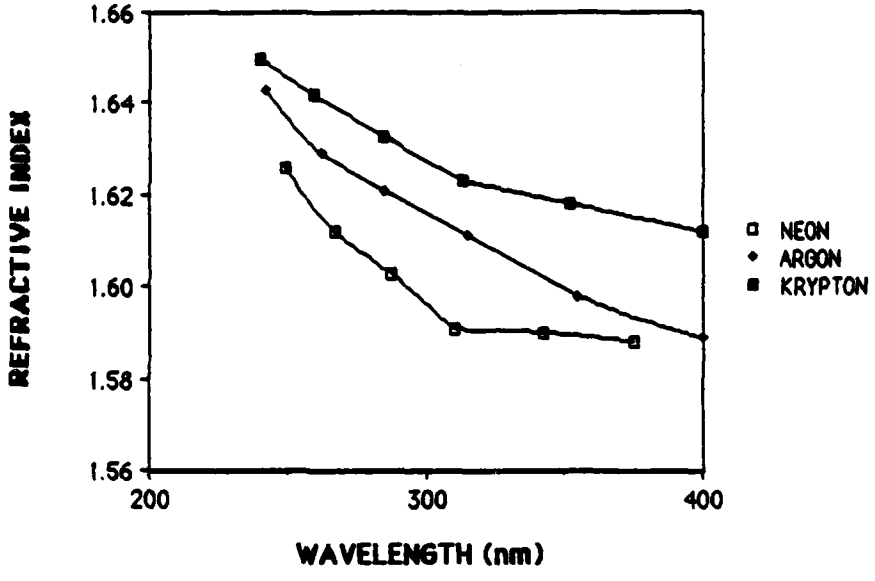

Figure 10 The refractive index of lanthanum fluoride films deposited by IAD with various noble gas ion beams, all at 60 $\mu A/cm^2$ current density and 500 eV energy.

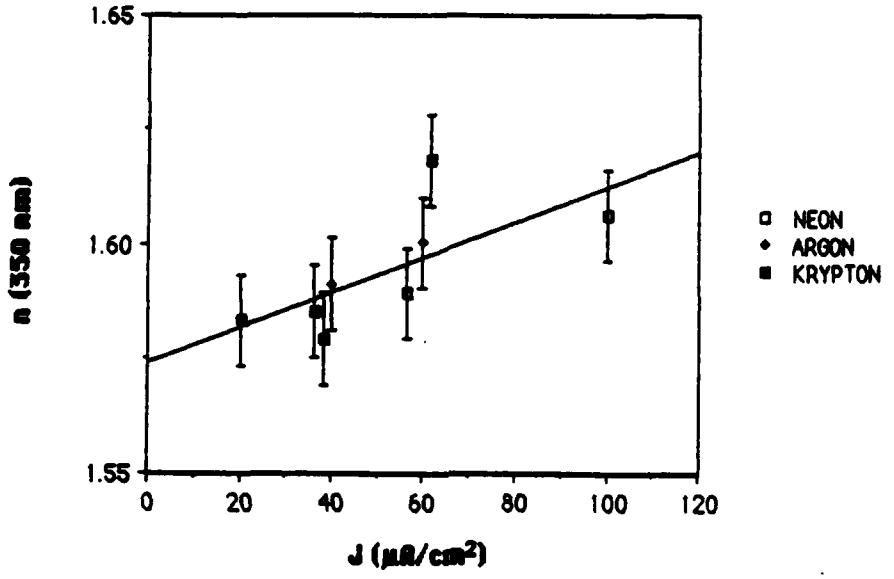

Figure 11 The refractive index of the lanthanum fluoride films at 350 nm plotted against current density. Ion energy in all cases is 500 eV. Agreement is not good.

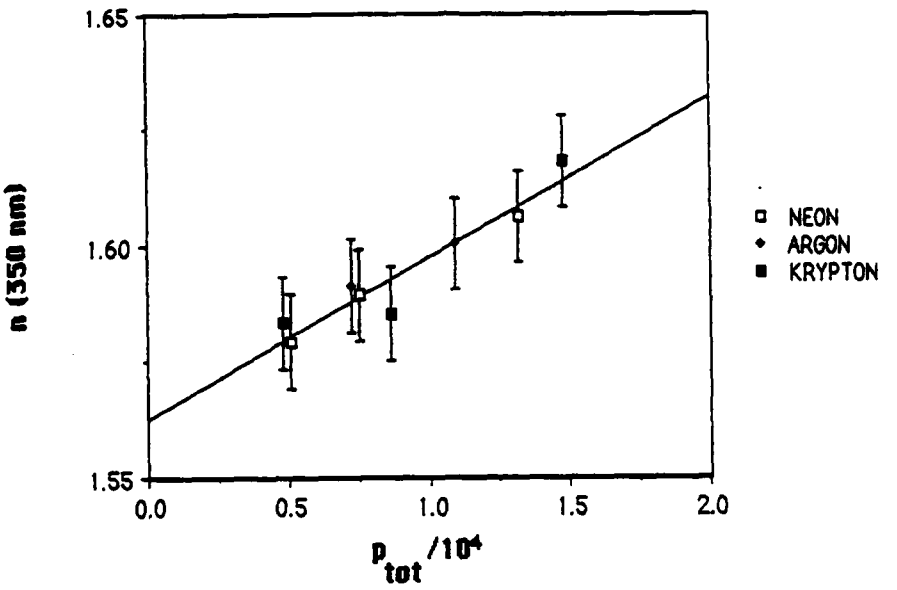

Figure 12 The refractive index of the lanthanum fluoride films of Figure 9 plotted as a function of the total momentum transfer rate in units of ($\mu A/cm^2$) $(amu.eV)^{1/2}$. The agreement is good.

implied consequences: uniformity defects in homogeneity, anisotropy variations, etc ...

We have already described the technique of characterization used (guided waves); let us see now the results related to these uniformity problems.

With the more classical materials used for Fabry-Perot filters, such as zinc sulfide and cryolite, the problem of uniformity of refractive index is not very critical. The condition $U(z) = 1$ essentially concerns the geometrical thickness of the deposits. nevertheless, we have displayed the fact that U could eventually depend on time t: The evaporant distribution varies during the evaporation and this can have important consequences on the performances of the filters realized [7].

With materials such as oxides, indices depend considerably on the deposition conditions and the problem of index uniformity becomes very important.

We dealt particularly with layers produced by IAD (Ion Assisted Deposition). **Figure 13** and **Table III** give the distribution measured for a TiO_2 layer. The surface studied is about 20 cm in diameter and we have, over the diameter, the law of index distribution (here we give n_2 and n_3, the principal indices with the model of anisotropic layer). Together with the thickness distribution. It is interesting to compare these values with those concerning the uniformity of the ion beam (see figure 13), but the interpretation of the phenomena is still not complete . In the case of single Fabry-Perot filters, these techniques allowed us to improve the conditions of uniformity in our evaporating plant. For triple half wave Fabry-Perot filters, tolerances are more severe and further progress is still necessary.

Anisotropy

The experimental aspects concerning anaisotrcpy have been seen in the chapter related to indices. We saw that guided wave measurements are still of large use. In Arizona, the major work has been in the development of software to calculate the properties of general

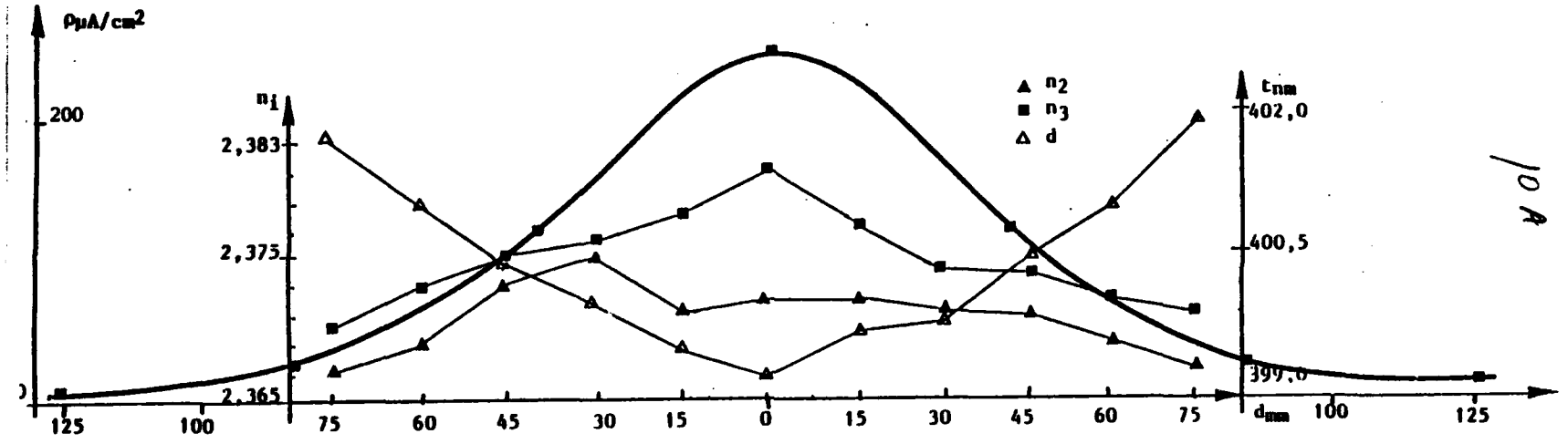

Figure 13

Ion Assisted Deposition. Study of the uniformity of the thickness (d) and the indices (n_2, n_3) of a TiO_2 layer deposited on a rotating substrate (20 cm in diameter). The uniformity of the ion beam is also given. The numerical data concerning this figure are given in Table III.

d (mm)	75	60	45	30	15	0	15	30	45	60	75
n_1	2,371	2,373	2,383	2,384	2,371	2,370	2,376	2,378	2,376	2,374	2,366
n_2	2,367	2,369	2,373	2,375	2,371	2,372	2,372	2,371	2,371	2,369	2,367
n_3	2,370	2,373	2,375	2,376	2,378	2,381	2,377	2,374	2,374	2,372	2,371
t	401,8	401,3	400,4	400,0	399,5	399,2	399,7	399,8	400,5	401,0	401,9

↑
center

Table III

Measurement of uniformity: Indices and anisotropy of a TiO_2 layer on a rotating substrate (see figure 13)

anisotropic, absorbing and optically active multilayers. The objective has been principally in the field of optical data storage and the system based on the Kerr magneto-optical effect. However, the program can be used in any application.

Scattering and surface roughness

Work under this heading has continued under several different subheadings.

In Marseille we have an extremely high performance apparatus for recording scattering curves (Measurements for the wavelength λ_0 = 632.8 nm only). We have also developed a theoretical model, derived from that of Elson and Bennett, to account for scattering in layers or in multilayers. In this model it is assumed that interfacial roughness is the main source of scattering. The validity of this model has been proved for the problem we are interested in: coated or uncoated surfaces of good optical quality.

A great deal of work (see USAF 86) has been devoted to the study of single layers and we have extracted information on the "grain size", one of the important microstructure characteristics for a material in thin film form. The layers studied have been produced in our laboratory. We have studied, for different dielectric materials, the dependence of the grain size on the preparation conditions of the layers.

Concerning interfacial roughness, the granularity corresponds to a correlation rate between the two interfaces, glass-layer and layer-air. The models of layer growth simulation developed in Tucson can thus be applied to compare our results, but this gives rise to numerous difficulties.

Let us also recall the alminum overcoating technique: an opaque aluminum layer is deposited on a dielectric coating, allowing the measurement of the scattering curve and thus the roughness of the top interface of the coating.

At Marseille, we have been particularly interested this year in two different subjects:

- For the Optical Society of America, we have systematically measured scattering on TiO_2 single layers produced by some 20 different laboratories. (in fact, this is the continuation of the operation concerning index determinations).

- On the other hand, we have extended our scattering studies to multilayer systems, especially to quaterwave stacks such as mirrors or Fabry-Perot filters. All these coatings are produced in our laboratory for different applications (for exampie, demultiplexing in optical telecommunications between satellites).

Multilayer study

Let us begin with this second aspect of our activity in Marseille.

Calculations of scattering curves for a multilayer involve a great number of parameters (in practice, 5 parameters for each interface: 4 parameters to describe the roughness and 1 for the crosscorrelation rate of the interfaces). Evidently, it is impossible to determine each of them from a limited number of experimental results. In a first step, we make simplifying assumptions:

- identical interfaces;

- limitation to two extreme hypothesis corresponding to the cases where the interfaces are completely correlated ($\alpha = 1$) or totally uncorrelated ($\alpha = 0$).

The Al overcoating technique on the multilayer allows us to determine the 4 roughness parameters for the top interface, layer-air. The measurement of the scattering curve of the multilayer can then be compared with the calculated values. We arrive at the following conclusions with TiO_2 and SiO_2 materials:

- For mirrors, we must admit that the interfaces are practically correlated (**fig. 14**).

- For Fabry-Perot filters (single, DHW or THW), the interfaces are uncorrelated (**fig 15**).

Contrary to appearences, these results are not inconsistent. This for two reasons

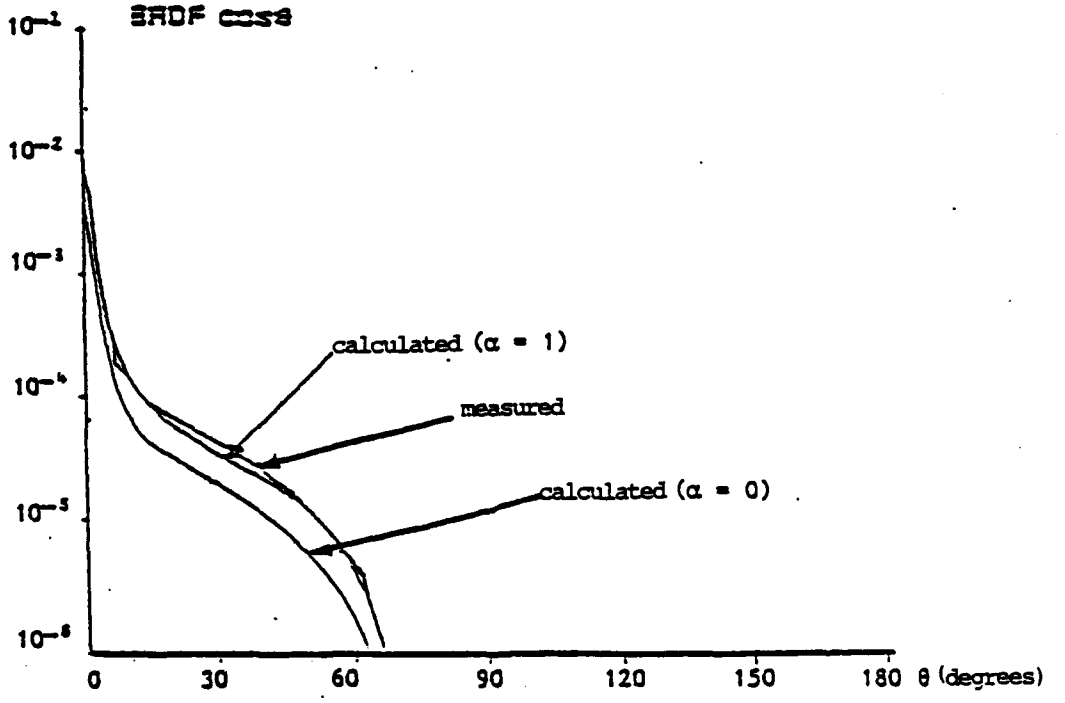

Figure 24

Measurement and calculation of the scattering curve of a mirror:
substrate HL HL HL HL HL HL HL H air
We theoretically consider the two extreme cases:
$\alpha = 1$ interfaces perfectly correlated
$\alpha = 0$ uncorrelated interfaces
By comparison with experiment, we deduce that the interfaces are correlated.

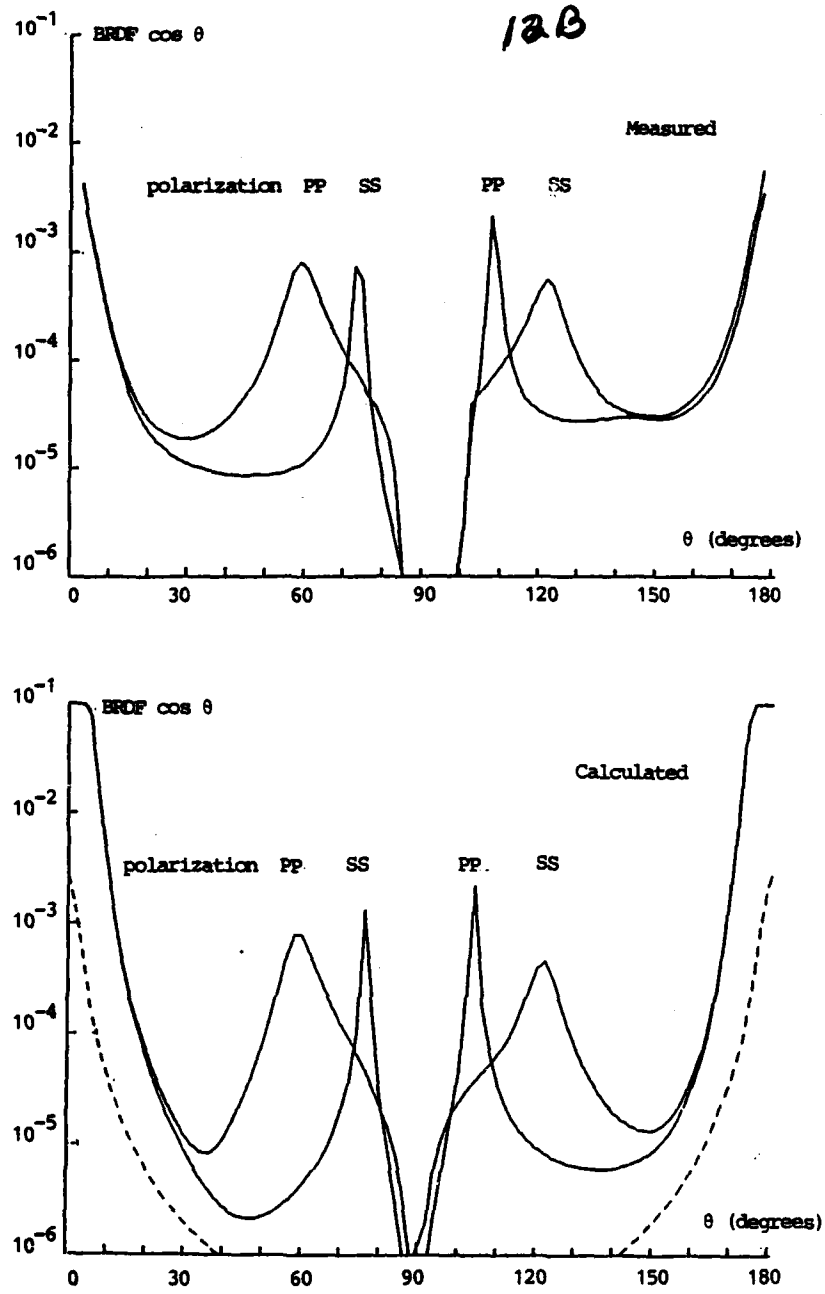

Figure 15

Measurement and calculation of the scattering curves of a Fabry-Perot filter:
substrate HL HL HL 18H LH LH LH air
The measurements are performed for the pp and the ss polarizations. The better agreement is obtained by assuming uncorrelated interfaces in the calculations.

- In a mirror and in a Fabry-perot filter, the same interfaces have significantly different influence;
- Theoretically the state $\alpha = 1$ which corresponds to a perfect correlation, gives a spatial distribution law of scattering which is very unstable. The effect of destructive interference disappears with the slighest trace of uncorrelation.

Obviously, our model is overly simplified; we must consider intermediate values for α (between 0 and 1), that is partial correlation. And finally, experiments show that we must take account of the fact that α is not a number but a function of the spatial frequency of the defects.

Here also, all these considerations meet those which have motivated the development in Tucson of the model of layer growth, and this is an important subject of common work for the two groups in the coming years.

Measurements of the OSA samples

A brief survey of the measurements made for the Optical Society of America, on single TiO_2 layers follows. We have tried to handle this problem statistically, but we have had serious difficulties and the conclusions can be subject to controversy. Fortunately, we have the dynamic help of Jean Bennett to aid in this matter.

We must remember here that we have reliable experience concerning the evaporation conditions for TiO_2. Many results [8] have been published on the grain size of layers made of this material, these results having been obtained from scattering measurements. Our aim was to apply the same technique to the mesaurements made for the O.S.A.

If we limit ourselves here to the opinion of the research workers in Marseille on their measurement results, our conclusions are rather restricted.

Starting from the measurements, the scattering curves measured on TiO_2 layers, and the scattering curve measured after deposition of aluminum on these layers, we can calculate, by integrating in the whole space, the total amount of light front- and backscattered by the layer,

and the global front scattering for the aluminum layer. The comparison of all these results shows a very large disparity from one layer to another (fig. 16). It is obvious that the quality of the substrates is involved perhaps together with the cleanliness of the studied samples.

From scattering measurements, is it possible to obtain information concerning the microstructure of the material TiO_2? On this set of samples, we are tempted to answer no, because the necessary experimental precautions, in our opinion, have not been taken:

- we have not an exact idea of the substrate quality;
- the dust particles on the substrate or included in the layer are probably responsible for the measured scattering.

Of course, we have attempted to get a better utilization of our measurements by studying the shape of the scattering curve, which is very characteristic for some samples. Here we have only limited conclusions. Jean Bennett keenly encourage us to question again our point of view ... and obviously this discussion is only at its beginning. It is thus a subject to which we will return. However, it seems interesting to give our own conclusions: due to lack of experimental precautions, our scattering measurements cannot lead to good information on TiO_2 layer microstructure; too many artefacts mask the interesting phenomenon. A poster on this subject has been presented at the Tucson Conference last April [9].

Publications - Participation in conferences

The Laboratory of Marseille was anxious to massively participate in Conferences in the USA particularly those devoted to subjects related to its own domain of research: The Boulder Damage Symposium (Nov. 87) and mainly, the Conference on Optical Interference Coatings which was held in Tucson (April 1988). 8 persons of the laboratory attended this conference; 6 papers (including an invited paper) were presented. The manuscripts of these conferences have been submitted to O.S.A. for publication.

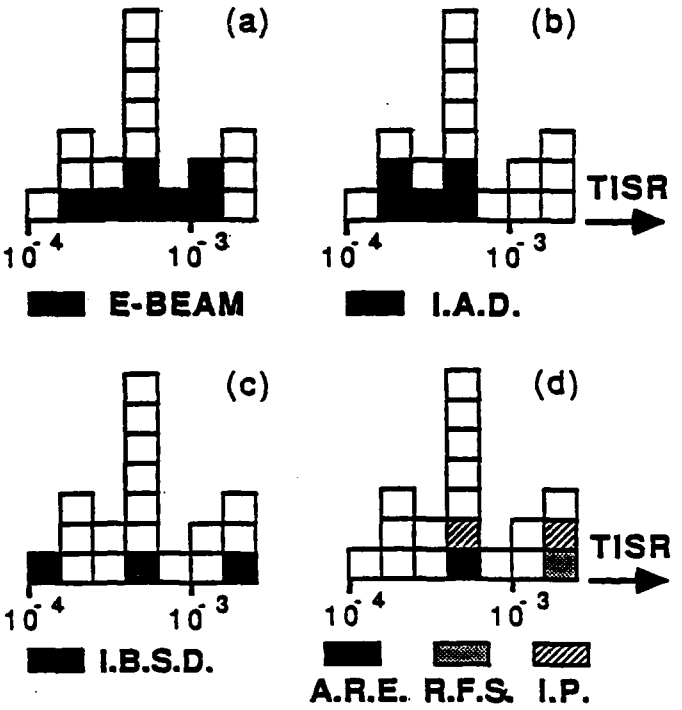

Figure 16

To tal amount of front scattered light (TISR) measured on the 19 single layers of titania films of OSA.
The histogram is repeated 4 times in order to show the portion of samples produced by the indicated deposition techniques:

Electron beam (EB)
Ion Assisted deposition (IAD)
Ion Beam sputter Deposition (IBSD)
Activated Reactive evaporation (ARE)
RF Diode Sputtering (RFS)

In appendix I, we give the abstracts of the papers presented at Tucson. The complete articles are available on request. A copy of each is enclosed with this report.

In appendix II, we give some other recent publications of the two laboratories in Tucson and Marseille, which concern the subjects developed in this final report.

Conclusion

The interest presented by the Ion Assisted Deposition technique has been obviously a great motivation for the two laboratories by involving them in the study of very different materials (Ag, LaF_3, Ta_2O_5,...).

Concerning characterization techniques of layers, we can note the analogy between guide wave optics techniques applied in one case to metals and in the other case to dielectrics.

Detecting anisotropy in the layers is a well advanced technique and its application to multilayers is of great interest for both laboratories.

Scattering studies in Marseille and studies of models for computing film growth in Tucson must now meet together to study the crosscorrelation laws between interfaces in a stack.

Application to studies of optical rough surfaces gives rise to difficult problems and we have to pay a particular attention to solve them.

References

1 J.P. BORGOGNO, B. LAZARIDES, E. PELLETIER, Automatic determination of the optical constants of inhomogeneous thin films. - Applied Optics, 21, 4020-4029, (1982)

2 F. HOROWITZ, Ph. Dissertation, University of Arizona, Optical Sciences Center, 1983
I.J. HODGKINSON, F. HOROWITZ, H.A. MACI EOD, M. SIKKENS, J.J. WHARTON, Measurement of the principal refractive indices of thin films deposited at oblique incidence, J. Opt. Soc. Am., 2, 1693-1697, (1985)

3 E. PELLETIER, F. FLORY, Y. HU, Optical characterization of thin films by guided waves. - Invited paper presented at: "Fourth topical meeting on OPTICAL INTERFERENCE COATINGS", April 12-15, 1988, Tucson, Arizona - Submitted to Applied Optics

4 J.M. BENNETT, C. CARNIGLIA, K.M. GUENTHER, E. PELLETIER, et al., Comparison of the properties of titanium dioxide films prepared using different techniques. To be published.

5 J.P. BORGOGNO, E. PELLETIER, Determination of the extinction coefficient of dielectric thin films from spectrophotometric measurements. - Conf. presented at: "Fourth topical meeting on OPTICAL INTERFERENCE COATINGS", April 12-15, 1988, Tucson, Arizona - Submitted to Applied Optics

6 F. FLORY, E. PELLETIER, G. ALBRAND, Surface optical coatings by Ion Assisted Deposition techniques: study of uniformity. - Conf. presented at: "Fourth topical meeting on OPTICAL INTERFERENCE COATINGS", April 12-15, 1988, Tucson, Arizona - Submitted to Applied Optics

7 C. GREZES-BESSET, R. RICHIER, E. PELLETIER, Layer uniformity obtained by vacuum evaporation. Application to fabry-Perot filters. - Conf. presented at: "Fourth topical meeting on OPTICAL INTERFERENCE COATINGS", April 12-15, 1988, Tucson, Arizona - Submitted to Applied Optics

8 C. AMRA, G. ALBRAND and P. ROCHE, Theory and application of antiscattering single layers; antiscattering antireflection coatings., Applied Optics, 25, 2695-2702, (1986)

9 C. HICKEY, C. AMRA, E. PELLETIER, Scattering study of single layer titania films. - Conf. presented at: "Fourth topical meeting on OPTICAL INTERFERENCE COATINGS", April 12-15, 1988, Tucson, Arizona - Submitted to Applied Optics

APPENDIX I

Abstracts of the conferences presented at Tucson (Optical Interference Coatings, 12-15 April 1988)

OPTICAL CHARACTERIZATION OF THIN FILMS BY GUIDED WAVES

E. Pelletier

Ecole Nationale Supérieure de Physique de Marseille - Laboratoire d'Optique des Surfaces et des Couches Minces - Unité associée au CNRS, U.A.1120 -Domaine Universitaire de St Jérôme - 13397 Marseille Cedex 13 - France

Abstract

The study of guided waves in a thin layer allows a precise characterization of refractive index and thickness. Optical anisotropy can also be measured. We show how this technique can be applied to the characterization of a multilayer structure.

I - INTRODUCTION

It is easy to justify the interest in a precise optical characterization of thin layers: if we know their refractive indices with a good accuracy, we can correctly predict the effective optical properties of a multilayer stack when the layer thicknesses are previously determined. For optical coatings, it is a decisive step and a main condition for obtaining the desired optical properties when attempting to manufacture coating. However, all this is based on two principles that are unfortunately not always perfectly true:

- we know how to individually characterize single layers. The models used in calculations do not accurately account for the microstructure of the layers, particularly when they are obtained by classical evaporation.

- the optical constants of a single layer are not perturbed when such a layer is sandwiched in a stack.

Numerous studies have been developed for single layer optical characterization. As a first approximation, it is generally admitted that they are homogeneous, isotropic, and with plane and parallel surfaces. In these conditions, from an optical point of view, characterization is reduced to a simultaneous knowledge of the refractive index, which is a complex number, and of the thickness.

With the precision which is now required, the above principles are no longer sufficient.

In our laboratory in Marseilles, we have systematically developed studies which avoid inadequacies of the model. Most of the results have been published in different conferences:

J.P. BORGOGNO, B. LAZARIDES, E. PELLETIER, **Automatic determination of the optical constants of inhomogeneous thin films**. - Applied Optics, 21, 4020-4029, (1982) - J.P. BORGOGNO, P. BOUSQUET, F. FLORY, B. LAZARIDES, E. PELLETIER, P. ROCHE, **Inhomogeneity in films: limitation of the accuracy of optical monitoring of thin films**. - Applied Optics, 20, 90-94, (1981) - F. FLORY, B. SCHMITT, E. PELLETIER, H.A. MACLEOD, **Interpretation of wide band**

scans of growing optical thin films in terms of layer microstructure. - S.P.I.E.(The Society of Photo-Optical Instrumentation Engineers) VOL. 401, Thin Film Technologies, 109-116, (1983) - J.P. BORGOGNO, F. FLORY, P. ROCHE, B. SCHMITT, G. ALBRAND, E. PELLETIER, H.A. MACLEOD, **Refractive index and inhomogeneity of thin films.**- Appl. Opt., 23, 3567-3570, (1984) - P. ROCHE, E. PELLETIER, **Characterizations of optical surfaces by measurement of scattering distribution**, App. Opt., 23, 3561-3566, (1984) - B. SCHMITT, J.P. BORGOGNO, G. ALBRAND and E. PELLETIER, **In situ and air index measurements: influence of the deposition parameters on the shift of TiO_2/SiO_2 Fabry-Perot filters.** Applied Optics, 25, 3909-3915, (1986) - M. COMMANDRE, L. BERTRAND, G. ALBRAND, E. PELLETIER, **Measurement of absorption losses of optical thin film components by Photothermal Deflection Spectroscopy**, - The Hague, The Netherlands, 30 mars-3 avril 1987 - SPIE PROCEEDINGS,"Optical Components and Systems", 805, 128-135, (1987) - F. FLORY, HU YOULIN, E. PELLETIER, **Optical anisotropy of thin film materials measured with guided waves techniques**, Conférence présentée à : "1986 Optical Society of America Annual Meeeting" - Seattle, Washington, October 19-24, 1986.

Measurements by guided waves techniques, with their complementary aspect, have an unquestionable interest, at least for studying layers in the surrounding atmosphere.

Compared with the other methods, two essential advantages appear, in addition to its inherently high precision:

- optical anisotropy can be detected without any ambiguity and correlated with the layer evaporation conditions.

- this method can be extended to multilayer stacks. Thus it will be possible to compare the refractive index in different environmental conditions: the single layer, the layer on the top of a stack and the layer sandwiched in a multilayer system.

Through several examples, we will give a rapid evaluation of recent progress in the development of this characterization technique and show its potential interest for future studies.

II - DETERMINATION OF OPTICAL CONSTANTS BY GUIDED WAVES TECHNIQUES

This method is summarized in **figure 1**. For the simple case of a single homogeneous layer, light coupling is made with a prism and we measure the synchronous angles corresponding to the propagation modes. For an incident light with wavelength λ_0, there are, theoretically, two unknown parameters: the index n and thickness d. Two values of synchronous angles are sufficient to determine these parameters when the method of successive approximations is employed (**fig. 2**). If more than 2 modes are present, our results can be verified: any chosen pair of modes must yield the same values for n and d.

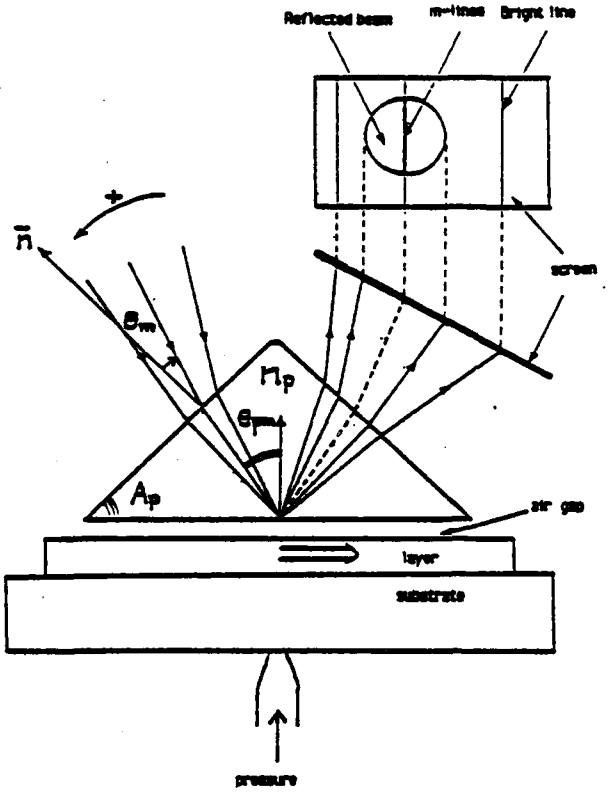

Figure 1

Prism coupling and measurement of effective indices of the guide.

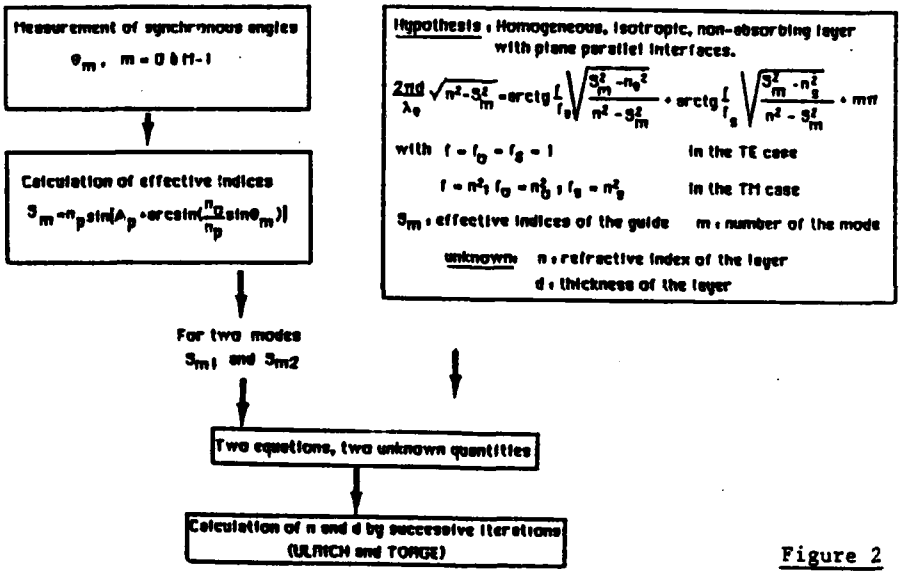

Figure 2

III - STUDY OF AN ANISOTROPIC LAYER

Layers obtained by classical evaporation exhibit a columnar microstructure. It can be admitted that the medium has a biaxial crystal structure (fig. 3) and the problem is to determine the principal indices n_1, n_2, n_3 and thickness d. To solve

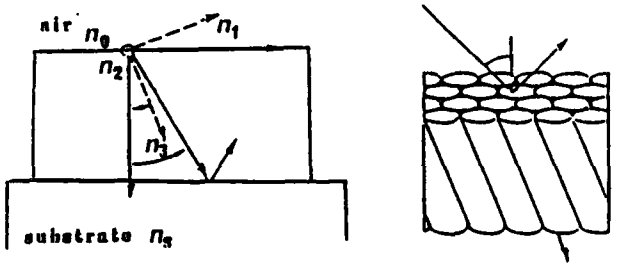

Figure 3

Columnar structure model (after Horowitz and Macleod)

these 4 unknown values, we use the measurement of 2 TE polarized modes and 2 TM polarized modes.

If we compare film samples, from substrates positioned in different places in the evaporating chamber, and then simultaneously coated with a layer of low packing density (material such as TiO_2), we can show that the detected anisotropy is directly correlated with the incident angle of deposited material.

This technique offers a way to compare the uniformity observed in coatings on the calotte in the evaporating chamber, with variation laws concerning thickness, index and anisotropy as a function of the position on the surface. In addition, we can determine the projected direction of the growth columnar axis on the surface of each sample.

IV - STUDY OF MULTILAYER SYSTEMS

The number of unknown parameters increases rapidly with the number of layers in a coating, and quickly becomes unmanageable. In the case of a multilayer stack consisting of alternating layers of two materials, we can assume that indices do not depend on the position of a layer in the stack. This hypothesis can be verified by measuring the different modes of propagation in. The problem is simplified by assuming the optical thicknesses of the different layers are known. These thicknesses can be calculated from spectrophotometric data obtained during monitoring of the stack growth.

We will present some results comparing the refractive index of a top layer with that of a sandwiched layer. In this study, it is difficult to account for anisotropy and much theoretical and experimental progress must be made to further develop this characterization technique.

5

DETERMINATION OF THE EXTINCTION COEFFICIENT OF DIELECTRIC THIN FILMS FROM SPECTROPHOTOMETRIC MEASUREMENTS

J.P. Borgogno, E. Pelletier

Ecole Nationale Supérieure de Physique de Marseille - Laboratoire d'Optique des Surfaces et des Couches Minces - Unité associée au CNRS, U.A.1120 -Domaine Universitaire de St Jérôme - 13397 Marseille Cedex 13 - France

Abstract

Data obtained from reflectance and transmittance measurements are used to determine the extinction coefficient. We show that accuracy is limited by the substrate quality and by interface roughnesses of the layer.

Introduction

The complex refractive index of a thin layer is usually determined from reflectance (R) and transmittance (T) mesurements over a wide spectral range. With layers of low absorption, successive approximations methods are used for a simultaneous determination of refractive index, extinction coefficient and layer thickness [1]. In a recent publication [2], we have shown that we can theoretically calculate $k(\lambda)$ from $1 - R(\lambda) - T(\lambda)$.

Here we deal with experimental results obtained for $k(\lambda)$ in the case of very low absorption losses. These measurements are very useful for calibration of absorption measurements by the photothermal effect (mirage effect) [3].

II - Some results

In the proximity of the absorption band, k varies rapidly versus λ and, for many applications, it is important to determine the decreasing law, together with the residual value of $k(\lambda)$ in the transparent region. A typical example is a TiO_2 layer given in fig. 1. The decreasing law is quite apparent yet partially masked by a periodic modulation. This modulation is often in phase with the variation law $R(\lambda)$. Our goal is to find the origin of this defect in order to get eliminate it. The difficulty lies in the fact that R and T measurements must be very accurate (errors lower than some thousandths) if we want to detect extinction coefficients lower than some 10^{-4}.

III - Analysis of the error origins

Two sources of error must be distinguished: a defect in the calibration of the $R(\lambda)$ and $T(\lambda)$ measurement, or a defect in the computing technique for the determination of $k(\lambda)$.

III-1) Principle of the R(λ) and T(λ) measurements

The method consists in the ratio of two values obtained by two successive measurements: first we measure the flux ϕ_C reflected by the layer, and then the flux ϕ_O reflected by the bare substrate. Knowing the substrate index n_S, we can calculate its reflectance R_S and then, with the ratio ϕ_C/ϕ_O, determine R.

Obviously, if the substrate refractive index is not known with sufficient accuracy, the value of R_S is incorrect, and produces an error in R. Practically, transmittance calibration gives rise to the same difficulties, which must include the perturbing phenomena due to the back surface of the substrate.

In all cases, a good quality substrate is of prime importance; theoretically, the surface must be perfectly polished, without a transition layer. We will try to show the consequences of a scattering surface, or of a substrate perturbed by a transition layer, but we will first examine the reasons why the calculation of k(λ) can fail.

III-2) Method for determining k(λ)

In our models, it has always been supposed that each layer was homogeneous, isotropic and with plane par allel surfaces. In some cases, we have accounted for the variation of the real part of the refractive index in the volume of the layer; for this a model with a constant index gradient is often used [4]. However, with respect to absorption, it is always implied that the extinction coefficient does not vary in the layer, but this hypothesis is obviously unrealistic.

For very low absorption, a serious difficulty arises from the fact that scattering has been neglected. The relation A = 1 - R - T is valid only if scattering, D, can be completely neglected. This is not always the case, and furthermore, D should be divided in two parts: the external scattering D_O which can be measured, and the volume scattering D_i, which corresponds to large angle scattering inside the layer. Thus, light is trapped and even absorbed by volume scattering.

In these conditions, we write the energy balance as: $R + T + A + D_O + D_i = 1$, where the value of A would be used for the k(λ) computation. Some numerical examples can display the relative importance of these different phenomena to explain the k(λ) modulation observed in our experimental results.

IV - Effects of a transition layer in the substrate and of layer interface roughness

Some examples will be given here to illustrate our conclusions.

IV-1) Transition layer

The BK7 substrate, index ns, is presumed to have a thin transition region, index n_T and thickness e = 50 nm. This prevents the correct calibration of R_S and perturbs the measurement of R and T. As a consequence, we have a change in the value of k. The results of a computer simulation are presented here: ideally, we should have k = O; instead we obtain the graph given in fig. 2; a modulation of k between 1.10^{-3} and a few 10^{-4} is seen. The extremums of k are practically in phase with those of R(λ).

IV-2) Consequences of scattering

In our laboratory, we can theoretically calculate the distribution law for the scattered light.

For this precise application, we have used [5] the laws of variation of D_0 as a function of wavelength by separately considering D_0^R and D_0^T, which respectively represent scattering integrated in the half-space near the front surface and the half-space near the back surface. In a first apporoximation, we let the measured values of reflectance R and of transmittance T be $(R - D_0R)$ and $(T - D_0T)$ for the determination of k.

A numerical example serves to display expected result.

On a BK7 substrate, the layer has an index given by $n = A + B/\lambda^2 + C/\lambda^4$

with $A = 2.2382$

$B = 2.845\ 10^4\ nm^2$

$C = 5.378\ 10^9\ nm^4$

The roughness of the interfaces [5] is given by a r.m.s. of 3 nm and a correlation length of 2000 nm. The interfaces are assumed to be perfectly correlated. We successively calculate R, T, D_0R and D_0T for a series of different wavelengths. Then, by successive iterations, we can determine $n(\lambda)$, e and $k(\lambda)$ (given in fig. 3)

We can thus conclude that both scattering and a transition layer in the substrate play a role in the anomalous modulation of $k(\lambda)$ that has been experimentally observed.

References

1 J.P. BORGOGNO, B. LAZARIDES, E. PELLETIER, Automatic determination of the optical constants of inhomogeneous thin films. - Applied Optics, 21, 4020-4029, (1982)

2 J.P. BORGOGNO, B. LAZARIDES, P. ROCHE, An improved method for the determination of the extinction coefficient of thin film materials. - Thin Solid Films, 102, 209-220, (1983)

3 M. COMMANDRE, L. BERTRAND, G. ALBRAND, E. PELLETIER, Measurement of absorption losses of optical thin film components by Photothermal Deflection Spectroscopy - Conf. présentée à: "4th Int. Symp. on OPTICAL and OPTOELECTRONIC APPLIED SCIENCE and ENGINEERING" - The Hague, The Netherlands, 30 mars-3 avril 1987 - SPIE PROCEEDINGS, "Optical Components and Systems", 805, 128-135, (1987)

4 - J.P. BORGOGNO, P. ROCHE and G. ALBRAND, Un modèle de couche inhomogène valable dans un large domaine spectral et pour une incidence quelconque, Thin Solid Films, 146, 145-154, (1987)

- see [1] above

5 C. AMRA, C. GREZES-BESSET, Laboratoire d'Optique, Marseille, Private communication.

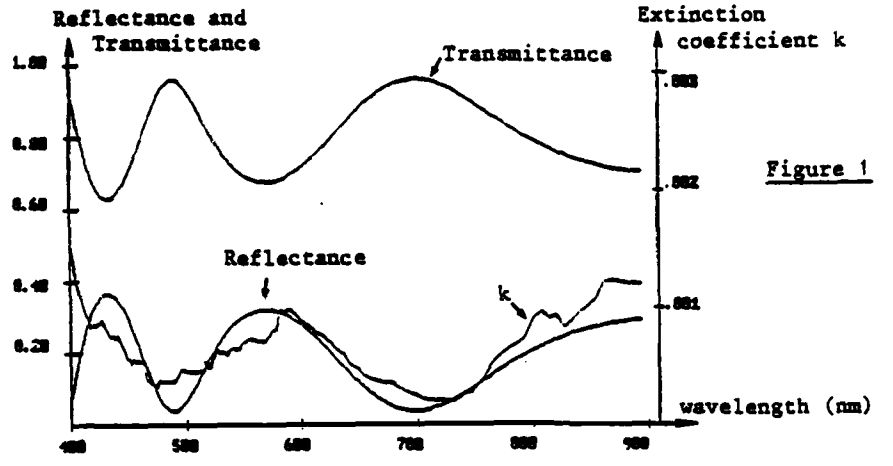

Figure 1

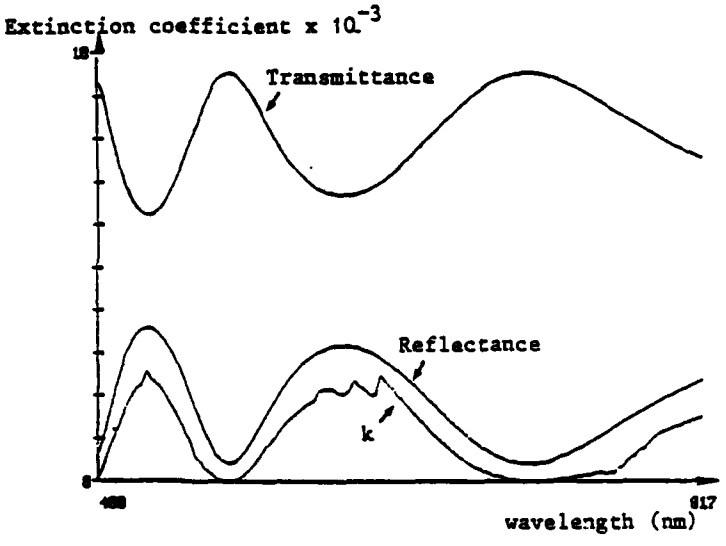

Figure 2

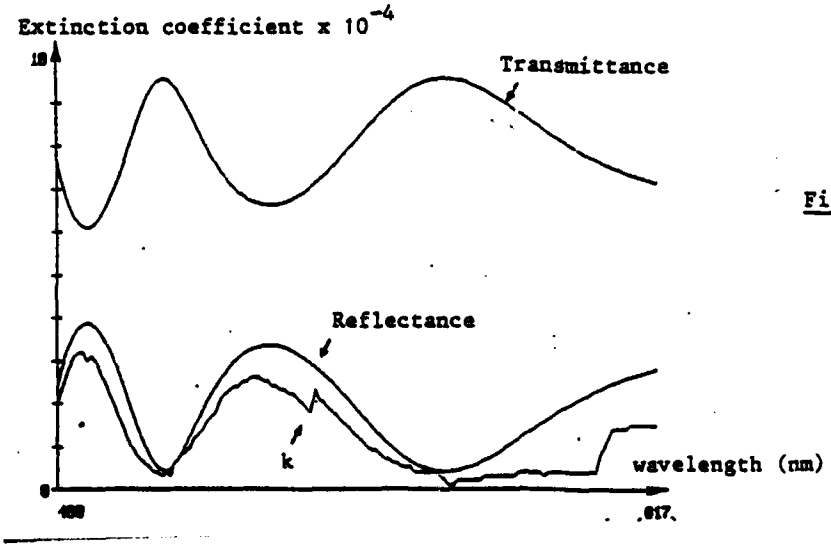

Figure 3

SURFACE OPTICAL COATINGS BY Ion Assisted Deposition TECHNIQUES: STUDY OF UNIFORMITY

F. Flory, E. Pelletier, G. Albrand

Ecole Nationale Supérieure de Physique de Marseille - Laboratoire d'Optique des Surfaces et des Couches Minces - Unité associée au CNRS, U.A.1120 -Domaine Universitaire de St Jérôme - 13397 Marseille Cedex 13 - France

Abstract

Uniformity of layers produced by I. A. D. strongly depends on the characteristics of the ion beam: optical characterization is made by guided wave measurements.

Introduction

For industrial applications, it is important to obtain uniform coatings on large surfaces. To have this results, not only must the thickness of the deposited layer be uniform over the surface, but the refractive index must also be constant. This last condition obviously concerns both imaginary (extinction coefficient) and real parts of the index for materials in the layers and also other parameters related to the film microstructure at different points of the surface.

Spectrophotometric measurements allow us to carry out these studies, but the characterization by the guided wave technique is very useful for a more detailed analysis.

Ion Assisted Deposition

As in many other laboratories, we have developed the technique of Ion Assisted Deposition, mainly for application in the visible spectral range, with material such as oxides: TiO_2, Ta_2O_5, SiO_2 ... [1] , [2].

The primary advantage of this technology is to give layers with a very dense microstructure. As a consequence, layers are practically insensitive to the humidity in the surrounding atmosphere. The problem is to define the conditions of layer realization. Our techniques of spectrophotometric measurements during deposition and in the surrounding air show that the optical properties can be identical for these two cases. The refractive index and optical thickness are therefore stable, in contrast to those layers produced by classical evaporation.

In many applications, it is necessary to minimize losses due to absorption and scattering; this leads to a detailed study of evaporation conditions together with the various ion gun parameters used: current density, ions energy, gas mixture (Ar and O_2).

Layer deposition uniformity

Is it possible to obtain the same uniformity as that obtained with classical evaporation? We attempt to answer this question by studying the conditions of ion bombardment to have the best result. Classical spectrophotometric measurements allow this study to be carried out.We show that characterization by guided waves is a powerful means for extending this analysis.

The study is made on a plane disc 20 cm in diameter: we try to avoid uniformity defects of about one thousandth.

From reflectance and transmittance measurements in air of different points of the disc, we can determine the uniformity of the optical thickness of the coating. It is possible to go further by computing [3], for each point of measurement, refractive index $n(\lambda)$, extinction coefficient $k(\lambda)$ and thickness e.

For each coating, the law of uniformity can be represented as a radial distribution where separately intervene n as a function of the distance r to the center of the disc and e as a function of r. For some materials, experiments show that the variation law k(r) cannot be neglected. In this way, we can show to what extent the ion gun parameters influence the uniformity. With these photometric techniques, the precision on the measurement of optical thickness ne is about one thousandth, but precision on n is barely sufficient to deduce the law of uniformity n(r). Obviously we can also investigate the uniformity of optical properties for multilayer stacks, but photometric measurements do not allow direct access to the laws n(r) and e(r) for each material. Layer characterization by guided waves allows us to go further in this analysis.

Characterization by guided waves technique

For determining refractive index and thickness of a single layer, it is sufficient to measure two synchronous angles corresponding to two guided modes. The precision for determination of n and e is about 1 to 2‰.

By measuring 2 TE modes and 2 TM modes, we have access to the optical constants n_1, n_2, n_3 of an assumed biaxial medium. It is interesting to show that layers produced by IAD exhibit almost negligible anisotropy. We then give results concerning the uniformity of n(r), e(r) and the anisotropy.

By measuring synchronous angles, we can also study multilayer systems: employing some assumptions to limit the number of parameters, we can determine the index pairs (n_H, n_L) of alternating materials in a multilayer system, the thicknesses of which are known. It is possible to verify the results by comparing them with those given by spectrophotometric methods.

For example, we have determined the values n_H and n_L for a Fabry-perot filter, starting from synchronous angles measured for wavelength λ = 0.63 nm (He-Ne laser). Knowing the dispersion laws $\partial n/\partial\lambda$ for each material, it is possible to predict the optical properties of this stack for a large spectral range. These predicted values are compared with values measured for manufactured filters: the two profiles are identical (fig.1).

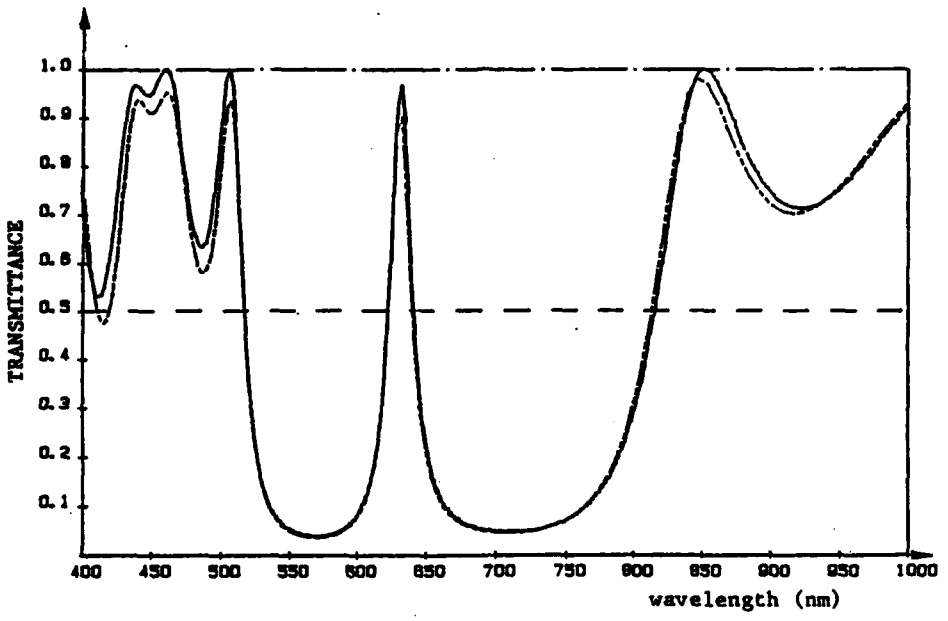

Figure 1 - *Verification of the validity of index measurements: Multilayer stack of design: glass HL HL 4H LH LH, with H: λ/4 layer of TiO_2 and L: λ/4 layer of SiO_2.*

----- *Measured profile*

——— *Profile calculated from index measurements made with guided wave technique at wavelength λ = 623 nm. The dispersion law ∂n/∂λ is assumed to be known, and layers are strictly λ/4.*

This concordance confirms the quality of this characterization method. We can thus study the uniformity of multilayer systems with a good precision.

References

1 F. FLORY, G. ALBRAND, C. MONTELYMARD, E. PELLETIER, Optical study of the growth of Ta2O5 and SiO2 layers obtained by Ion Assisted Deposition - SPIE Proceedings, Thin Film Technologies II, 652, 248-253, (1986)

2 P.J. MARTIN, H.A. MACLEOD, R.P. NETTERFIELD, C.G. PACEY, W.G. SAINTY, Ion beam deposition of thin films., Appl. Optics, 22, 178, (1982)

3 J.P. BORGOGNO, B. LAZARIDES, E. PELLETIER, Automatic determination of the optical constants of inhomogeneous thin films. - Applied Optics, 21, 4020-4029, (1982)

12

DESCRIPTION OF A SCATTERING APPARATUS APPLICATION TO THE PROBLEMS OF CHARACTERIZATION OF OPAQUE SURFACES

C. Amra, C. Grèzes-Besset, P. Roche, E. Pelletier

École Nationale Supérieure de Physique de Marseille - Laboratoire d'Optique des Surfaces et des Couches Minces - Unité associée au CNRS, U.A.1120 -Domaine Universitaire de St Jérôme - 13397 Marseille Cedex 13 - France

Abstract

We show how the complexity of a micropolished optical surface can be investigated in detail by measurement of the distribution of scattered light.

Minimization of scattering in optical multilayers, such as Fabry-Perot filters and laser mirrors, is an important problem because of the stringent demands of many optical applications. Recent results have shown that reduction of scattering requires the use of super smooth substrates. Therefore, efforts to improve the polishing techniques are currently under way. Polishing skills have now advanced to the point where, for certain materials, surface roughness does not exceed some 0.2 nm.

Characterization tools have improved in parallel with this increase in the quality of optical surfaces. Among the different methods that give access to the roughness of an optical micropolished surface, the measurement of light scattered by the sample in each direction of space is particularly well adapted to the characterization of opaque surfaces,because this technique yields additional information on the anisotropy of the surface roughness.

We developed in Marseilles a scatterometer capable of measuring the distribution of scattered light in all directions, and a vector theory of light scattering to interpret the experimental results. The combined tools of theory and experiment provide the roughness spectrum and autocorrelation function (roughness and

autocorrelation length) of substrate defects, as well as the uniformity and anisotropy of the roughness. The detection level of the apparatus must be very low since we know that the Total Integrated Scattering (TIS) from a super-smooth surface is less than some 10^{-6} of the incident flux. A rapid description of the apparatus will be given.

With this experimental set up we have been able to undertake a systematic study of the quality of black samples produced by different optical shops. In particular we have studied the polish homogeneity within several series of samples (fig.1); we have also studied the problems of cleaning and "sample degradation" .

Since scattering levels and residual roughness seen in multilayer stacks are often due to the reproduction of substrate defects, it is essential to specify which defect periods our optical method is sensitive to. A detailed study of the apparatus function emphasizes the limits of validity of the method. We are also interested in the problem of approximating a roughness spectrum with analytic functions .

Fig. 1 -

Calculated and measured mean plane sections of angular scattering curves for four black glasses (a, b, c and d). Experimental and theoretical curves are in good agreement. For these samples, we find rms roughnesses of 0.6 nm (a), 1.4 nm (b), 3.1 nm (c) and 3,6 nm (d). BRDF cos θ is the scattered flux per unit of solid angle and surface, normalized to the incident flux. The angular range (0 → 90°) corresponds to scattering by reflection. Curves A, B and D are anisotropy curves of samples a, b and d. These curves are a representation in polar coordinates of angles θ and α that lead to the same level of scattering.

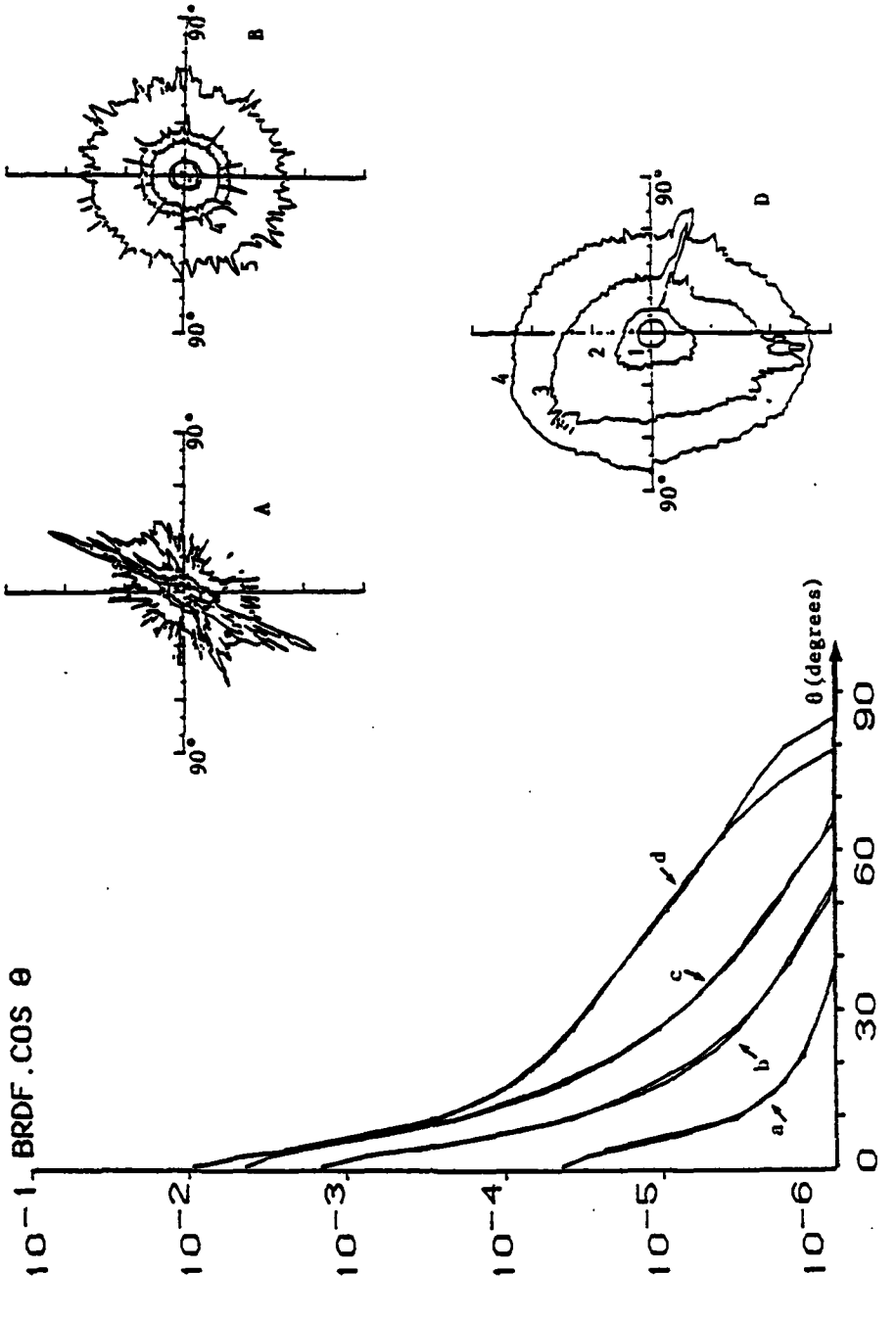
A
B
D
90°
1
2
3
4
5
BRDF . COS θ
10⁻¹
10⁻²
10⁻³
10⁻⁴
10⁻⁵
10⁻⁶
0
30
60
90
θ (degrees)
a
b
c
d

Figure 1

LAYER UNIFORMITY OBTAINED BY VACUUM EVAPORATION. APPLICATION TO FABRY-PEROT FILTERS

C. Grèzes-Besset, R. Richier, E. Pelletier

Ecole Nationale Supérieure de Physique de Marseille - Laboratoire d'Optique des Surfaces et des Couches Minces - Unité associée au CNRS, U.A.1120 -Domaine Universitaire de St Jérôme - 13397 Marseille Cedex 13 - France

Abstract

We show how we can measure with accuracy the uniformity of layer thickness for different materials obtained by vacuum deposition. Generalization to multilayer stacks raises many difficulties due to time dependence of evaporant distribution.

Introduction

Optical telecommunication between satellites are of growing interest today. Through a collaboration with the Centre National d'Etudes Spatiales, the Optical Laboratory of Marseilles is interested in wavelength multiplexing and demultiplexing systems between several telecommunication tracks. In order to separate and isolate each track, it is necessary to use multiple half wave Fabry-Perot filters because of their high rejection : the pass-band may be less than 10 nm, and the cross-talk levels are easily about 10^{-4}. Fabrication of these filters does not pose any serious problems. On the other hand, the simultaneous treatment of several filters raises many difficulties that we try to clear up in this presentation.

II - Realization techniques of multiple half-wave Fabry-Perot filters

With materials such as zinc sulfide and cryolite, the realization of quarter wave layer stacks does not raise particular problems other than thickness monitoring during deposition. In our Laboratory, monitoring techniques have been developed which meet the design requirements [1]. We record the evolution of the filter optical properties during deposition and the variation of the two signals $(\partial T/\partial t)_{\lambda_0}$ and $(\partial T/\partial \lambda)_{\lambda_0}$ (derivatives of transmittance versus time and versus wavelength, at the peak wavelength λ_0). It is easy to locate the transmittance extrema which correspond to

a zero of the derivative $(\partial T/\partial t)\lambda_0$. The great advantage of this technique is that it allows self-correction of thickness errors during deposition [2]. For the substrate which is used for direct optical monitoring, one can consider that the problem of manufacturing multiple half wave Fabry Perot filters is well solved.

III - Layer uniformity

In order to simultaneously manufacture many filters with identical optical properties, the film thickness distribution for each material must be very uniform.

The magnitude of errors which can be tolerated in multiple cavity Fabry-Perot filters is very low, and the layers deposited on different substrates must all have a quarterwave optical thickness at the right wavelength λ_0.

Uniformity is generally studied through the measurement of the optical properties of single layers simultaneously deposited on several glass substrates. This yields information on refractive index, extinction coefficients and layer thicknesses. With materials such as zinc sulfide and cryolite, the refractive index does not greatly depend on the position of the sample in the chamber and so the optical thickness is sufficient for determining the distribution of layer thickness. However, the transmittance and reflectance modulations versus wavelength are often small for a single layer. Thus this method cannot have a precision better than 10^{-2} for thickness measurement.

In order to improve sensitivity in the measurement of uniformity, we studied all dielectric Fabry-Perot filters. It is well known that the location of the transmittance peak strongly depends on layer thickness.

For a perfect quarterwave multilayer (no error during deposition), measurement of the peak wavelength directly leads to the layer thickness: one can write that the thickness distribution is given by $U(s) = \lambda_S/\lambda_0$, where λ_0 and λ_S are the peak wavelengths at the monitor position 0 and the substrate S respectively. Owing to an accurate positionning of the samples (within 1/10 mm), quasi identical filters can therefore be manufactured.

IV - Application to high rejection filters

In spite of all these adjustments, experimental results show that with multiple cavity filters there are some complications. From one layer to another of the same material, reproducibility of the distribution law is not systematically perfect. The tolerances on individual layer thicknesses are so small that we must account for the time dependence of the distribution during deposition.

Self-correction occurs for the monitor plate, but for the other substrates the smallest shift in distribution prevents production of successful filters and the shape of the bandpass filters is not correct. In this case, it is not possible to extract valuable information on uniformity from the measurement of the peak wavelength of the filters. We show how we can experimentally solve this problem and we present numerous results.

References

1 A. FORNIER, R. RICHIER, E. PELLETIER, B. BOVARD, G. SALVINI

Contrôle optique du dépôt de couches multidiélectriques quart d'onde: techniques hybrides de traitement du signal utilisées pour améliorer les performances. "Annales ds Télécommunications", 42, 140-148, (1987)

2 - P. BOUSQUET, A. FORNIER, R. KOWALCZYK, E. PELLETIER, P. ROCHE

Optical filters: Monitoring process allowing the auto-correction of thickness errors. - Thin Solid Films, 13, 285-290, (1972)

- E. PELLETIER, R. KOWALCZYK, A. FORNIER

Influence du procédé de contrôle sur les toiérances de réalisation des filtres interférentiels à bande étroite. - Optica Acta, 20, 509-526, (1973)

- H.A. MACLEOD

Turning value monitoring of narrow-band all-dielectric thin-film optical filters, Optica Acta, 19, 1-28, (1972)

18

SCATTERING STUDY OF SINGLE LAYER TITANIA FILMS

C. Hickey, C. Amra, E. Pelletier

Ecole Nationale Supérieure de Physique de Marseille - Laboratoire d'Optique des Surfaces et des Couches Minces - Unité associée au CNRS, U.A.1120 -Domaine Universitaire de St Jérôme - 13397 Marseille Cedex 13 - France

Abstract

Light scattering measurements further characterize a series of TiO_2 thin film samples. Previous analyses were given at the 1986 and 1987 O.S.A. annual meetings.

Introduction

This paper continues the characterization analysis performed for the Optical Materials and Thin Films topical meetings at the 1986 and 1987 Optical Society of America conferences. Single layer films of titania oxide were analyzed for their optical and surface roughness properties. Optical properties included measurement of the refractive index, its inhomogeneity, and the extinction coefficient. Over twenty four films, prepared by 18 different laboratories and using nearly a dozen different deposition processes, were measured for these presentations. The aim of this work is to study the scattering properties of the TiO_2 samples and to look for correlations between our experimental results and the information already acquired.

Surface scattering measurements

The scatterometer employed in this analysis illuminates the sample, at quasi-normal incidence, with a 1 mW HeNe laser (λ=0.6328 mm). It measures the spatial distribution (at 25,000 different points in space) of the light scattered in all directions by the sample. A convenient means to examine the data is to consider the average angular scattering curve , BRDFcosθ(θ) (fig. 1). Averaging is made over 250 separate measurement planes, all containing the surface normal. The function BRDFcosθ(θ) represents the flux scattered per unit area into a unit solid angle and normalized against the incident light flux. Two angular regions are considered, one (0°-90°) corresponding to scattering by reflection, and another (90°-180°) corresponding to scattering by transmission. In addition, the global integrated scattering for the two half-spaces (D_R for light scattered in reflection and D_T for light scattered in transmission) and the Total Integrated Scattering ($TIS=D_R+D_T$) are measured for each sample.

We are also interested in the anisotropy of the surface roughness. Therefore, curves such as that shown in fig. 2 are drawn for the samples. Each curve represents a given scattering level plotted against polar coordinates (θ,α), where θ and α

characterize the scattering directions. We can see in figure 2 two scattering level curves (a = 2.10^{-5} and b= 8.10^{-6}); for each curve, θ is the radius and α the polar angle. The departure of successive curves from concentric circles indicates the degree to which surface defects are anisotropic.

A survey of data for the samples will be given in the form of scattering histograms so that the dependence of scattering properties for different film characteristics can possibly be seen. The range of scattering values is greater than 100 over all the samples. Selected anisotropy and BRDFcosθ(θ) curves will also be presented.

Discussion

Preceeding work has shown that the refractive index of thin films is lower when films are prepared by classical evaporation techniques. This is not surprising in view of a more compact microstructure seen in films prepared by other techniques (for example, by Ion Assisted Deposition: P.J. Martin, H.A. Macleod, R.P. Netterfield, G.C. Pacey, W.G. Sainty, Appl. Op. 22, 178 (1983); C.M. Kennemore III and U.J. Gibson, Appl. Op. 23, 3608 (1984); and F. Flory, G. Albrand, C. Montelymard, and E. Pelletier, SPIE Proc., Thin Film Tech. 652, 248 (1986)). This analysis investigates the possibility that scattered light measurements can also give information on thin film microstructure and thereby permit characterization of different preparation techniques. It is not obvious a priori that such is the case for two reasons:

1) Since all the TiO_2 samples were deposited on transparent substrates, the analysis must account for the influence of the substrate surfaces. In past work we have seen that, for extremely careful deposition conditions, a thin film does not substantially modify the scattering characteristics of the uncoated substrate. The scattering characteristics of the film are therefore overwhelmed by those of the substrate and it is impossible to separate out information concerning the film microstructure. One way to solve this problem consists of aluminizing each side of the sample and measuring separately the surface roughness of the front film surface and back substrate surface.

2) Substrate cleanliness and film inclusions (such as dust or chunks of material) may also have a critical effect on the scattering distribution. In order to separate out this influence, we attempt to correlate the global scattering factors with the number of dust or impurity spots observed in a phase contrast microscope.

Even if a systematic study of light scattered by the TiO_2 samples does not lead to a precise characterization of the microstructure, it is nonetheless interesting to compare our scattering measurements with the roughness measurements obtained by Jean Bennett (O.S.A. 1987 Annual Meeting Technical Digest) or a Talystep. The two methods ought to be sensitive to approximately the same range of measureable defect periods.

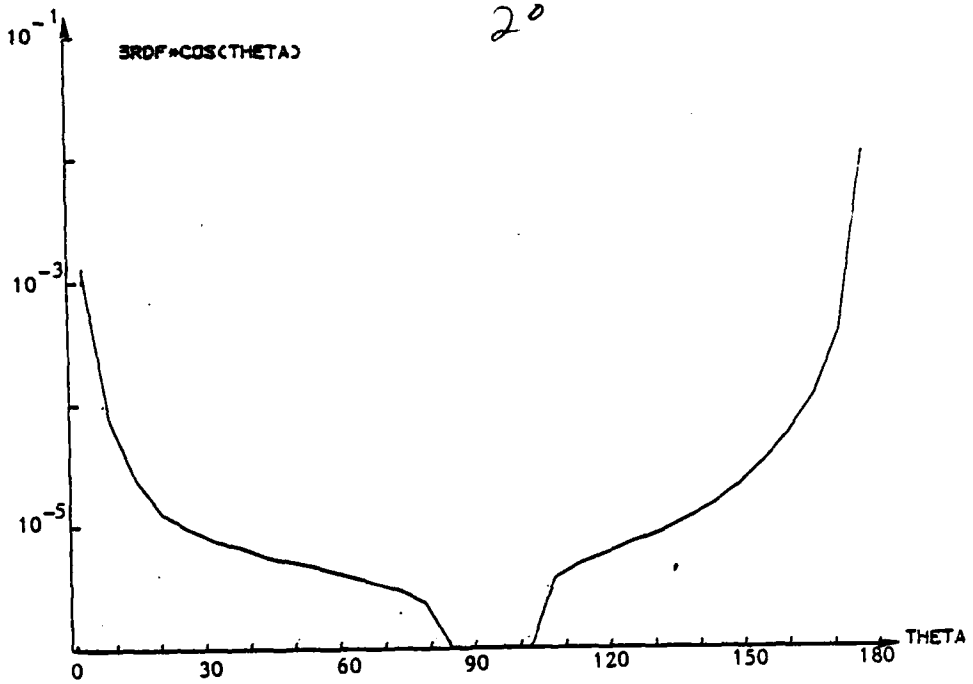

Figure 1

Mean angular scattering curve for a single layer of TiO_2 on a transparent substrate (OSA sample n° 135)

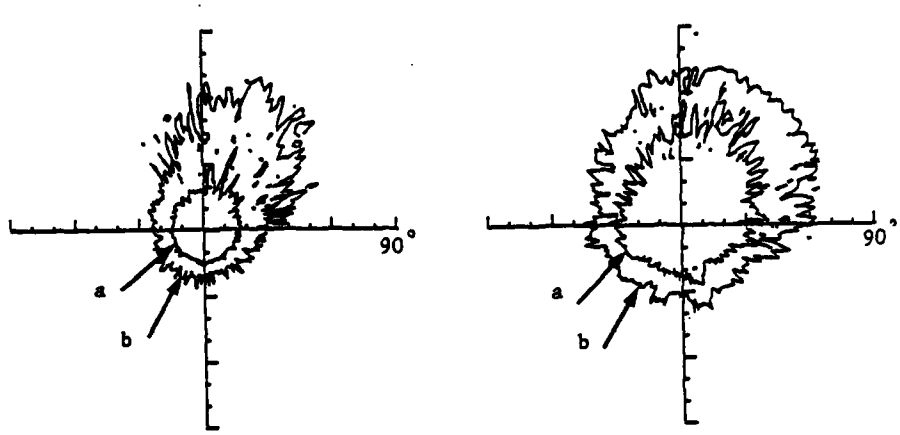

Figure 2

Anisotropy curves for a single layer of TiO_2 on a transparent substrate (OSA number n° 135).
The curve to the left represents scattering by reflection while the curve to the right represents scattering by transmission.

APPENDIX II

Recent publications

Reprinted from Applied Optics, Vol. 26, page 3733, September 1, 1987

Ion-assisted deposition of lanthanum fluoride thin films

James D. Targove, John P. Lehan, Linda J. Lingg, H. Angus Macleod, J. A. Leavitt, and L. C. McIntyre, Jr.

Ion-assisted deposition has been used to deposit lanthanum fluoride thin films with near-unity film packing densities and no significant increase in absorption. Rutherford backscattering analysis has determined the effect of ion bombardment on the film stoichiometries including the degree of fluorine deficiency. Oxygen atoms or compounds appear to occupy most of the available anion vacancies if sufficient oxygen is available in the ion beam or the residual atmosphere.

I. Introduction

Thin films deposited by thermal evaporation are known to possess a columnar microstructure that strongly influences many of their properties.[1] This microstructure is characterized by packing densities of less than one, refractive indices of less than the bulk value, and degraded moisture resistance. More energetic deposition processes can reduce this columnar microstructure and increase packing density.[2] Ion-assisted deposition (IAD), the bombardment of a growing thermally evaporated film with an energetic ion beam, is one such technique. The applicability of IAD to a wide range of materials has already been demonstrated.[3] The majority of this work, however, has been directed toward metal–oxide materials. Fluorides, with the exception of MgF_2,[4,5] have only briefly been addressed.[6]

Rare-earth fluoride thin films are of great interest because of their excellent transmission from the UV (even the vacuum UV[7]) to the IR.[8] LaF_3 is the most popular material in this family; it is transparent from ~130 nm to 10 μm and has a very high laser damage threshold.[9] However, it suffers like most fluorides, from large tensile stress[9] and has a packing density of only 0.80 when deposited onto ambient-temperature substrates.[10] We have, therefore, investigated ion-assisted deposition as a means of improving lanthanum fluoride coatings.

All authors are with University of Arizona, Tucson, Arizona 85721; J. A. Leavitt and L. C. McIntyre, Jr., are in the Physics Department, the other authors are in the Optical Sciences Center.
Received 17 April 1987.
0003-6935/87/173733-05$02.00/0.

II. Deposition Conditions

The films were deposited in a Balzers BAK 760 box coater using the geometry shown in Fig. 1. Glass, fused silica, germanium, and graphite substrates were used for compatibility with various forms of analysis. We precleaned the substrates before deposition and bombarded them during deposition with oxygen or argon ions from a 3-cm aperture Kaufman hot-cathode ion source equipped with tungsten filaments and graphite grids. The source-to-substrate separation was 40 cm, with the substrates held stationary during the deposition. A filament neutralizer emitted electrons to neutralize the beam, preventing charge build-up on the dielectric substrates. A Faraday cup measured the ion current density at the substrate. All coating runs were performed at room temperature with a residual pressure of 1.5–3 × 10^{-6} Torr and at a deposition rate of 0.6 nm/s. The LaF_3 films were evaporated from resistively heated molybdenum boats, while the MgF_2 layers of multilayer coatings (see Sec. III. E) were evaporated using an electron-beam source.

III. Characterization

A. Refractive Index and Packing Density

We will follow Ogura[10] in using an increase in refractive index to quantify an increase in packing density. We calculated the refractive index and extinction coefficient (see Sec. III. B) of single-layer coatings using the envelope method of Manifacier *et al.*[11] This method assumes a homogeneous thin film and, therefore, only requires a measurement of transmittance. These data are then fit by least squares to a dispersion relation of the form

$$n^2 = A + \frac{B}{\lambda^2}, \tag{1}$$

which is a first-order approximation to the Sellmeier

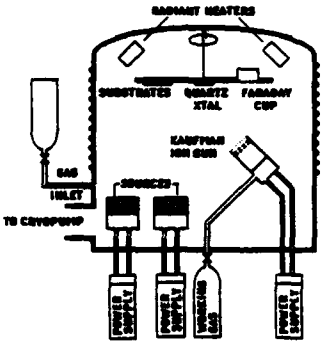

Fig. 1. Schematic of Balzers BAK 760 coating plant configured for ion-assisted deposition.

dispersion relation away from resonance.[12] The index of refraction is then converted into packing density using a linear formula for refractive index as a function of packing density, which assumes that the film is a mixture of columns and voids[13]

$$n_f = pn_s + (1 - p)n_v , \qquad (2)$$

where n_f = the measured refractive index of the film,
n_s = the refractive index of the material in the film columns,
n_v = the refractive index of the film voids, and
p = the packing density of the film.

We assume that the columns have the bulk index of the material and that the voids are filled with water. This assumption and choice of the linear model both result in a lower bound for the packing density, which obviously improves as the packing density approaches unity.

The variation in refractive index at a wavelength of 350 nm with ion beam current density is shown in Fig. 2 for the bombardment of films with a physical thickness of 500 nm by 300- and 500-eV argon and 300-eV oxygen ions. The bulk index is taken to be 1.624 at 350 nm, an average of the ordinary and extraordinary bulk refractive indices.[14] These curves show that the refractive index, and thus the packing density, is substantially increased by argon bombardment at both 300 and 500 eV. The indices of the oxygen-bombarded films cannot be related to packing density in a similar manner: n_s probably lies between the refractive indices of LaF_3 and La_2O_3 because of the implanted oxygen in the coatings.

The packing densities of the argon-bombarded films are then calculated by substituting the data from Fig. 2 into Eq. (2), with the refractive index of the water in the voids taken to be 1.35 at 350 nm.[15] Packing densities have been calculated from the refractive-index data assuming a bulk index for n_s (Fig. 3). However, Ogura[10] has pointed out that n_s is not necessarily the bulk index and instead used 1.59 at 500 nm for LaF_3 in place of the bulk index. We have thus also calculated packing densities using the refractive index data at 500 nm. These results are compared in Fig. 3 for n_s equal

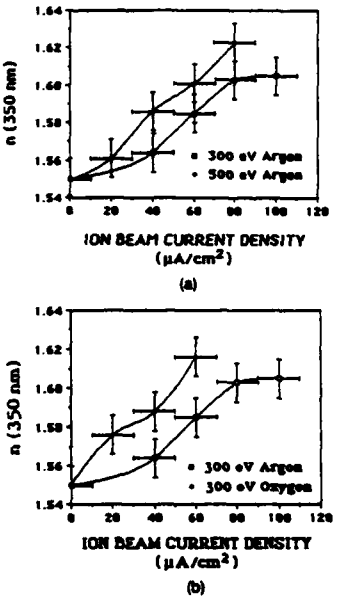

Fig. 2. Index of refraction at 350 nm of LaF_3 films bombarded with (a) 300- and 500-eV argon ions and (b) 300-eV argon and oxygen atoms as a function of ion beam current density.

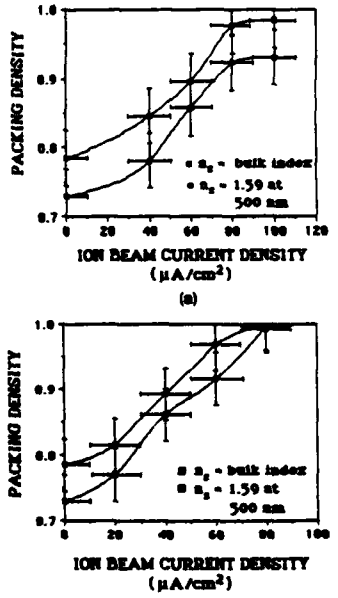

Fig. 3. Packing density of IAD LaF_3 films as a function of ion beam current density for bombardment by (a) 300- and (b) 500-eV argon ions. The vertical error bars represent only the uncertainty in the refractive indices of the films.

to the bulk value and to 1.59. The packing densities obtained using $n_s = 1.59$ agree closely with Ogura's value of 0.80 for conventional coatings deposited onto ambient-temperature substrates and exceed those obtained with a bulk column index by 0.04–0.06. Unity packing density has been achieved by bombardment at 500 eV with a current of 80 $\mu A/cm^2$ and a packing density >90% resulted from 300-eV 100-$\mu A/cm^2$ bombardment.

B. Extinction Coefficient

The extinction coefficients of the single-layer films are also calculated with an envelope method.[11] The argon-bombarded films all have extinction coefficients at $\lambda = 250$ nm below the accuracy of the calculation ($\sim 3 \times 10^{-4}$) with the exception of the 500-eV 80-$\mu A/cm^2$ bombardment (Fig. 4). With oxygen bombardment, however, the films begin to show a short-wavelength absorption edge characteristic of lanthanum oxide (Fig. 4).[16] This absorption edge shifts toward longer wavelengths as the ion beam current density increases because of increasing oxygen implantation (see Sec. III. C).

C. Rutherford Backscattering Analysis (RBS)

Rutherford backscattering (RBS) has proved to be an excellent tool for studying compositional changes within thin films caused by IAD.[17] High-energy (1.892 MeV in this work) singly ionized helium ions from a Van de Graaff accelerator are scattered by a thin sample in vacuum.[18] The measured number of scattered helium ions per unit solid angle per incident helium ion, combined with known scattering cross sections, provides the absolute number of each atomic species in the film in units of atoms per unit area. Film stoichiometries can thus be measured very accurately. Graphite substrates are used in this work because the silicon and oxygen peaks from glass substrates overwhelm the fluorine and oxygen peaks from the film, decreasing measurement accuracy and complicating the analysis.

Rutherford backscattering, a nuclear scattering process, does not address the nature of the chemical bonding in the films. In particular, the oxygen content of the films cannot be divided between oxygen atoms and water or OH^- complexes.

Samples bombarded with 300-eV argon and oxygen ions at varying ion beam current densities as well as unbombarded samples have been measured. These samples are ~100 nm thick; for thicker films, the backscattered peaks attributable to oxygen and fluorine atoms overlap. Writing the film stoichiometries as LaF_xO_y, a perfectly stoichiometric film would have $x = 3$ and $y = 0$. Our unbombarded films have $x = 2.91$–3.00 and $y = 0.11$–0.15.

We previously noted that unbombarded MgF_2 films sometimes are slightly fluorine deficient.[17] Figure 5 shows that all the bombarded films suffer a preferential sputtering of fluorine over lanthanum, as expected from simple sputtering theory.[19] The argon-bombarded films contain a fairly constant amount of oxygen, probably a result of residual water vapor in the chamber. When oxygen ions are used, ion implantation sharply increases the oxygen content of the films. This extra oxygen compensates for the larger fluorine deficiency in the oxygen-bombarded films and explains their lack of absorption in the visible.

The anion-to-cation ratio $x + y$ is also plotted in Fig. 5. The unbombarded films have a ratio greater than three, suggesting that more water molecules are adsorbed from the residual gases in the chamber than are needed to simply fill the fluorine vacancies in the film. With an ion current density of 20 or 40 $\mu A/cm^2$, the

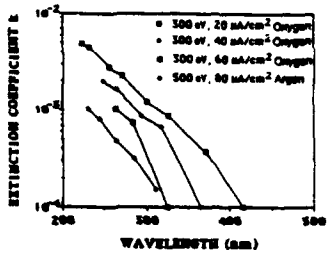

Fig. 4. Ultraviolet extinction coefficient of LaF_3 films bombarded with 300-eV oxygen and argon ions.

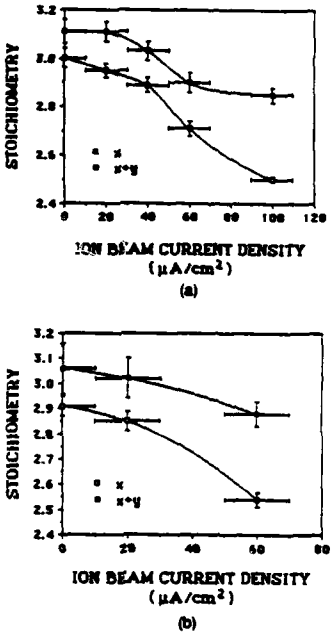

Fig. 5. F-to-La ratio x and anion-to-cation ratio $x + y$ of IAD LaF_3 films bombarded with 300-eV (a) argon and (b) oxygen ions as a function of ion beam current density with the stoichiometry expressed as LaF_xO_y.

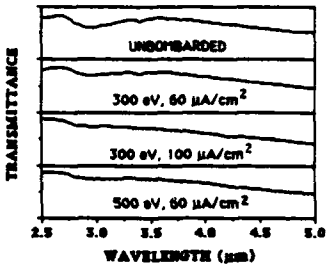

Fig. 6. Transmittance of IAD LaF_3 films in the 3-μm water absorption band for varying argon-ion beam energies and current densities. The transmittance scale is 45–65% for each film.

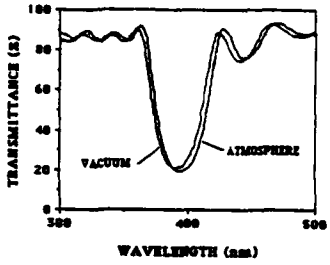

Fig. 7. Air-to-vacuum shift of a twenty-three layer conventionally deposited LaF_3/MgF_2 stack.

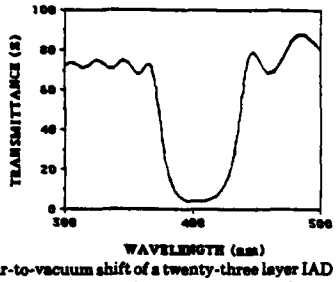

Fig. 8. Air-to-vacuum shift of a twenty-three layer IAD LaF_3/MgF_2 stack deposited with the ion beam parameters of Table I. The shift is < 1 nm.

anion-to-cation ratio remains greater than three. Films deposited with these ion-beam parameters do not show the UV absorption edge typical of anion vacancies.[20] This suggests that most of the anion vacancies caused by the preferential sputtering are filled by oxygen atoms or complexes; but as mentioned above, oxygen-bombarded films do show an oxide absorption edge because of the oxygen implanted into the films. For 60-$\mu A/cm^2$ argon bombardment, however, $x + y$ is ~2.9, and the films begin to show a slight UV absorption attributable to anion vacancies not filled by oxygen or water. This absorption increases with larger current densities as the anion-to-cation ratio in the films decreases further.

The bombarded samples all have a tungsten concentration of < 0.02 at. % caused by erosion and sputtering from the tungsten filaments of the ion gun. In addition, argon-bombarded films contain 0.4–2.0 at. % of argon implanted by the ion bombardment. As shown above, these impurities appear to be much less important than oxygen content to the optical properties of the films.

D. Infrared Water Absorption Band

The amount of water present in a film is a good measure of its packing density. Allen[21] has previously employed the magnitude of the 3-μm water-absorption band as a qualitative measure of the densification caused by ion-assisted deposition. The IR transmittance of films deposited on germanium substrates was measured with a Perkin-Elmer 983 FTIR spectrometer at OCLI. All these films were deposited in the same batches as the fused-silica samples used to calculate the refractive indices of the films and are thus ~450 nm thick.

These measurements show that the water content of the films decreases drastically as the ion-beam current density increases (Fig. 6). There is still a slight absorption band present in the 300-eV 100-$\mu A/cm^2$ and 500-eV 60-$\mu A/cm^2$ samples. From Fig. 3, the packing densities of the identical films on fused silica were >90%.

Table I. Deposition Conditions of IAD LaF_3/MgF_2 Stack

Material	Dep. rate (nm/s)	Ion beam species	Ion beam energy (eV)	Ion beam current density ($\mu A/cm^2$)
MgF_2	0.6	Ar	300	40
LaF_3	0.6	Ar	300	100

E. Multilayer Coatings

Once single-layer coatings had been characterized, two multilayer coatings were deposited to demonstrate the utility of the IAD process. These coatings were $(HL)^{11}$ H stacks with $H = LaF_3$ and $L = MgF_2$ and a design wavelength of 400 nm. The bombardment parameters for the IAD multilayer are given in Table I. The conventionally deposited coating contained cracks from the cumulative tensile stress of both coating materials, while the IAD coating contained no cracks because of the previously observed tensile stress reduction associated with ion-assisted deposition.[22] The air-to-vacuum shift of these coatings was then measured using a specially constructed vacuum cell in a Cary 14 double-beam spectrophotometer. The transmittance spectrum of the conventionally deposited coating shifted 5 nm between atmosphere and 15 mTorr as the adsorbed water was pumped from the coating (Fig. 7), while the transmittance of the IAD coating showed no measurable shift (Fig. 8), suggesting that the IAD process resulted in a near-unity packing density. In addition, both the width of the reflectance band and peak reflectance of the IAD coating are larger than for the conventional coating because the index

contrast between the two materials has increased with bombardment. The index of the LaF_3 layers increase more with bombardment than that of the MgF_2 layers. The IAD coating does, however, have ~2% absorption at peak reflectance.

IV. Conclusion

Ion-assisted deposition has increased the packing density of lanthanum fluoride thin films to near-unity values with little or no increase in film absorption, even with large ion fluxes. Bombardment with oxygen ions results in the expected oxide absorption edge in the near UV.

The films deposited by ion-assisted deposition show a slight fluorine deficiency caused by the preferential sputtering of lighter atoms out of the films. These anion vacancies are filled by oxygen atoms or complexes (such as water or OH^-) and, therefore, do not contribute to absorption at wavelengths longer then 300 nm in our bombardment conditions. Extra fluorine could be added to the films to fill these vacancies by bombarding the films with fluorine (which raises obvious safety concerns) or a fluorine-rich gas such as Freon.[20]

This research was sponsored by the Los Alamos National Laboratory under contract 9-X56-0322C-1 and by OCLI. The authors would like to thank Bertrand Bovard, Ross Potoff, and Rick Swenson for their assistance with this research. We also wish to acknowledge Thomas Allen of OCLI for stimulating discussions and providing FTIR spectrometer measurements. The University of Arizona Ion-Beam Analysis Facility is supported by IBM-Tucson and Motorola; the authors thank P. Stoss, M. D. Ashbaugh, B. Dezfouly-Arjomandy, M. F. Hinedi, J. Oder, J. Serveld, and G. van Zyll for assistance with RBS data acquisition.

References

1. H. A. Macleod, "Microstructure of Optical Thin Films," Proc. Soc. Photo-Opt. Instrum. Eng. 325, 21 (1982).
2. H. A. Macleod, "Overview of Coating Techniques," Proc. Soc. Photo-Opt. Instrum. Eng. 476, 128 (1984).
3. P. J. Martin and R. P Netterfield, "Optical Films Produced by Ion-based Techniques," Prog. Opt. 23, 113 (1986).
4. C. M. Kennemore III and U. J. Gibson, "Ion Beam Processing for Coating MgF_2 onto Ambient Temperature Substrates," Appl. Opt. 23, 3606 (1984).
5. P. J. Martin and R. P. Netterfield, "Ion Assisted Deposition of Magnesium Fluoride Films on Substrates at Ambient Temperature," Appl. Opt. 24, 1732 (1985).
6. W. C. Herrmann, Jr., and J. R. McNeil, "Ion Beam Applications for Optical Coating," Proc. Soc. Photo-Opt. Instrum. Eng. 325, 101 (1982).
7. L. J. Lingg, J. D. Targove, C. C. Weng, and M. R. Jacobson, "Rare Earth Fluorides for Ultraviolet Coatings," J. Opt. Soc. Am. A 3, (13) P20 (1986).
8. H. K. Pulker, "Characterization of Optical Thin Films," Appl. Opt. 18, 1969 (1979).
9. F. Rainer, W. H. Lowdermilk, D. Milam, C. K. Carniglia, T. T. Hart, and T. L. Lichtenstein, "Materials for Optical Coatings in the Ultraviolet," Appl. Opt. 24, 496 (1985).
10. S. Ogura, Ph.D. Thesis, Newcastle upon Tyne Polytechnic (1975).
11. J. C. Manifacier, J. Gesiot, and J. D. Fillard, "A Simple Method for the Determination of the Optical Constants n, k and the Thickness of a Weakly Absorbing Thin Film," J. Phys. E 9, 1002 (1976).
12. D. Smith and P. W. Baumeister, "Refractive Index of some Oxide and Fluoride Coating Materials," Appl. Opt. 18, 111 (1979).
13. K. Kinosita and M. Nishibori, "Porosity of MgF_2 Films—Evaluation Based on Changes in Refractive Index due to Adsorption of Vapors," J. Vac. Sci. Technol. 6, 730 (1969).
14. W. G. Driscoll, Ed., *Handbook of Optics* (McGraw-Hill, New York, 1978).
15. J. L. Lauer and P. H. Miller, Jr., " An Instrument for the Measurement of the Index of Refraction of Liquids in the Wavelength Range 200 mμ to 1000 mμ," J. Opt. Soc. Am. 37, 664 (1947).
16. G. Hass, J. B. Ramsey, and R. Thun, "Optical Properties of Various Evaporated Rare Earth Oxides and Fluorides," J. Opt. Soc. Am. 49, 116 (1959).
17. M. J. Messerly, Ph.D. Dissertation, U. Arizona (1987).
18. W. K. Chu, J. W. Mayer, and M. A. Nicolet, *Backscattering Spectrometry* (Academic, New York, 1978).
19. G. Betz and G. K. Wehner, "Sputtering of Multicomponent Materials" in *Sputtering by Particle Bombardment II*, R. Behrisch, Ed. (Springer-Verlag, Berlin, 1983).
20. U. J. Gibson and C. M. Kennemore III, "Ambient Temperature Deposition of MgF_2 with Noble and Chlorofluorocarbon Ion Assistance," Proc. Soc. Photo-Opt. Instrum. Eng. 678, 130 (1986).
21. T. H. Allen, "Properties of Ion Assisted Deposited Silica and Titania Films," Proc. Soc. Photo-Opt., Instrum. Eng. 325, 93 (1982).
22. S. D. Jacobs, A. L. Hrycin, K. A. Cerqua, C. M. Kennemore III, and U. J. Gibson, "Adhesion Enhancements and Internal Stress in MgF_2 Films Deposited with Ion Beam Assistance," Thin Solid Films 144, 69 (1986).

The grating chirp is caused by the holographic exposure geometry shown in Fig. 4. As a consequence of the grating formation by the interference of two beams radiating from two pointlike spatial filters, the resonant wavelength changes across the grating is given by

$$\Delta\lambda \approx \lambda\left(\frac{2\delta x\cos\theta}{R}+\frac{3x^2}{2R^2}\right), \quad (4)$$

where R, δ, θ, and x are defined in Fig. 4. If the sample is properly aligned so that the tilt angle δ of the exposure plane is zero, the linear chirp vanishes. The remaining quadratic chirp, for the conditions of holographic exposure shown in Fig. 4, is plotted in Fig. 3. The quadratic chirp can be removed by the use of collimating lenses in front of the spatial filters. However, these lenses may introduce wavefront aberrations due to imperfections, misalignments, finite apertures, and dust.

Our Bragg reflector waveguide is sketched in Fig. 1. It is formed from a Si_3N_4 rib waveguide core layer surrounded by SiO_2 cladding layers above a Si substrate. The thickness of the Si_3N_4 layer is ~1200 Å, which results in n_{eff} being about ~0.05 greater than the cladding refractive index. Variations of the core layer thickness change n_{eff}, and the Bragg wavelength shifts ~0.5 Å for each angstrom change in the core layer. The layers are formed by low pressure chemical vapor deposition (LPCVD). The CVD geometry results in a minimum layer thickness at the center of the wafer and an approximately quadratic change in core thickness with increasing distance away from the center. The shift in Bragg wavelength from the center of the wafer with distance is plotted in Fig. 3.

Figure 3 shows the three contributions to bandwidth as a function of the length of L_B for a grating $2L_B$ long. The sum of these contributions is also plotted in Fig. 3 with the assumption that the minimum chirp occurs at the center of the grating. There is a broad minimum value for a bandwidth of 2.8 Å centerd at grating length of 8 mm. The minimum approximately accounts for our minimum observed spectral width. If the minimum chirp occurs at the edge of the grating, the smallest bandwidth increases to 4.2 Å. These simple calculations slightly overestimate the minimum bandwidth because they do not take into account that Bragg reflection takes place over about $1/2L_B$, and, therefore, there will be no Bragg reflection associated with the extreme ends of the grating.

In summary: We have made Bragg reflectors with spectral widths as narrow as ~2.5 Å and with the resonance at 1.52 μm. The minimum spectral width can be understood when the broadening of the spectrum by grating chirp and waveguide nonuniformity is taken into account. The spectral width of a uniform Bragg reflector decreases inversely with length, but layer nonuniformities and grating chirp increase the spectral width in proportion to length squared. This leads to a minimum achievable width, which, for our material nonuniformity and holographic conditions, is ~2.8 Å. This bandwidth is not a fundamental limit. It represents what is avaievable using conventional LPCVD and holographic grating fabrication. Both grating and waveguide chirp could be reduced by modifications of the holographic and LPCVD processing.

References

1. R. P. Kazarinov and C. H. Henry, "The Relation of Line Narrowing and Chirp Reduction Resulting from the Coupling of a Semiconductor Laser to a Passive Resonator," IEEE J. Quantum Electron. QE-23, 1401 (1987).
2. N. A. Olsson, C. H. Henry, R. F. Kazarinov, H. J. Lee, and K. J. Orlowsky, "Extremely Low Chirp Narrow Linewidth External Silicon Chip Bragg Reflector (SCBR) Laser," in *Postdeadline Papers, Optical Fiber Communication Conference–Sixth International Conference on Integrated Optics and Optical Fiber Communication* (Optical Society of America, Washington, DC, 1987), paper 8.
3. C. H. Henry, R. F. Kazarinov, H. J. Lee, K. J. Orlowsky, and L. E. Katz, "Low Loss Si_3N_4–SiO_2 Optical Waveguides on Si," Appl. Opt. 26, 2621 (1987).
4. H. J. Lee, C. H. Henry, R. F. Kazarinov, and K. J. Orlowsky, "Low-Loss Bragg Reflectors on SiO_2–Si_3N_4–SiO_2 Rib Wavguides," Appl. Opt. 26, 2618 (1987).
5. S. L. McCall and P. M. Platzman, "An Optimized π/2 Distributed Feedback Laser," IEEE J. Quantum Electron. QE-21, 1899 (1985).

Effect of oxygen incorporation on the structure of ion-beam-assisted LaF_3 thin films

James D. Targove, Linda J. Lingg, John P. Lehan, and H. Angus Macleod

When this work was performed all the authors were with University of Arizona, Optical Sciences Center, Tucson, Arizona 85721; J. D. Targove is now with Air Force Institute of Technology, Department of Engineering Physics, Wright-Patterson Air Force Base, Ohio 45433.

Received 10 August 1987.
0003-6935/88/020213-03$02.00/0.

Ion-assisted deposition (IAD) has been investigated by a number of groups as a means of improving the properties of thin films of metal fluorides, particular MgF_2.[1-6] A problem with this technique is the incorporation of oxygen from the residual atmosphere of the vacuum chamber into the films. This oxygen has been shown to degrade the moisture resistance of the MgF_2, although it also reduces absorption of films in the visible.[4,5] The method of incorporation of the oxygen into the films has been speculated at by most of these groups, with the formation of an oxide component in the films being most commonly suggested.[4,6] Unfortunately, there has been no way to directly answer this question for MgF_2.

We recently investigated the ion-assisted deposition of LaF_3 thin films.[5,7] These films are highly crystalline, enabling us to perform x-ray diffraction measurements of the IAD films and identify their crystalline structure. While it is not discussed here, identical results have also been observed for NdF_3, another material which forms highly crystalline films.

The thin films have been resistively evaporated in a vacuum chamber described in detail elsewhere[5,7] with a base pressure of ~$1–2 \times 10^{-6}$ Torr. Films 4500–5000 Å thick were deposited onto ambient temperature fused silica substrates. These films were used for both x-ray diffraction in a Siemens x-ray diffractometer and x-ray photoelectron spectroscopy (XPS) in a Perkin-Elmer 5100 series Electron Spectroscopy for Chemical Analysis system. Films 800 Å thick were deposited onto graphite substrates in separate depositions for Rutherford backscattering spectrometry (RBS).

The unbombarded LaF_3 films show strong crystalline peaks in x-ray diffraction, with all the peaks corresponding to a tysonite structure (Fig. 1), the only phase for bulk LaF_3.[8] These peaks are still present for IAD films bombarded with

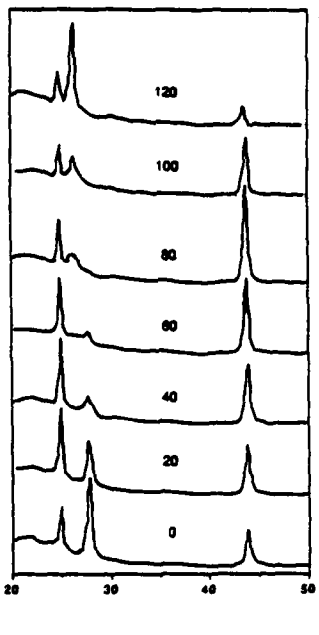

Fig. 1. X-ray diffraction spectra of IAD LaF_3 films bombarded with 300-eV argon ions. The ion beam current densities for each sample are indicated on the graph in $\mu A/cm^2$.

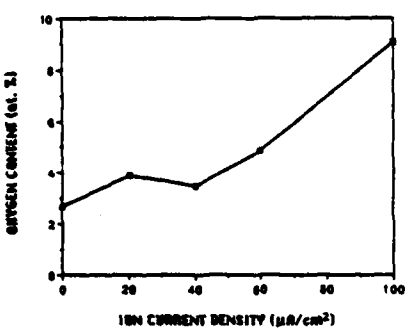

Fig. 2. Oxygen content of IAD LaF_3 films bombarded with 300-eV argon ions as a function of ion beam current density.

low fluxes of 300-eV argon ions (Fig. 1), but at a threshold ion flux density of 100 $\mu A/cm^2$, the (111) peak at $2\theta = 27.6°$ (all angles reported here are 2θ values) shrinks and a new peak appears at 26.5°. This peak does not correspond to any LaF_3 tysonite orientation. RBS analysis shows that the oxygen content of the films increases with ion bombardment (Fig. 2). This suggested that the new peak represents the formation of an oxide or oxyfluoride phase.

Zachariasen[9] has studied the oxidation of bulk LaF_3 during thermal annealing in air, identifying three distinct oxidized phases. A tetragonal lanthanum oxyfluoride phase

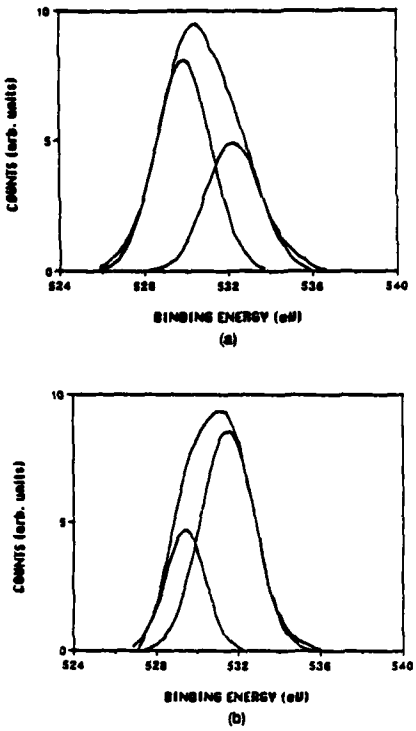

Fig. 3. XPS spectra of oxygen 1s binding state for (a) unbombarded and (b) IAD (300-eV, 100-$\mu A/cm^2$ Ar) LaF_3 films. The two Gaussian peaks which best fit each spectrum are also shown.

was first observed with a stoichiometry in the range LaO_nF_{3-2n} with $0.7 < n < 1.0$. The unit cell of this phase shrank with increasing oxygen content, shifting the x-ray peaks toward larger values of 2θ. When $n = 1$, a phase transition to a rhombohedral LaOF phase was observed. This phase had only one stable stoichiometry. Finally, this phase oxidized into a true La_2O_3 phase.

Unfortunately, both oxyfluoride phases have peaks near this angle: the tetragonal (101) and rhombohedral (222) oxyfluoride phase orientations are at 26.6 and 26.5°, respectively. The oxide can thus be ruled out, but we cannot yet differentiate between the two oxyfluoride phases. We next thermally annealed the 300-eV, 120-$\mu A/cm^2$ film for 3 h at 500°C. The (300) LaF_3 peak at 43.6° now disappeared, and a new peak appeared at 44.3°. The nearest La_2C_3 peak is at 44.9°, showing that the crystallites are still not fully oxidized, even after this anneal. The new peak could be either the (200) tetragonal or (332) rhombohedral oxyfluoride orientation.

The size of crystallites in a film can be determined from the linewidth of the x-ray peaks using the Scherrer equation.[10] The linewidth of the oxyfluoride peak at 26.6° for the 300-eV 120-$\mu A/cm^2$ film is approximately the same as the linewidth of the 27.6° LaF_3 peak for the more lightly bombarded films, suggesting that entire fluoride crystallites ~200 Å large are being transformed to an oxyfluoride phase.

Three of the LaF_3 films were also examined with XPS. The only meaningful differences between the films are ob-

served in the O 1s binding energy peaks (Fig. 3). These peaks are actually superpositions of two peaks separated by ~2 eV. As the ion flux increases, the higher energy peak contributes a greater portion of the total area of the peak: Gibson and Kennemore[4] have observed a similar effect in MgF_2 films, with films possessing a higher oxygen content having a larger contribution from the higher energy peak. Comparing the XPS result to the x-ray diffraction data, we can equate the higher energy O 1s state with oxygen filling anion sites in the crystalline lattice, as only oxygen in the lattice could drive the phase transformation to the oxyfluoride state.

A critical percentage of oxygen is apparently required to cause oxyfluoride crystallites to appear. Since the oxyfluoride phase first appears for an ion current density between 80 and 100 $\mu A/cm^2$, this critical percentage is between 7 and 9 at. %.

We have shown that the percentage of oxygen in the crystalline lattice of IAD LaF_3 thin films deposited in high vacuum increases with increasing ion beam current density. This oxygen must strain the fluoride lattice until the incorporation of a sufficient amount of oxygen into the lattice results in a phase transition by individual LaF_3 crystallites into an oxyfluoride phase. There is no evidence for the formation of an oxide phase. This contradicts the normal assumption that the oxygen forms a segregated oxide in the films at all significant levels of oxygen incorporation.

Support for this work was provided by the Los Alamos National Laboratory under contract 9-X56-0322C-1 and the Air Force Office of Scientific Research through the University Research Initiative Program. The authors wish to thank Charles Kennemore for performing the XPS measurements and data reduction and John Leavitt and Larry McIntyre and their co-workers in the Ion Beam Analysis Facility of the University of Arizona Department of Physics for performing the RBS measurements.

References

1. W. C. Herrmann and J. R. McNeil, "Ion Beam Applications for Optical Coating," Proc. Soc. Photo-Opt. Instrum. Eng. 325, 101 (1982).
2. C. M. Kennemore III and U. J. Gibson, "Ion Beam Processing for Coating MgF_2 onto Ambient Temperature Substrates," Appl. Opt. 23, 3608 (1984).
3. P. J. Martin and R. P. Netterfield, "Ion Assisted Deposition of Magnesium Fluoride Films on Substrates at Ambient Temperature," Appl. Opt. 24, 1732 (1985).
4. U. J. Gibson and C. M. Kennemore III, "Ambient Temperature Deposition of MgF_2 with Noble and Fluorocarbon Ion Assistance," Proc. Soc. Photo-Opt. Instrum. Eng. 678, 130 (1986).
5. J. D. Targove *et al.*, "Ion-Assisted Deposition of Fluorides," Proc. Soc. Photo-Opt. Instrum. Eng. 678, 115 (1986).
6. P. M. Martin *et al.*, "Influence of Ion Assistance on the Optical Properties of MgF_2," Appl. Opt. 26, 1235 (1987).
7. J. D. Targove, J. P. Lehan, L. J. Lingg, H. A. Macleod, J. A. Leavitt, and L. C. McIntyre, Jr., "Ion-assisted Deposition of Lanthanum Fluoride Thin Films," Appl. Opt. 26, 3733 (1987).
8. Joint Committee on Powder Diffraction Standards, Inorganic File, Plate 8-461 (1967).
9. W. H. Zachariasen, "Crystal Chemical Studies of the 5*f*-Series of Elements. XIV. Oxyfluorides, XOF," Acta Cryst. 4, 231 (1951).
10. B. D. Cullity, *Elements of X-ray Diffraction* (Addison-Wesley, Reading, MA, 1978).

Phase-gradient reconstruction from photon-limited stellar speckle images: erratum

G. J. M. Aitken and R. Johnson

Queen's University, Department of Electrical Engineering, Kingston, Ontario K7L 3N6, Canada.
Received 18 November 1987.
0003-6935/88/020215-01$02.00/0.

In this paper[1] we did not indicate that a MAMA detector was crucial to the acquisition of the high-quality photon-event data, taken on the Steward Observatory 2.3-m telescope, and used in our β-del reconstructions. We wish to acknowledge with thanks the contribution to the data acquisition by Jeffrey Morgan, Centre for Space Science and Astrophysics, Stanford University, who provided the MAMA detector for these observations.

Reference

1. G. J. M. Aitken and R. Johnson, "Phase-Gradient Reconstruction from Photon-Limited Stellar Speckle Images," Appl. Opt. 26, 4246 (1987).

Lightweight mirror structures best core shapes: a reversal of historical belief; comment

William P. Barnes

Precision Optics Corporation, 22 East Broadway, Gardner, Massachusetts 01440-3338.
Received 27 August 1987.
0003-6935/88/020215-01$02.00/0.

I would like to make the following comment on the paper by Sheng[1]:

The shortcomings of hexagonal and rectangular cell configurations for open back plate structures subjected to torsion loading are well known. With respect to the data I reported in 1972,[2] my faith in a well-conceived and well-tested physical model still transcends my belief in finite element mathematical models. Our testing showed no detectable differences in deflection for either construction for the three-point support case with the supports moved 30° circumferentially.

References

1. S. C. F. Sheng, "Lightweight Mirror Structures Best Core Shapes; a Reversal of Historical Belief," Appl. Opt. 27, 354 (1988).
2. W. P. Barnes, "Hexagonal vs Triangular Core Lightweight Mirror Structures," Appl. Opt. 11, 2748 (1972).

To be published in Thin Solid Films (1988).

9

Anisotropic effects in thin film multilayers

K. Balasubramanian, A. S. Marathay, and H. A. Macleod
Optical Sciences Center, University of Arizona, Tucson, Arizona 85721 USA

Abstract:

Vacuum evaporated thin films are known to exhibit a growth induced columnar microstructure causing a small anisotropy in their optical constants. We have developed a code to model the optical performance of anisotropic thin film multilayers based on Yeh's 4 x 4 matrix formalism[10] and applied it to study the effect of growth induced anisotropy. We have computed the performance of a typical multilayer system, a narrow-band filter. Here we discuss the results which show considerable shift in the performance of the filter when a small anisotropy is introduced.

Introduction:

Several papers in the literature[1-7] have presented computer models of thin film growth and have shown remarkable columnar microstructure. Experimental observations have been made of these columns and scanning electron micrographs of such microstructures have been published[1,2]. One of the immediate effects of the columnar microstructure is anisotropy in the optical constants of the film. Moisture penetration into the voids in the films would also produce further changes in the refractive index and hence a multilayer stack, for example, a narrow band filter would show considerable shift[8] in the performance of the device from the intended design. A general scheme to calculate the reflection, and transmission characteristics of anisotropic multilayer thin film systems is given by Pochi Yeh[10]. Details of the scheme and its extension to the study of optically active media are presented in another paper[13]. Here we adopt the scheme to study the effects of growth induced anisotropy in a multilayer thin film system.

The Design:

We study the performance of an all dielectric narrow band filter designed to operate at 632.8 nm. The design is air/$[HL]^p$ H^q $[LH]^p$/glass with p = 4 and q = 4. H denotes a quaterwave layer of Titanium oxide and L denotes a quarterwave layer of Silicon dioxide. Hodgkinson et al[9] fabricated such a filter and determined the principal refractive indices of the Titanium oxide layer. They deposited films at 27 degrees vapour angle and found a large anisotropy in the refracive index due to a very pronounced columnar microstructure oriented at about 14.29 degrees to the film normal. Here, to begin with, for the sake of simplicity, we assume that the films are deposited with vapour incident nearly normal to the substrate and assume that the principal indices of refraction coincide with the geometry of the substrate and that the anisotropy is quite small. Then we calculate the performance of the system for the case of the films deposited at oblique vapour incidence.

Results and Discussions:

We study the following five situations. The geometry of the film system is shown in figure 1.

1. All layers being isotropic: In this case we assume that there is no anisotropy in any of the layers and calculate the transmittance at normal incidence of such an ideal filter. Fig.2 shows the transmittance of an all dielectric filter of the design mentioned above with the refractive index of the H layer being 2.40 and that of the L layer being 1.45. The peak transmission wavelength is 632.8 nm and the filter shows the desired peak transmittance.

2. H layer being isotropic in the XY plane: This is the case when the H layer exhibits a uniaxial anisotropy with $n_x = n_y \neq n_z$. We further assume that all the L Layers are isotropic. Hodgkinson et al have shown that SiO_2 exhibits very little anisotropy and hence can be assumed isotropic. For the H layer we take $n_x = n_y = 2.2$ and $n_z = 2.4$. It is appropriate to assume that n_x and n_y would be smaller than n_z due to the nature of the columns in the film. For the L layer we take n = 1.45 as before. Fig.3 shows the normal incidence transmittance of the narrowband filter with the above values for the indices of the films. We see that the peak transmission is at 595.4 nm as against the desired peak wavelength of 632.8 nm.

3. H layer being biaxial: In this case we consider that the Titania layers exhibit biaxial anisotropy whereas the silica layers are still isotropic as suggested by Hodgkinson et al. We assume $n_x = 2.2$, $n_y = 2.3$ and $n_z = 2.4$ for Titania layers and n = 1.45 for the silica layers. Figs 4a & b show the normal incidence transmittance for the filter with the above indices. We see that the filter shows different peak wavelengths for p and s polarizations even for normal incidence as could be expected, s being shifted more towards the shorter wavelength than p. The peak wavelengths for s and p are 595.4 nm and 613.8 nm respectively.

4. Now we study the case of films deposited at oblique incidence of vapour. Let us assume that the columns in the films are oriented at 10 degrees to the normal as shown in fig.5. The dielectric tensor for the films are tranformed to the coordinate system given in fig.1 by means of the rotation of coordinates. If ϵ is the dielectric tensor of the film in the principal coordinates shown in fig.5, the dielectric tensor in the film system shown in fig.1 can be obtained by the equation $\epsilon' = R\,\epsilon\,R^{-1}$, where R refers to the rotation matrix given by

$$R = \begin{matrix} 1 & 0 & 0 \\ 0 & \cos(\alpha) & \sin(\alpha) \\ 0 & -\sin(\alpha) & \cos(\alpha) \end{matrix}$$

where α is the angle of inclination of the columns in the film relative to the film normal. On doing this transformation we get the following values for the dielectric tensor for the H layer

//

$$\epsilon = \begin{matrix} 4.840 & 0 & 0 \\ 0 & 5.30417 & 0.08037 \\ 0 & 0.08037 & 5.74577 \end{matrix}$$

Assuming the L layer to be isotropic and H layers characterized by the above values for the dielectric tensor, we get the filter transmission shown in fig.6a & b corresponding to s and p polarizations. The peak wavelengths are 595.4 nm for s polarization and 614.3 nm for p polarization. If we now assume that the columns are oriented at 20 degrees to the film normal, we get, similar characteristics as shown in fig. 7a & b. The peak wavelengths are 595.4 nm for s polarization and 615.8 nm for p polarization. Comparing with the cases where we assumed the columns to be oriented normal to the film plane, we see that the s polarization has the same peak wavelength and the p polarization shows one or two nm shift depending on the angle of tilt of the columns. This performance is in line with what one might expect.

5. Finally we study the case where we assume a small amount of anisotropy in the L layers as well. We assume that the columns are oriented at 10 degrees to the film normal for both the L and H layers and the L layer indices in the principal coordinates are $n_x = 1.35$, $n_y = 1.40$ and $n_z = 1.45$ whereas the corresponding indices for the H layers are 2.2, 2.3 and 2.4. The filter characteristics for such a system of films are shown in fig 8a & b. It is interesting to note that the p and s polarization peaks get further separated from the desired peak wavelength.

Conclusions:

From the foregoing theoretical calculations we can conclude that columnar microstructures found in vacuum evaporated thin films would produce a significant shift in the performance of the device particularly when the device is made for narrow band applications. Furthermore, there could be polarization dependent effects if the films exhibit biaxial anisotropy or if they are used at non normal incidence. Columnar microstructure combined with stress and moisture penetration could lead to greater changes in the performance of the device. While one could consider such shifts as potential problems, one might also design devices with anisotropic films so as to work favorably as tuning devices in applications with polarized light.

Acknowledgements:

The authors wish to acknowledge the support of IBM corporation and the Optical Data Storage Center at the University of Arizona for their support.

References:

1) Karl H. Guenther, "Microstructure of vapour-deposited optical coatings", Appl Optics, Vol.23, No.21, pp 3806-3816 (1984)

2) Karl H. Guenther, "Columnar and nodular growth of thin films", Proc. SPIE, Vol.346, pp 9-18, (1982)

3) H. K. Pulker, "Characterization of optical thin films", Appl. Optics, Vol.18, No.12, pp 1969-1977 (1979)

4) J. A. Thornton, "Structure and topography of sputtered coatings", J. Vac. Sci. Technol., Vol.11, No.4, pp 666-670 (1974)

5) M. Sikkens, I. J. Hodgekinson, F. Horowitz, H. A. Macleod, J. J. Wharton, "Computer simulation of thin film growth: applying the results to optical coatings" Optical Engineering, 25, pp 142-147 (1986)

6) B. Bartholomeusz, Karl-Heinz Muller, M. R. Jacobson, "Computer simulation of the nucleation and growth of optical coatings", Proc. SPIE Vol. 821, (in press) (1987)

7) R. B. Sargent, and H. A. Macleod, "Computer simulation of the growth of two-element films", Technical Digest, OSA Annual Meeting, Rochester, New York, 1987

8) Steven G. Saxe , M. J. Messerley, Bertrand Bovard, L. De Sandre, Fred J. van J Milligan aand H. A. Macleod, "Ion bombardment induced moisture absorption in optical thin films", Appl. Optics, 23, 3633, (1984)

9) L. J. Hodgkinson, F. Horowitz, H. A. Macleod, M. Sikkens, and J. J. Wharton, "Measurement of the principal refractive indices of thin films deposited at oblique incidence", JOSA, A, 2, 1693-1697 (1985)

10) P. Yeh, "Electromagnetic propagation in birefringent layered media", JOSA Vol.69, p 742, (1979)

11) S. Visnovsky, "Magneto-optical ellipsometry", Czech. J. Phys., B 36, pp 625-650, (1986)

12) K. Balasubramanian, A. S. Marathay and H. A. Macleod, "Design technique for anisotropic multilayer thin film systems", Technical Digest, OSA Annual Meeting, Rochester, N. Y., (1987)

13) K. Balasubramanian, A. S. Marathay and H. A. Macleod, "Modelling magneto-optical thin film media for optical data storage" Seventh International Coneference on Thin Films (ICTF-7) , New Delhi, December 7-11, 1987.

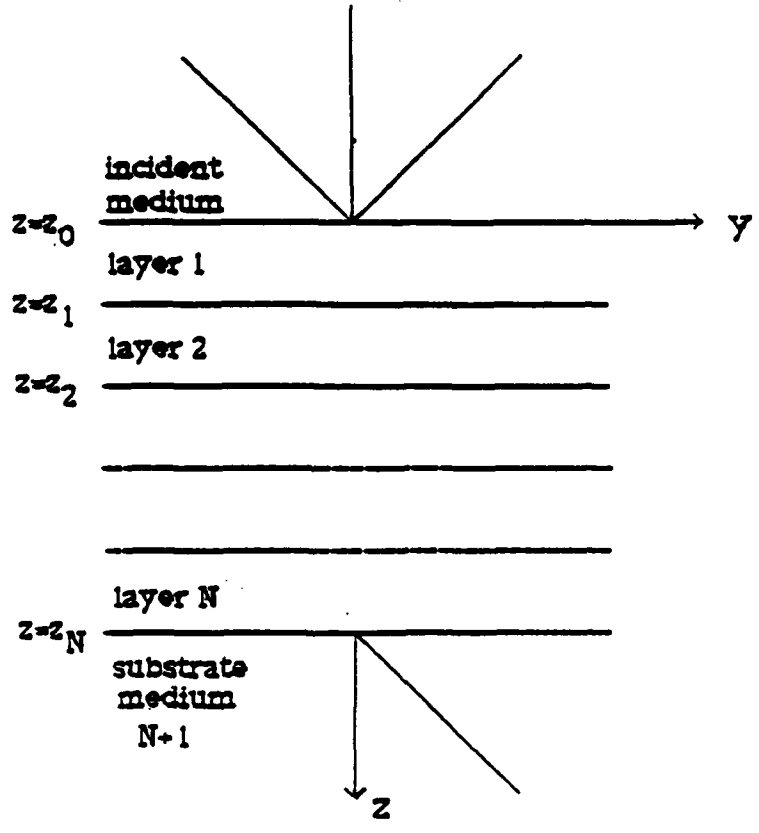

1. Geometry of the film system

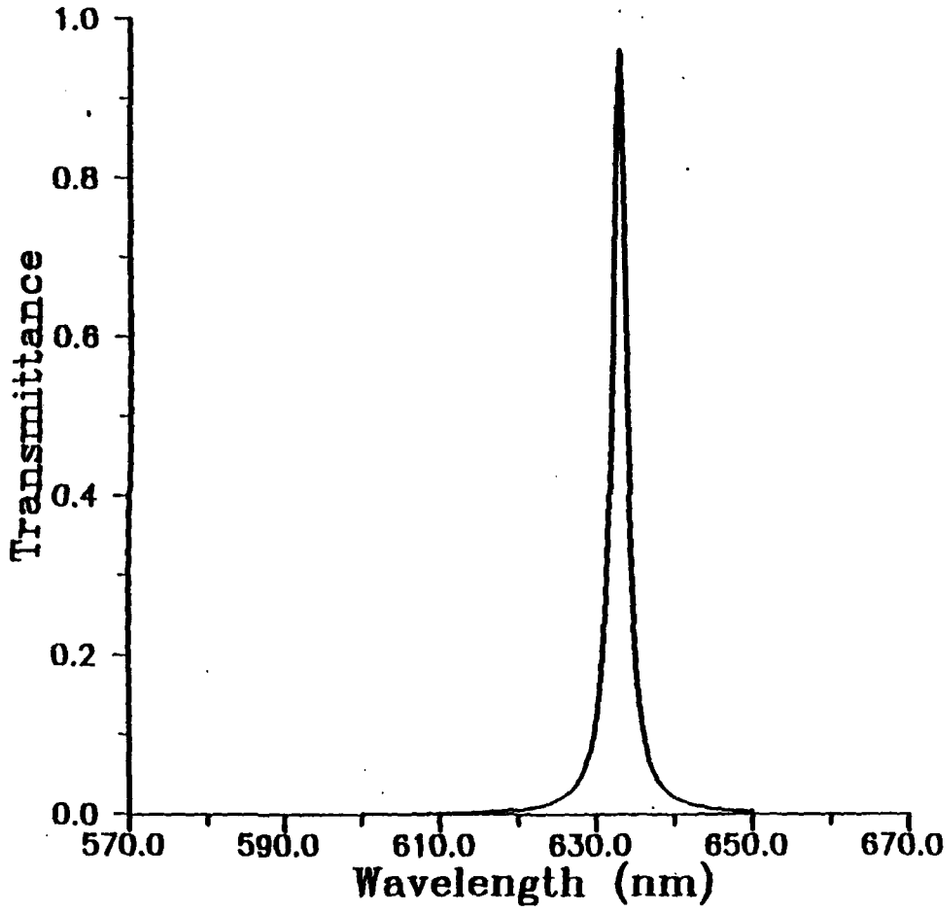

2. Filter performance at normal incidence
Design: air/(HL)^4 4H (LH)^4/glass; all layers are assumed isotropic
$n_H = 2.4$; $n_L = 1.45$; H and L denote quarterwave films of the high and low index materials; peak wavelength = 632.8 nm

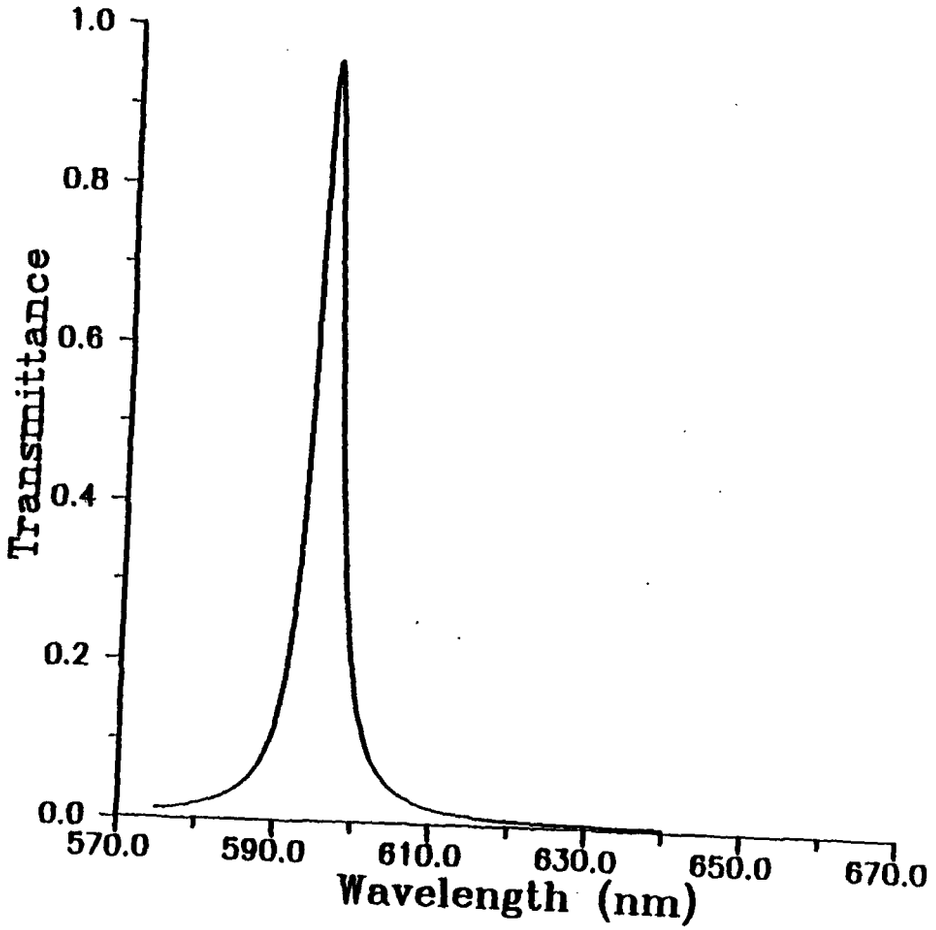

3. Filter performance at normal incidence for the same design as for fig.2; H layer is assumed anisotropic with columns of the film oriented normal to the film; $\alpha = 0$; $n_x = 2.2$, $n_y = 2.2$ and $n_z = 2.4$ for the H layer; L layer is assumed isotropic; peak wavelength for s and p polarizations = 505.4 nm

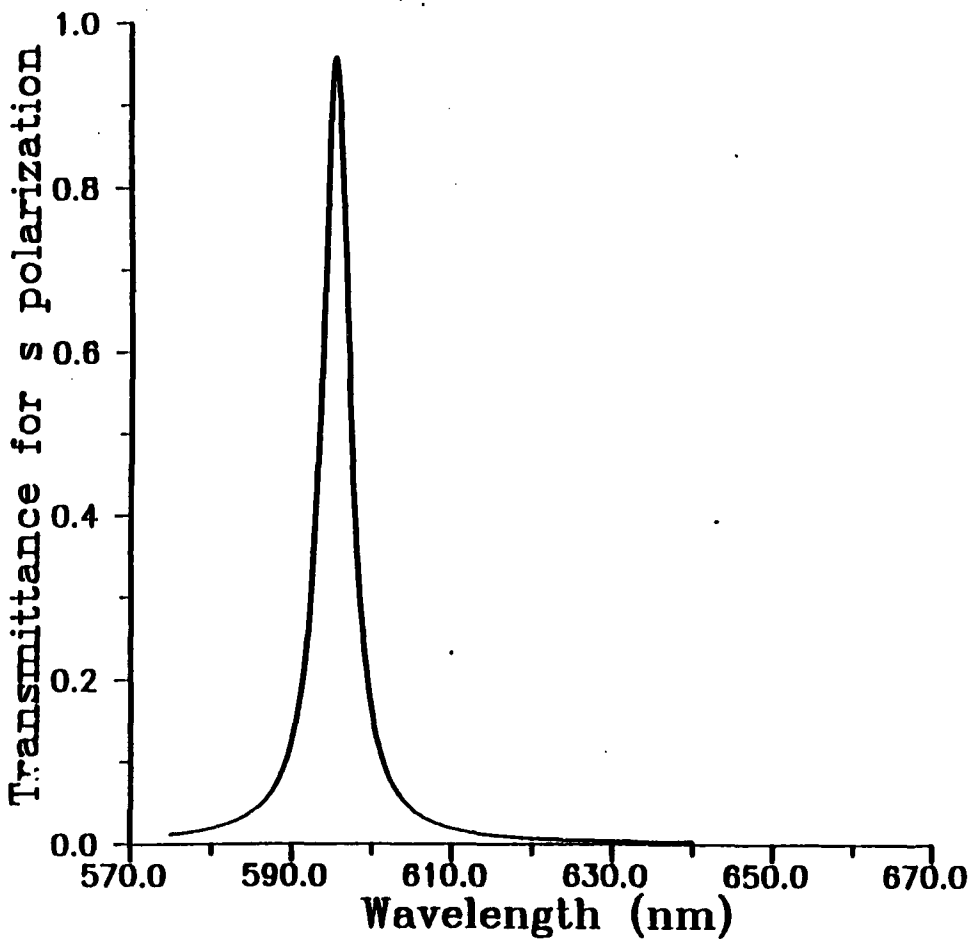

4. Filter performance at normal incidence for the same design as for fig.2; H layer is assumed anisotropic with columns of the film oriented normal to the film; $\alpha = 0$; $n_x = 2.2$, $n_y = 2.3$ and $n_z = 2.4$ for the H layer; L layer is assumed isotropic; peak wavelengths are 595.4 nm and 613.8 nm for s and p polarizations respectively

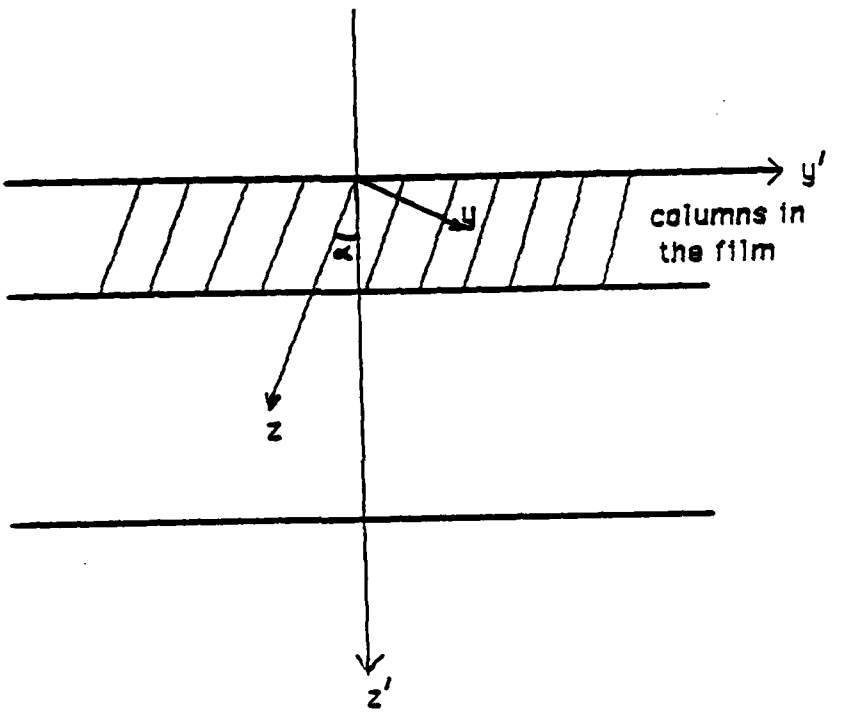

5. Geometry of the columns in the film

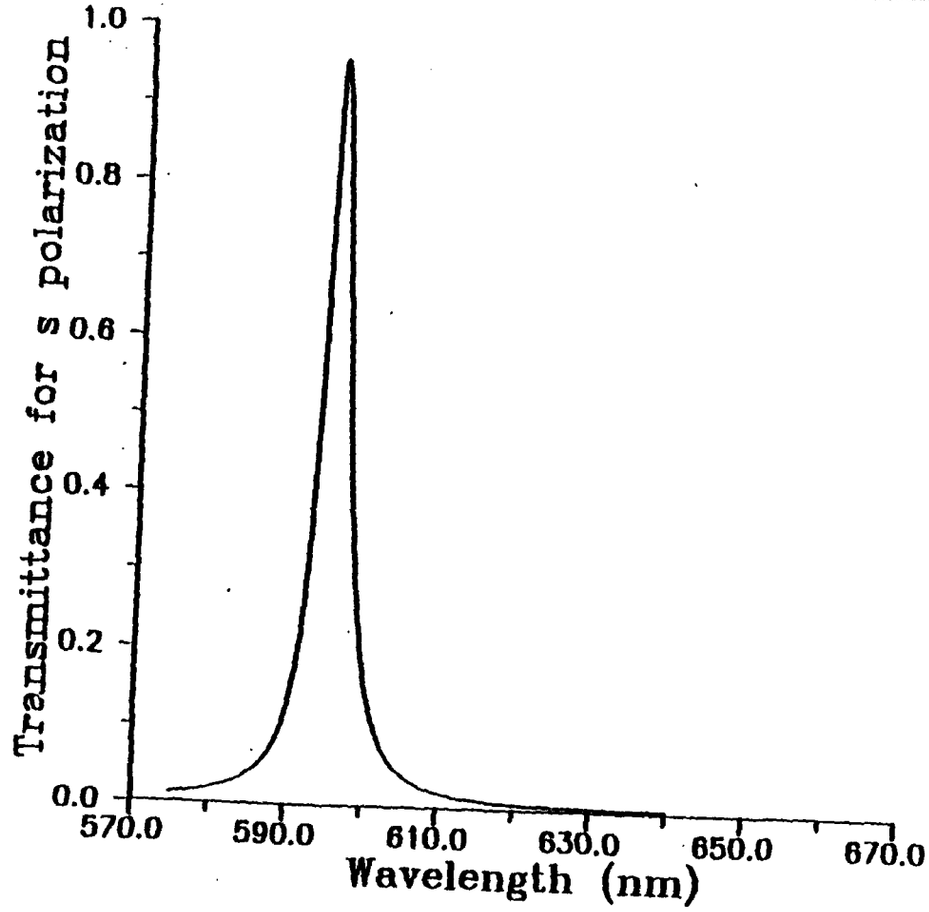

6. Filter performance at normal incidence for the same design as for fig.2; H layer is assumed anisotropic with columns of the film oriented at 10 degrees to the film normal ; α = 10 degrees; n_x = 2.2, n_y = 2.3 and n_z = 2.4 for the H layer; L layer is isotropic; peak wavelengths are 595.4 nm and 614.3 nm for s and p polarizations

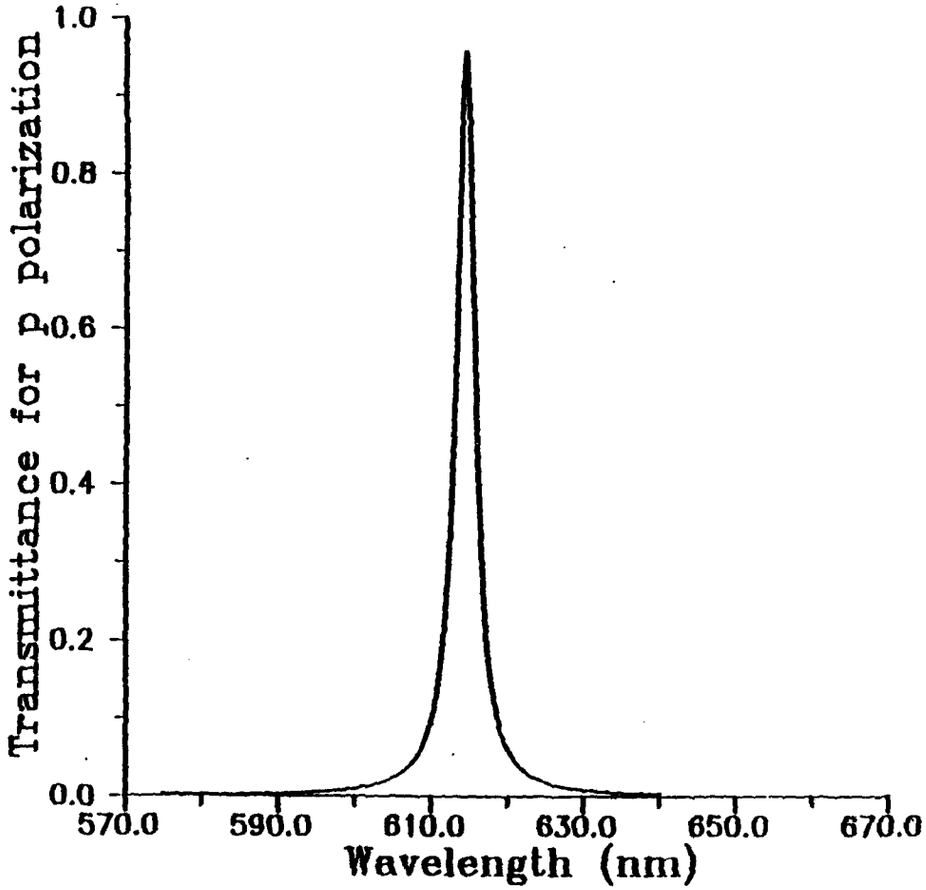

6. Filter performance at normal incidence for the same design as for fig.2; H layer is assumed anisotropic with columns of the film oriented at 10 degrees to the film normal ; α = 10 degrees; n_x = 2.2, n_y = 2.3 and n_z = 2.4 for the H layer; L layer is isotropic; peak wavelengths are 595.4 nm and 614.3 nm for s and p polarizations

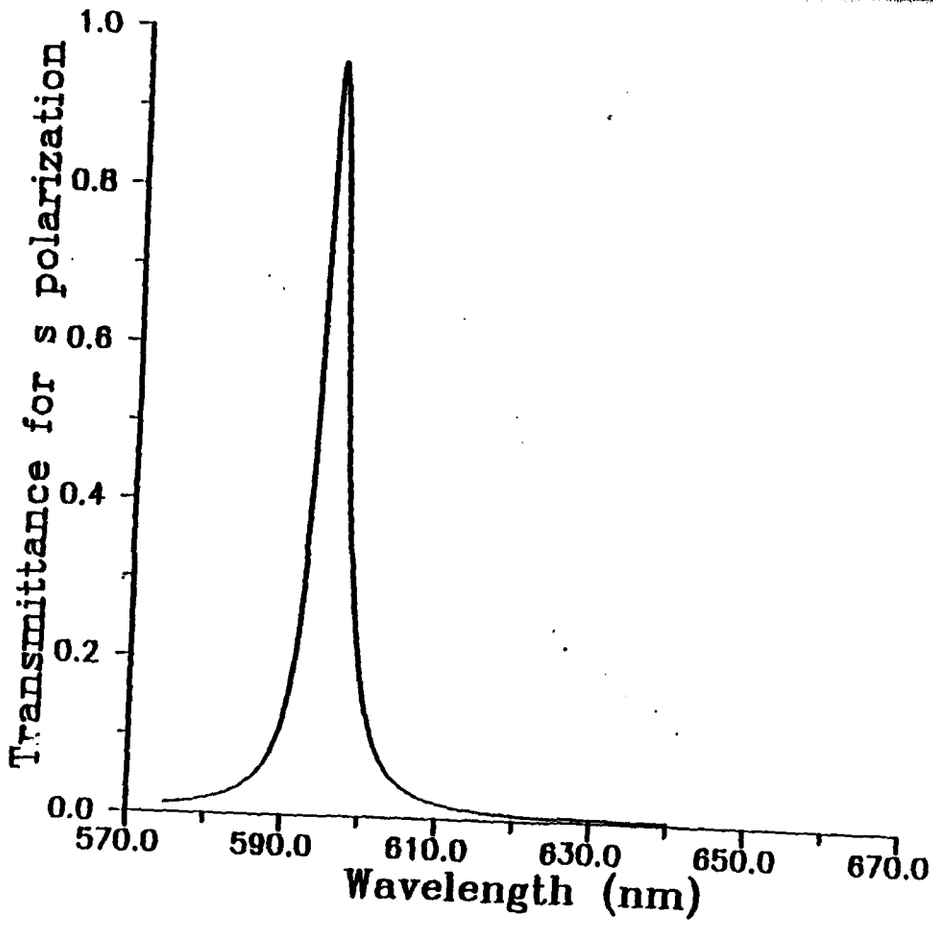

7. Filter performance at normal incidence for the same design as for fig.2; H layer is assumed anisotropic with columns of the film oriented at 20 degrees to the film normal ; α = 20 degrees; n_x = 2.2, n_y = 2.3 and n_z = 2.4 for the H layer; L layer is isotropic; peak wavelengths are 595.4 nm and 615.8 nm for s and p polarizations

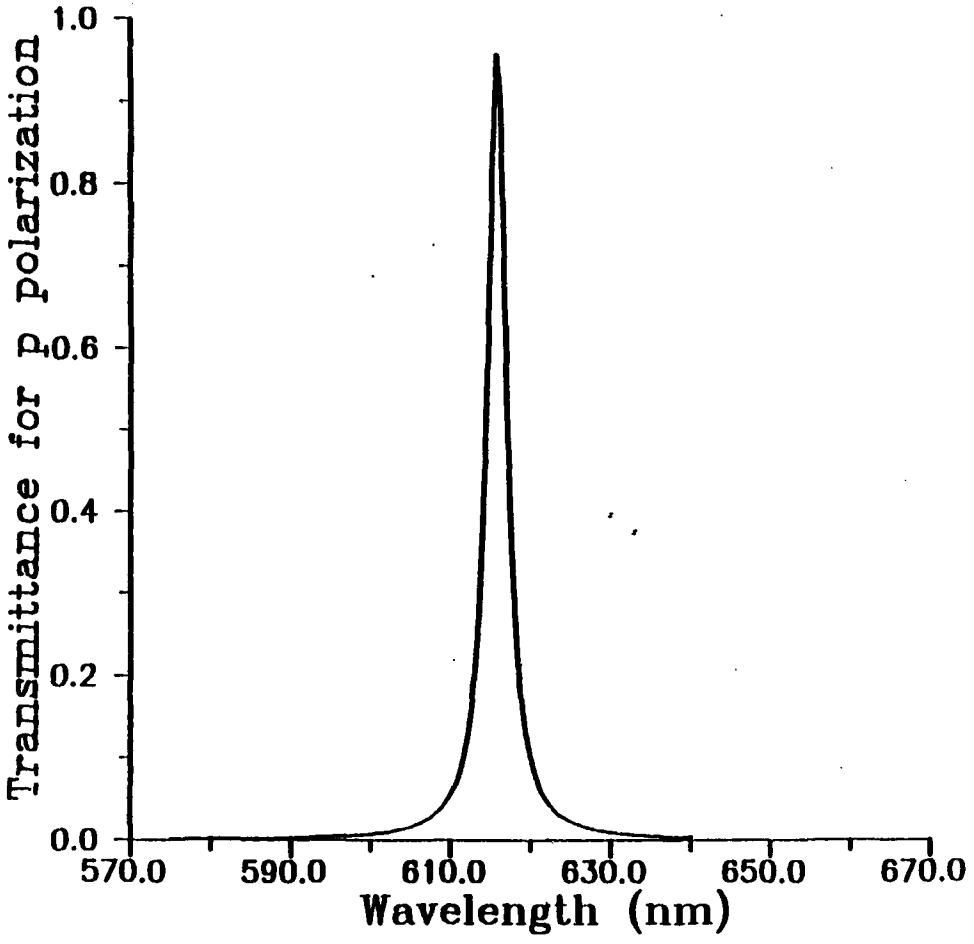

7. Filter performance at normal incidence for the same design as for fig.2; H layer is assumed anisotropic with columns of the film oriented at 20 degrees to the film normal ; α = 20 degrees; n_x = 2.2, n_y = 2.3 and n_z = 2.4 for the H layer; L layer is isotropic; peak wavelengths are 595.4 *nm* and 615.8 *nm* for s and p polarizations

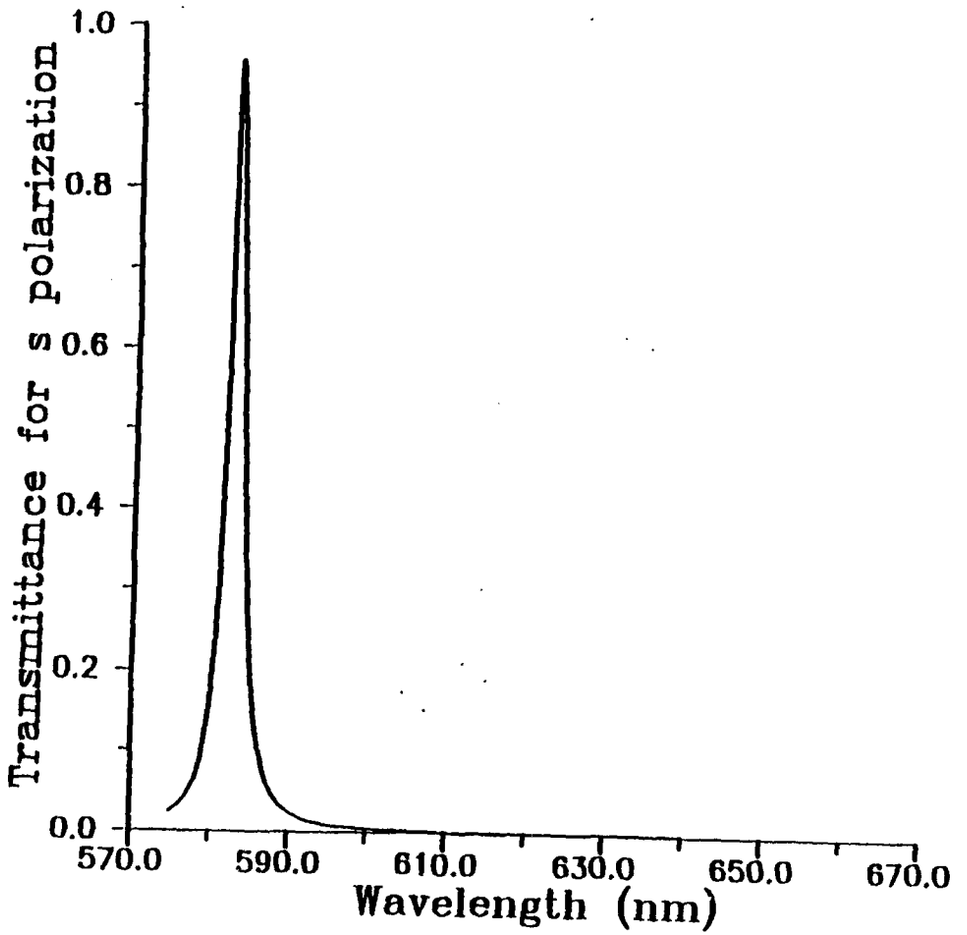

8. Filter performance at normal incidence for the same design as for fig.2; H layer and L layer are both assumed anisotropic with columns of the film oriented at 10 degrees to the film normal; α = 10 degrees; n_x = 2.2, n_y = 2.3 and n_z = 2.4 for the H layer; n_x = 1.35, n_y = 1.40 and n_z = 1.45 for the L layer; peak wavelengths are

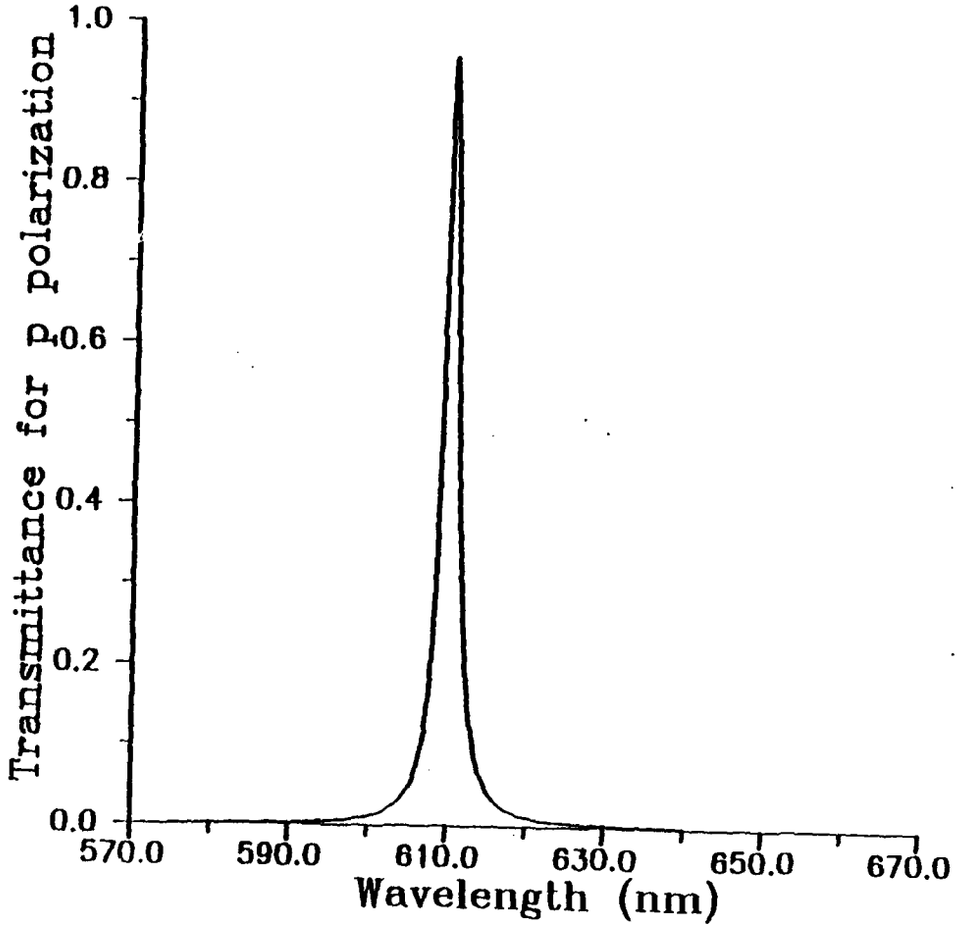

8. Filter performance at normal incidence for the same design as for fig.2; H layer and L layer are both assumed anisotropic with columns of the film oriented at 10 degrees to the film normal; α = 10 degrees; n_x = 2.2, n_y = 2.3 and n_z = 2.4 for the H layer; n_x = 1.35, n_y = 1.40 and n_z = 1.45 for the L layer; peak wavelengths are

24

Reprinted from Journal of the Optical Society of America B, Vol. 4, page 1087, July 1987

Interface roughness cross-correlation laws deduced from scattering diagram measurements on optical multilayers: effect of the material grain size

C. Amra, P. Roche, and E. Pelletier

Laboratoire d'Optique des Surfaces et des Couches Minces, Unité Associée (1120) au Centre National de la Recherche Scientifique, Ecole Nationale Supérieure de Physique de Marseille, Domaine Universitaire de St Jérôme, 13397 Marseille Cedex 13, France

Received January 28, 1987; accepted April 3, 1987

It is well known today that scattering phenomena in multilayer coatings are of great importance, and we have already shown how and why it was necessary to understand this mechanism in detail if we want to increase the performances of optical systems. Among the numerous parameters involved in the calculation of the scattered waves (roughnesses, autocorrelation lengths, cross-correlation coefficients, indices, and thicknesses of the layers, etc.), the cross-correlation laws inside the stack are essential, because they are largely responsible for the form and the magnitude of the flux scattered from a coating. Moreover, knowing these laws provides us with valuable information concerning the grain structure of thin-film materials. First we show how some specific effects (such as the antiscattering effect) permit us to determine the cross-correlation laws in the case of a coating with a small number of layers and how a carefully done comparison between theory and experiment can be used to characterize the grain size of materials. In the case of a coating with many layers, the phenomena are obviously more complicated to interpret. Nevertheless, an investigation is possible (using an aluminum-layer technique), and we present our results for a mirror.

INTRODUCTION

Optical filters are required today to have extremely high performance both for the position of the transmission spectral window (in the case of Fabry–Perot filters used in optical multidemultiplexing) and for the magnitude of losses by absorption and scattering (especially for laser mirrors). The monitoring and production techniques of these filters obtained by vacuum evaporation of dielectric materials have been considerably improved, and it now appears that the main key factors that limit their performance lie in the fine microstructure of the materials that the stack is made of: absorption, surface scattering, volume scattering, adsorption, anisotropy, inhomogeneity, oxidation, and stress; these are all factors that can be responsible for the differences observed between theoretical calculation and experimental results.

We are interested here in the study of light scattering from structure irregularities of the interfaces of a multilayer stack, according to the commonly admitted hypothesis[1] that it is 1 order of magnitude higher than scattering from the bulk of the evaporated materials. For this purpose, our laboratory in Marseilles has developed an extremely high performance apparatus[2] that can measure, in each direction of space, the scattered flux of some billionths of the incident flux. However, it is obvious that a detailed analysis of experimental results requires the use of a vector theory of light scattering from rough surfaces, which takes into account the polarization states of the incident and scattered light. Among the vector theories of light scattering from slightly rough surfaces, the theories of Elson[3] and Bousquet *et al.*[4] are noteworthy because they can also be applied to multilayer optical coatings. In the laboratory, the theory of Bousquet *et al.* was developed and computed, and we demonstrated that it was equivalent[5] to Elson's theory.

When scattering originates only from one rough surface, we know that through theory and experiment we can determine the autocorrelation function of the surface defects[2,4,6,7]; this is an accurate method to characterize the optical polish on the surface of an absorbing material. On the other hand, such a method cannot be applied to the case of a multilayer optical coating, because we must take into account both the roughnesses of each interface and the cross-correlation functions between these interfaces. The knowledge of these cross-correlation laws is of a fundamental interest, since these laws are mainly responsible for the shape and the magnitude of the scattering distribution. Moreover, these laws can provide us with valuable information concerning the fine microstructure of thin-film materials. Nevertheless, their determination is rather difficult because the number of parameters involved is high (the scattering calculation for a p-layer stack involves $5p + 4$ parameters). We show in this paper how the use of particular techniques, such as the antiscattering effect and the deposition of a thin opaque metallic layer, enables us to investigate the roughness of each interface and the cross-correlation laws between these interfaces. The origin of roughness is discussed along with its associated cross-correlation law. We consider both the influence of the substrate defects and that of the fine microstructure of the material. This work refers to numerous studies that were previously carried out; the overall viewpoint given here permits us to understand the key scattering parameters.

0740-3224/87/071087-07$02.00

THEORY AND CROSS-CORRELATION LAWS: INFLUENCE OF THE MICROSTRUCTURE OF MATERIALS

A detailed analysis of the experimental results requires a good knowledge of cross-correlation laws; let us recall certain facts. The present paper points out that the coherence of scattered waves from different interfaces depends on the scattering direction. We deal with the origin of roughness and with the influence of the fine microstructure of the material.

Autocorrelation Function and Roughness Spectrum

Since a slightly rough surface can be considered to be the result of an infinite sum of gratings, the scattered wave that can be measured at infinity in a direction (θ, ϕ) of space (Fig. 1) is due to the presence, on the rough surface, of a sinusoidal grating with grooves perpendicular to the scattering plane (ϕ). The magnitude of this grating is twice the modulus of the Fourier transform of the function h that describes the surface irregularities. The grating period is $c = 2\pi/\sigma$ under normal incidence, where $\sigma \approx |\sigma|$ is the spatial frequency under study, that is,

$$\sigma = \frac{2\pi}{\lambda} \sin\theta \begin{cases} \cos\phi \\ \sin\phi \end{cases},$$

where λ is the wavelength under study in the incident medium (air).

Then the scattered intensity can be written as the product of two factors: $I(\theta, \phi) = C(\theta, \phi)\,\gamma(\theta, \phi)$, where the first factor C, which is called the ideal coefficient, depends only on the indices of the two media and on the illumination and observation conditions (wavelength, incidence, and polarization). The roughness spectrum γ, which contains all the information related to the surface defects, is the Fourier transform of the autocorrelation function of the surface irregularities.

For more convenience, this roughness spectrum is usually approximated in the range of measurable spatial frequencies with the Fourier transform of the sum of an exponential and a Gaussian function, of parameters (δ_e, L_e) and (δ_g, L_g), respectively. This can be interpreted in the following way: the surface profile h is due to the superposition of two independent functions h_1 and h_1' (Fig. 2), of large and small spatial periods, respectively. The exponential function characterizes large-period defects—responsible for scattering at small angles—while the Gaussian function characterizes small-period defects, which give rise to scattering at large angles, θ.

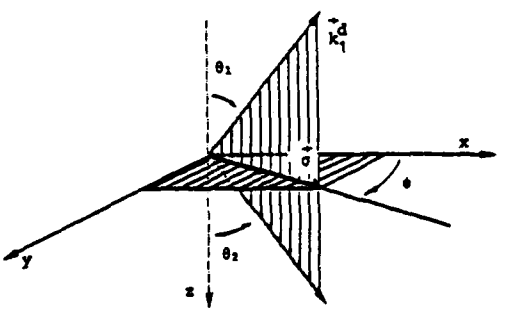

Fig. 1. Reference coordinates for the scattered wave vectors. z is an axis normal to the mean plane of the rough surface.

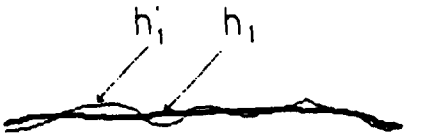

Fig. 2. The surface profile h can be considered to be the result of the superposition of two functions, h_1 and h_1', of large and small spatial periods, respectively.

Cross-Correlation Functions: Influence of the Microstructure of Materials

In the case of a multilayer stack, each rough interface is a source of scattered light, and we must consider the multiple reflections of each scattered wave throughout the entire stack. Moreover, interferences can occur among these various scattering sources, for which reason we introduce cross-correlation functions, which take into account the degree of coherence among the waves emitted from different interfaces. The expression of the scattered intensity can then be written as

$$I(\theta, \phi) = \sum_{i=1}^{p} |a_i|^2 \gamma_{ii} + \sum_{i \neq j} a_i \bar{a}_j \gamma_{ij}, \tag{1}$$

where the a_i coefficients (ideal coefficients) are given by theory and depend only on the indices and thicknesses of the layers and on the illumination and observation conditions. The γ_{ii} term represents the roughness spectrum of interface i and characterizes the statistical properties of the surface defects. If we suppose that the scattered waves from different interfaces show no degree of coherence, intensity is reduced to

$$I(\theta, \phi) = \sum_{i=1}^{p} |a_i|^2 \gamma_{ii},$$

which shows that the γ_{ij} terms of expression (1) take into account the interferential phenomenon between the waves scattered from interfaces i and j. In other words, γ_{ij} represents a degree of similitude between the profiles of interfaces i and j and takes into account the coherence between the waves scattered by these two surface defects. γ_{ij} is the Fourier transform of the cross-correlation function between the h_i and h_j profiles of surfaces i and j.

Let us now develop these terms; as a multilayer stack is obtained by vacuum evaporation of materials with small thicknesses (of the order of the wavelength), we can imagine a relation between cause and effect for the roughnesses of the various interfaces. Let us write, for instance,

$$i \leq j \Rightarrow h_j = h_i * a_{ij}, \tag{2}$$

where the symbol $(*)$ indicates a correlation product.

We thus obtain by Fourier transform

$$\hat{h}_j(\sigma) = \bar{a}_{ij}(\sigma)\hat{h}_i(\sigma),$$

where $a_{ij}(\sigma) = \mathrm{FT}[a_{ij}(x, y)]$ and $a_{ij} + \bar{a}_{ij} = 2$ real part (a_{ij}).

Hence we can see that each spectral component of the profile of interface j is a spectral component of the profile of

interface i multiplied by a α_{ij} coefficient, depending on the spatial frequency in question. That is, that each sinusoidal grating of interface i is more or less exactly reproduced by the evaporated layer, and the relative ratio of the magnitudes of those two gratings is taken into account by a cross-correlation coefficient, depending on the period of the grating.

We can now expect these cross-correlation laws to be strongly dependent on the microstructure of the materials: a material with a fine microstructure will reproduce surface defects over the entire range of measurable spatial frequencies (α_{ij} close to 1), whereas a material with a rather rough microstructure will not reproduce gratings of small periods (α_{ij} decreases to vanishing as σ increases). Broadly speaking, large-period gratings (analogous to function h_1 of Fig. 2) can be easily reproduced, whereas information about short-period gratings will be lost, depending on the evaporation conditions of the layers. For this reason, our data-calculation programs dissociate two spatial-frequency domains, using different cross-correlation coefficients for the exponential and the Gaussian functions.

According to relation (2), we can write

$$\alpha_{ii}(\sigma) = 1, \qquad \gamma_{ij}(\sigma) = \alpha_{ij}(\sigma)\gamma_{ii}(\sigma),$$

and then for the scattered intensity

$$I(\theta, \phi) = \sum_{i=1}^{p} |a_i|^2 \gamma_{ii} + 2 \sum_{i<j} R_e(a_i \bar{a}_j \alpha_{ij}) \gamma_{ii},$$

where the symbol $\bar{a}_j$ is the conjugate complex number of a_j.

So we say that α_{ij} represents the degree of coherence between the waves scattered from interfaces i and j. This coherence depends on the spatial frequency concerned and hence on the scattering direction.

It is also common to consider α_{ij} to be a constant real number over the entire range of measurable spatial frequencies, which means that the α_{ij} function is close to a Dirac function and that the profiles of the interfaces i and j are nearly proportional: $h_j \simeq \alpha_{ij} h_i$.

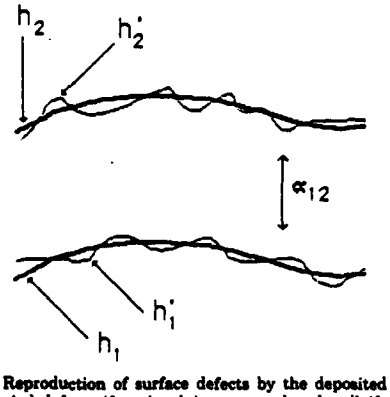

Fig. 3. Reproduction of surface defects by the deposited layer. Large-period defects (function h_1) are reproduced well (function h_2), with an associated cross-correlation coefficient close to unity. Short-period defects (function h_1') are not reproduced; the residual roughness (function h_2') is due to the microstructure of the material, and the cross-correlation coefficient between h_1' and h_2' is close to zero.

We must notice now that the model given by relation (2) is not applicable in the case when there is no link between the roughness statistics of the various interfaces. In fact, we must take into account a residual roughness originating from the fine microstructure of the materials that has only large spatial frequencies (scattering at large angles). This can be written as

$$i < j \rightarrow h_j = h_i * \alpha_{ij} + g_j,$$

where g_j characterizes the residual roughness. We must assume that all residual roughnesses are statistically independent, which leads to

$$\gamma'_{ij} = \gamma_{ij}, \qquad \gamma'_{jj} = \gamma_{jj} + |g_j|^2,$$

where the γ terms are relative to the preceding model of relation (2). This means that the scattered waves from different residual roughnesses do not show any degree of coherence; hence, for the scattered intensity, we have the expression

$$I'(\theta, \phi) = I(\theta, \phi) + \sum_{i=1}^{p} |a_i|^2 |g_i|^2,$$

where $I(\theta, \phi)$ is related to the model of relation (2).

Let us remark that the evaporated layers do not reproduce residual roughnesses, that is, $g_i * \alpha_{ij} = 0$. A good helpful representation of such a phenomenon is given in Fig. 3.

As a conclusion, we can see that the cross-correlation laws can depend strongly on the origin of roughness; such roughness can be due to two different phenomena that occur in two different spatial-frequency domains. It can be either *the result of surface-defect* reproduction (large-period defects are reproduced, and the associated cross-correlation coefficient is close to unity) or the effect of the grain size that characterizes the fine microstructure of the materials (such residual roughness introduces small-period defects, and the associated cross-correlation coefficient is close to zero). We now see how it is possible to investigate both roughnesses and cross-correlation coefficients for the case of a multilayer stack.

CASE OF A SINGLE LAYER. USE OF ANTISCATTERING EFFECT

A first approach of the cross-correlation coefficient can easily be obtained in the case of a single layer (Fig. 4). We know that the total integrated scattering from a single layer is strongly dependent on the cross-correlation function between the two layer roughnesses.[8,9] An analytical calculation[10] enabled us to demonstrate that the deposition of a single layer upon an absorbent substrate—in order to eliminate scattering from the back surface of the substrate—can lead to an appreciable reduction (or even elimination) of scattering, provided that the two interface defects are perfectly correlated ($\alpha_{10} = 1$). Elimination of scattering is obtained only for layers with optical thicknesses that are multiples of a quarter wavelength; in the case of a quarter-wave layer, we must have a low-index material, and the ratio of the roughnesses is given by

$$\frac{\delta_0}{\delta_1} = \left(\frac{n}{n_S}\right)^2 \frac{n_S^2 - n^2}{n^2 - n_0^2}.$$

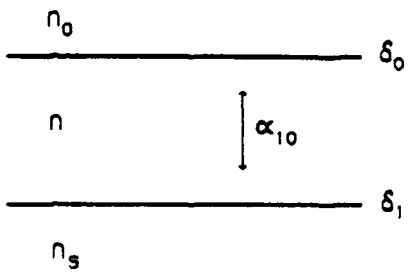

Fig. 4. Case of a single layer. δ_0 and δ_1 are the roughnesses of the two interfaces. α_{10} is the cross-correlation coefficient between these surfaces. n, n_0, and n_s are, respectively, the indices of the layer material, of the incident medium (air), and of the substrate.

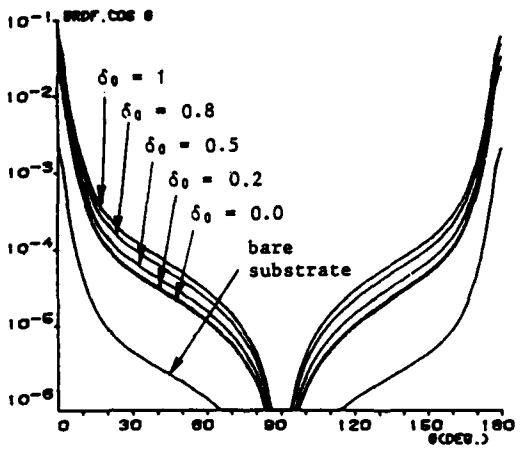

Fig. 5. Angular-scattering curves of a single layer of TiO_2 with optical thickness λ, calculated for different values of the top-interface roughness, in the case of uncorrelated interfaces. We observe no antiscattering effect. BRDF cos θ is the scattered flux per unit solid angle and per unit of incident flux. The wavelength under study is $\lambda = 0.6$ μm.

In the case of a half-wave layer, the material must be a high-index one, and the ratio of the roughnesses is given by

$$\frac{\delta_0}{\delta_1} = \frac{n^2 - n_s^2}{n^2 - n_0^2}.$$

Furthermore, the theory gives us the whole range of the values of this ratio $[a \le (\delta_0/\delta_1) \le b]$ for which the deposition of a half- or a quarter-wave layer leads to a single reduction of scattering. $I = [a, b]$ is called the antiscattering range.

In most cases, we find that $I = [0, a]$, with $a \ge 1$. This means that an antiscattering effect will occur, provided that the evaporated layer reproduces the substrate defects without increasing their magnitude (which is more probable) and that the cross-correlation coefficient is close to unity (homothetic surfaces).

The numerous layers that have been produced in our laboratory with five different dielectric materials [MgF_2, SiO_2, $Na_3(AlF_6)$, TiO_2, and ZnS] show an excellent agreement with theory (in the case of homothetic surfaces) and experiment[10]. Except for ZnS, nearly all the half-wave high-index layers and quarter-wave low-index layers led to reduction of scattering. Moreover, none of the high-index quarter-wave layers showed reduction of scattering, which is an additional confirmation of the theory.

For greater convenience, we drew in Fig. 5 the variations of the angular-scattering curve of a single layer of TiO_2 as a function of the top interface roughness (on the air side), in the case when the two interface defects are not correlated ($\alpha_{10} = 0$). We can see that scattering is never reduced, even in the case when the top interface is ideally flat ($\delta_0 = 0$). This theoretical result (using $\alpha_{10} = 0$) is in complete disagreement with the experimental result of Fig. 6, where scattering has been reduced to 58% of the substrate-scattering value. Then we can conclude that the cross-correlation coefficient between the two roughnesses of a single layer is close to unity. The aluminum-layer technique[11] enabled us to calculate the top-interface roughness of this layer and hence to verify that the ratio of the roughnesses was within the antiscattering range, which is another confirmation of the theory.

Because they are responsible for nearly 80% of the total integrated scattering, we have dealt until now only with large-period defects, and we gave α_{10} a constant real value over this period range. In the case of an antiscattering half-wave SiO_2 layer, we observed (Table 1) a decrease of the scattering ratio while the scattering angle became larger. This is probably due to a decrease of the cross-correlation coefficient as the spatial frequency increases, but it is not obvious. For ZnS, for instance, we sometimes observed[8] an increase of this coefficient at large scattering angles, which can be due to a microstructure with grains of large lateral dimensions.

An interesting feature of the antiscattering effect is that it

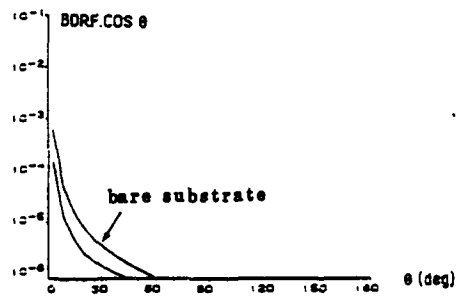

Fig. 6. Mean plane section of an angular-scattering curve measured from a TiO_2 layer with optical thickness λ. Scattering is reduced to 58%.

Table 1. Variation of the Scattering Ratio Before and After Coating in Different Angular Sectors in the Case of a Half-Wave SiO_2 Layer

Angular Sector (deg)	Scattering Ratio (%)
0 → 10	96
10 → 30	96
30 → 50	92
50 → 70	75
70 → 90	20

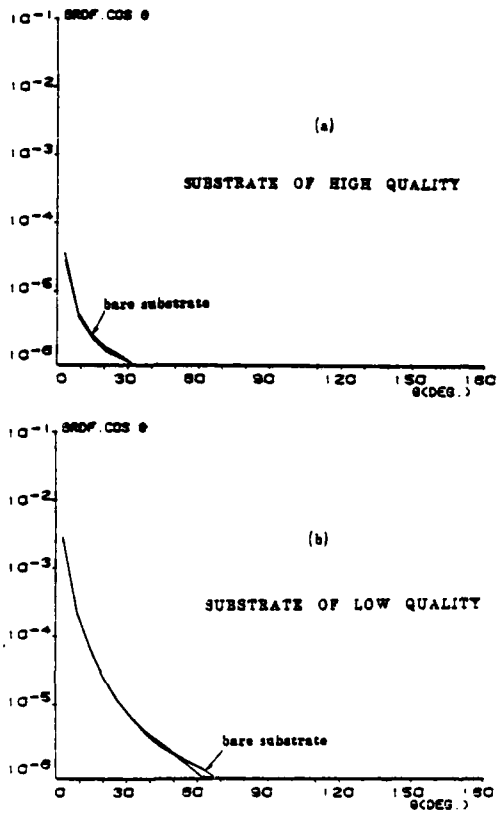

Fig. 7. Plane sections of the angular-scattering curves measured from a half-wave SiO_2 layer deposited upon a substrate: (a) of high quality (total integrated scattering = 5×10^{-6}) and (b) of low quality (total integrated scattering = 107×10^{-6}). In each case, the angular-scattering curves before and after coating are nearly the same.

Table 2. Comparison between the Total Integrated Scattering of Three Substrates Before [$D(v)$] and After [$D(\lambda)$] Deposition of a TiO_2 Layer with Optical Thickness λ[a]

Sample	$D(v)$ (ppm)	$D(\lambda)$ (ppm)	η (%)
1	9.0	46.5	520
2	61.6	35.6	58
3	127	67.3	53

[a] 1 ppm = 1 part in 10^6.

can be used to characterize the fine microstructure of thin-film materials. For example, a SiO_2 layer because of its fine microstructure will exactly reproduce substrate defects, whatever the quality of the polish; therefore, because the two interfaces have identical roughnesses, the two angular-scattering curves before and after coating (Fig. 7) are nearly the same ($I = [0, 1]$ for a half-wave SiO_2 layer). On the other hand, a TiO_2 layer with a rather rough microstructure will reduce the substrate defects and hence the total integrated scattering (Table 2); but if the substrate is of too high quality (sample 1), there is no antiscattering effect; the deposited layer cannot reproduce the defects of a substrate of low scattering (9 parts in 10^6), that is, of small roughness (0.7 nm), which is a limit that is due to the TiO_2 microstructure.

CASE OF A QUARTER-WAVE MULTIDIELECTRIC MIRROR: USE OF THE ALUMINUM-LAYER TECHNIQUE

Scattering distribution from a multilayer coating is not easy to interpret, because it does no seem possible *a priori* to isolate the flux scattered from only one interface. In the case of a quarter-wave multidielectric mirror, such a problem is slightly simplified by the fact that scattering has its origins in only two surface roughnesses where the electric field, which is the source of scattering, has its maximum.[12]

We previously showed that roughnesses and cross-correlation coefficients could depend strongly on each other; thus we must first deal with the origin of roughness in the stack. In order to demonstrate the influence of the substrate defects, we produced, under similar conditions, two identical quarter-wave TiO_2/SiO_2 mirrors of 15 layers on two substrates of different qualities. The aluminum-layer technique permitted us to calculate the top-interface (air-side) roughness of each stack and then draw our conclusions. Indeed,[11] it was demonstrated that it was possible to control the evaporation conditions of aluminum so that the metallic layer reproduces exactly the surface defects of the preceding interface with an accuracy of 0.1 nm in the entire range of measurable spatial frequencies. Hence a characterization of the top-interface roughness is obtained by deposition of a thin opaque metallic layer upon the mirror (in order to eliminate scattering from other interfaces) and then by characterization of the roughness of the air–metal interface, which is the same as that of the top interface of the mirror.

Some results are presented in Table 3, where we can note the following:

For large-period defects, the top-interface roughness of each mirror is close to the roughness of the bare substrate. This indicates that substrate defects are reproduced over the entire stack: the production of mirrors with very low scattering losses requires the use of supersmooth substrates.

As for short-period defects, the top-interface roughness is nearly the same for the two mirrors (whatever the substrate quality). It is probably a residual roughness that is due to the microstructure of the top-layer material (TiO_2). Let us note that such a value for the residual roughness shows good agreement with the fact that a TiO_2 layer cannot reproduce substrate defects with a roughness less than 0.7 nm (see the previous section).

Table 3. Influence of Substrate Defects on the Top-Interface Roughness of a Mirror

	Sample (nm)	Top Interface (nm)
δ_r, L_r	0.5; 3000	0.8; 2500
δ_g, L_g	<0.5	1.1; 200
δ_r, L_r	3; 2000	2.8; 2000
δ_g, L_g	0.5; 180	1; 200

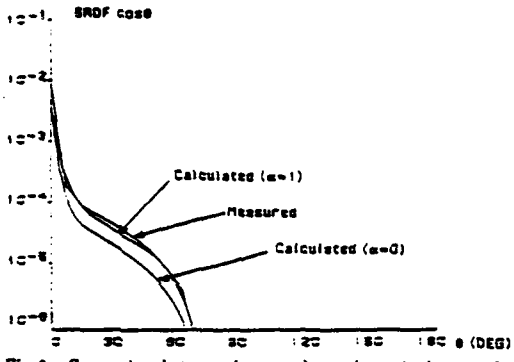

Fig. 8. Comparison between theory and experiment in the case of a multidielectric mirror. $\alpha = 1$ gives a better approximation than $\alpha = 0$.

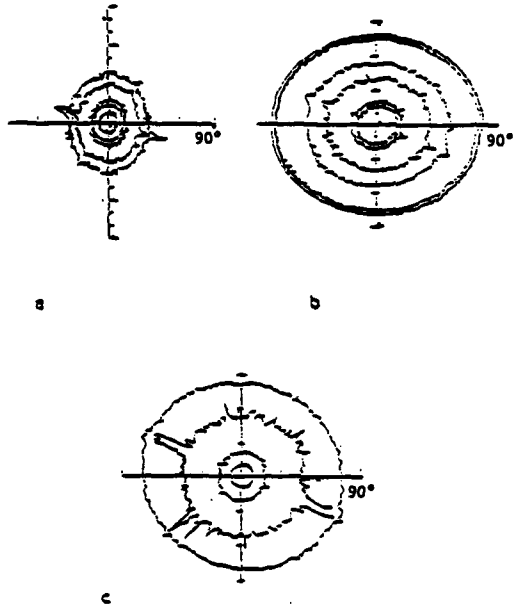

Fig. 9. Anisotropy curves[4] of a substrate before coating, after production of a mirror, and after deposition of aluminum upon the mirror.

What can we now deduce for cross-correlation laws? We know that large-period defects are reproduced throughout the entire stack. As they are responsible for most of scattering, we can expect that theory will show good agreement with experiments in the case of perfectly correlated interfaces. This is confirmed by Fig. 8, where we have drawn measured and calculated angular-scattering curves of a mirror produced upon a supersmooth substrate (Table 3). For the calculated curve, we considered that all the roughnesses of the stack were identical to that found for the top interface. This is not surprising, since in the case of a mirror, the two scattering rough interfaces are close to the top interface.

We can also verify (Fig. 9) that the deposition of layers does not modify the roughness anisotropy of the substrate. All these results show that substrate quality plays a key role in the scattering phenomenon.

We must note that nearly identical results on cross-correlation laws were found by Elson.[13]

CONCLUSION

We showed how the use of the antiscattering effect and aluminum-layer technique enabled us to investigate the key parameters of scattering from multilayer stacks. Roughness has its origins in two different phenomena, which occur in separate frequency ranges: It can be due first to reproduction of substrate defects by the evaporated layers (the associated cross-correlation coefficient is then close to unity) and second to the grain size that characterizes the fine microstructure of thin-film material (α close to zero).

For the coatings that have been produced in our laboratory, the agreement between theory and experiment is excellent in the case of perfectly correlated interfaces. Such a result is not surprising if we note that the layers have a thickness of the order of 0.1 μm, while defect periods responsible for practically the whole scattering lie approximately in the range (5–20 μm) and hence will probably be reproduced.

ACKNOWLEDGMENT

This work was presented at the 1986 Optical Society of America Annual Meeting, Seattle, Washington, October 19–24, 1986.

REFERENCES

1. H. E. Bennett and J. O. Porteus, "Relation between surface roughness and specular reflectance at normal incidence," J. Opt. Soc. Am. 51, 123 (1961).
2. P. Roche and E. Pelletier, "Characterizations of optical surfaces by measurement of scattering distribution," Appl. Opt. 23, 3561 (1984).
3. J. M. Elson, "Angle-resolved light scattering from composite optical surfaces," Proc. Soc. Photo. Opt. Instrum. Eng. 240, 296 (1980).
4. P. Bousquet, F. Flory, and P. Roche, "Scattering from multilayer thin films: theory and experiment," J. Opt. Soc. Am. 71, 1115 (1981).
5. C. Amra, "Développement et comparaison de deux théories vectorielles de la diffusion de la lumière par des surfaces peu rugueuses. Application à l'étude des surfaces et des empilements de couches," *Thèse de Doctorat d'Etat* (Université d'Aix-Marseille III, Marseilles, France, 1986).
6. P. Croce and L. Prod'homme, "Etude par diffusion lumineuse de la nature des surfaces de verre poli," Nouv. Rev. Opt. 7, 121 (1976).
7. J. M. Elson and J. M. Bennett, "Relation between the angular dependence of scattering and the statistical properties of optical surfaces," J. Opt. Soc. Am. 69, 31 (1979).
8. J. Garcin, "Diffusion de la lumière: étude expérimentale et représentation théorique des rugosités des interfaces de filtres multidiélectriques," *Thèse de Docteur-Ingénieur* (Université d'Aix-Marseille III, Marseilles, France, 1982).
9. P. Roche, E. Pelletier, and G. Albrand, "Antiscattering transparent monolayers: theory and experiment," J. Opt. Soc. Am. A 1, 1032 (1984).
10. C. Amra, G. Albrand, and P. Roche, "Theory and application of antiscattering single layers: antiscattering antireflection coatings," Appl. Opt. 25, 2695 (1986).

11. P. Roche, C. Amra, and E. Pelletier, "Measurement of scattering distribution for characterisation of the roughness of coated or uncoated substrates," presented at Third International Symposium on Optical and Optoelectronic Applied Sciences and Engineering, Innsbruck, Austria, April 14–18, 1986.
12. C. Amra, "Scattering distribution from multilayer mirrors—theoretical research of a design for minimum losses," presented at the 18th Annual Boulder Damage Symposium, Boulder, Colorado, November 3–5.
13. J. M. Elson, J. P. Rahn, and J. M. Bennett, "Light scattering from multilayer optics: comparison of theory and experiment," Appl. Opt. 19, 669 (1980).

Conférence présentée à "19th Annual Boulder Damage Symposium" - Oct. 26-28 , 1987, Boulder, Colorado - To be published in "Laser induced damage in optical material"

32

Minimizing scattering in multilayers: Technique for searching optimal realization conditions

C. Amra

Laboratoire d'Optique des Surfaces et des Couches Minces - Unité Associée au CNRS (U.A. 1120) - Ecole Nationale Supérieure de Physique de Marseille
Domaine Universitaire de St Jérôme - 13397 Marseille Cedex 13 - France

Reducing losses in optical coatings implies a search for optimal realization conditions of multidielectric coatings to obtain minimal absorption and scattering. Numerous works have been devoted to the absorption problem. Here we deal with scattering minimization. Scattering from a coated substrate is a function of numerous factors that can be successively measured: substrate roughness, interfaces roughness, cross-correlation state between interfaces. First, the substrate roughness is determined by scattering measurement before coating. Then, the interfaces roughness depends on the grain size of the material in thin film form. For a given material, we find that the grain is, in a large extent, function of the preparation conditions of the layer. And mainly, when a whole layer stack is concerned, the spatial distribution of the scattered light depends on the cross-correlation state between successive interfaces. With a scattering vector theory and an apparatus for measuring scattering curves at our disposal, we can show how it is possible to determine the interface roughness and the cross-correlation state, by a systematic comparison between theory and experiment. In order to eliminate any ambiguity in interpreting the experimental results, we must work with multilayer stacks the design of which is chosen so that the scattering curves have an aspect very different according to the cross-correlation state.

Key words: interface correlation; multilayers; optical filters; roughness; scattering.

1. Introduction

Though many works /1,2/ have been devoted to the study of absorption in optical multilayers, there are many applications (mirrors for lasers and gyrolasers, Fabry-Perot filters for optical multi-demultiplexing, ...) where scattering losses are mainly responsible for the limitation of filter performances. So we are dealing here with light scattering from surfaces and interfaces of optical multilayers.

We have already described the experimental /3/ and theoretical /4/ tools we developed in Marseilles for this study; let us recall that the scattering distribution can be measured in the whole space (25 000 data points), and then interpreted by matching the parameters involved in the theoretical model. Owing to these two tools that are theory and experiment, our investigations in scattering phenomenon have well gone forward:

- In a first stage, measurements of scattering from only one surface enabled us to show /3/ that the roughness spectrum, which characterizes the surface defects/5/ is independent of the illumination and observation conditions; such results are in good agreement with theory.
- Then we were interested in the study of scattering from one single layer /6, 7/, and we demonstrated that a deposited layer could exactly reproduce the substrate defects, provided that the deposition conditions have been well adapted. In such a case, the two interfaces (air/layer) and (layer/substrate) are quasi proportional and their cross-correlation coefficient is close to unity: the scattered waves from one and other interface are in phase cancellation, which leads to reduction of total integrated scattering ("antiscattering effect"). Then, by studying the ratio of the top interface (air/layer) roughness to the substrate roughness, we obtain precious information concerning the microstructure of the material in thin film form, and especially on the grain size which characterizes this microstructure.
- In the case of a multilayer mirror, the Aluminum technique /8/ pointed out the fact that roughness has its origins in two different phenomena: it can be due

to reproduction of substrate defects (case of perfectly correlated surfaces) or to the material microstructure (case of uncorrelated surfaces).

Now that such information is at our disposal, the question is to know whether it is possible to generalize "antiscattering effect" to multilayer systems, owing to destructive interferences between scattered waves. It is obvious that the first problem lies in the choice of the multilayer design; but as far as we know that scattering will only be reduced with perfectly correlated surfaces, we have first to make sure that we control the different parameters involved in scattering phenomenon. In spite of numerous results /9/ we obtained concerning the cross-correlation coefficient between interfaces, the determination of these parameters and of the associated roughnesses remains a difficult problem /10/, especially if the number of layers is high.

We show here how we can solve this problem, by using specific multilayer designs deduced from theory. The scattering of these stacks is so sensitive to the scattering parameters that we can determine them without any ambiguity. Such multilayers are then produced, using Ion Assisted Deposition, and both cross-correlation laws and roughnesses are deduced from scattering measurements. It then appears that we can characterize our deposition conditions with accuracy, from a point of view of scattering.

2. Search of specific multilayer design

In this section, we only present theoretical results, for a sample illuminated in natural light at normal incidence. The wavelength under study is λ_0 = 630 nm. The study is limited to scattering in the half space containing the specular reflection direction. We do not describe the analytical calculation that enabled us to choose the multilayer designs; we only verify by numerical computation that such designs are well adapted to our study.

The idea lies in the fact that (as an analogy with antiscattering effect),when a half-wave ($\lambda_0/2$) high-index layer is deposited on a substrate, the scattered waves from the new interface (air/layer) are in phase cancellation with those of the (layer/substrate) interface, which minimizes scattering losses. So we can expect that the same effect will occur if we deposit an odd number of successive alternated high- and low-index half-wave layers on a substrate: as the modulus of the electric field is the same at interfaces (Fig. 1), the corresponding scattering sources /11/ have magnitudes that are nearly the same; therefore scattering will be reduced, provided that these sources are in phase cancellation two by two. Obviously such phenomena only occur in the case where the interfaces are perfectly correlated; in such a case, we demonstrate (using analytical calculation) that scattering in the specular reflection direction do not depend on the number of layers. From a point of view of total integrated scattering, such results remain identical, as it is shown in table I:

For perfectly correlated surfaces and identical roughnesses at each interface, scattering losses do not change before and after coating, whatever the number of layers of the stack. On the other hand, we find in the case of uncorrelated surfaces that scattering losses are very sensitive to the number of layers: with 11 layers for instance, such losses are 138 times higher than that of the substrate before coating. It then appears that specific half-wave multilayer designs will give us access, using a careful comparison between theory and experiment, to the key parameters of scattering.

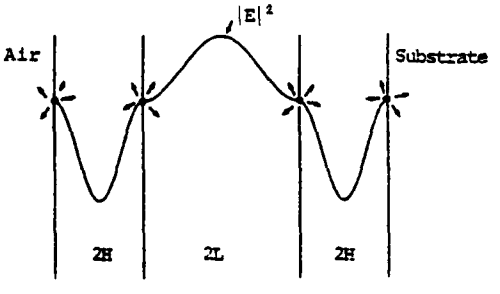

Figure 1:
Scattering phenomenon in a multilayer stack made of an odd number of alternated half-wave ($\lambda_0/2$) high index (2H) and low-index (2L) layers. We have plotted the square of the modulus of the electric field inside the stack. The sample is illuminated at λ_0 = 630 nm. The value of this field at interfaces is strongly related to the magnitude of the corresponding scattering source.

N	Coating	$D_0\ 10^6$	η_0	$D_1\ 10^6$	η_1
0	Bare substrate	23		23	
1	2H	649	28.2	23	1
3	2H 2L 2H	1153	50	24	1.1
5	2H 2L 2H 2L 2H	1660	72.2	26	1.2
11	2H 2L 2H ...	3175	138	28	1.2

Table I:
Scattering losses D integrated in the half-space containing the specular reflection direction, calculated before and after deposition of an odd number of alternated half-wave high-index (2H) and low-index (2L) layers. The substrate is a usual glass with refractive index n_s = 1.52. The materials are TiO_2 and SiO_2. N is the number of layers of the stack. Scattering is calculated at the wavelength λ_0 = 630 nm in the case of identical roughnesses at each interface, for two extreme values (α = 0 and α = 1) of the cross-correlation coefficient between interfaces. D_0 and D_1 are scattering losses that correspond to α = 0 and α = 1 respectively.
In the same way, η_0 and η_1 are the ratio of scattering after coating to scattering before coating, respectively for α = 0 and α = 1. For these theoretical results, we assume that the roughness spectra at each interface can be approximated with the Fourier Transform of the sum of an exponential and a gaussian function /3, 8/, with respective parameters: (δ_{exp}, L_{exp}) = (1.5 nm, 2000 nm) and (δ_G, L_G) = (1 nm, 200 nm).

3. Experimental results

We produced the preceding specific multilayers using Ion Assisted Deposition /12, 13/. The materials are TiO_2 and SiO_2. In order to point out the possible influence of the substrate quality, each multilayer was simultaneously produced on three black glasses with very different micropolishes. Scattering of every sample was measured before and after coating, at the wavelength λ_0 = 630 nm. The experimental results are presented in Table II, and they are concerning stacks that have one, three and five alternated half-wave ($\lambda_0/2$) high-index and low-index layers:

Sample	$D_N\ 10^6$	Coating	$D_T\ 10^6$	η
A27	8.9	2H	13.6	1.53
A20	41.6	2H	9.5	0.23
A23	82.6	2H	18.9	0.23
A31	9.7	2H 2L 2H	17.9	1.85
A22	40.1	2H 2L 2H	9.9	0.25
A32	80.6	2H 2L 2H	16.6	0.21
A36	25.2	2H 2L 2H 2L 2H	39.7	1.58
A21	42.0	2H 2L 2H 2L 2H	13.5	0.32
A33	110.5	2H 2L 2H 2L 2H	15.9	0.14

Table II:
Measured scattering losses from rough samples before (D_N) and after (D_T) deposition of an odd number of alternated half-wave high-index (2H) and low index (2L) layers. The materials are TiO_2 and SiO_2. All substrates were usual opaque glasses. Scattering is measured at the wavelength λ_0 = 630 nm. η is the ratio of scattering after and before coating: $\eta = D_T/D_N$.

First we notice that a unity value of η(predicted by theory in the case of identical roughnesses and perfectly correlated surfaces - see Table I) is not obtained. However, the curves of figure 2 and 3 will give us a complete understanding of these results.

Figure 2:
Calculated variations of the ratio $\eta = D_T/D_N$ (scattering after coating/scattering before coating) as a function of the cross-correlation coefficient α between interfaces, in the case of identical roughnesses at each interface. These results concern multilayer stacks made of an odd number of alternated half-wave ($\lambda_0/2$) high index (TiO_2) and low index (SiO_2) layers. Scattering is calculated at the wavelength λ_0 = 630 nm. N is the number of layers of the stack.

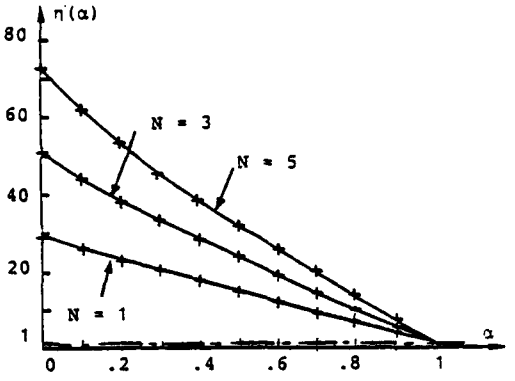

In figure 2 we plotted the calculated variations of the ratio η (scattering after coating/scattering before coating) as a function of the cross-correlation coefficient α /9/ between interfaces, in the case of identical roughnesses. Let us remark that, whatever the number of layers, only the value α = 1 (correlated surfaces) leads to a unity value for η: it is not possible to reduce scattering without modifying the interface roughnesses.

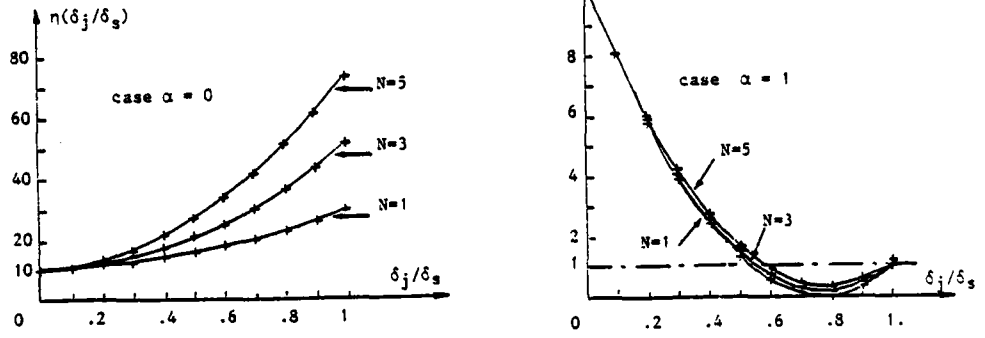

Figure 3:
Calculated variations of the ratio $\eta = D_T/D_N$ as a function of the ratio (δ_j/δ_s) of the roughness at interfaces, for two extreme values of the cross-correlation coefficient between interfaces. Figure 3a corresponds to α = 0, while figure 3b corresponds to α = 1. The stacks are made of an odd number of alternated half-wave ($\lambda_0/2$) high index (TiO_2) and low index SiO_2 layers. Scattering is calculated at the wavelength λ_0 = 630 nm. We assumed that all roughnesses δ_j at interfaces (except that of the substrate) were identical, but smaller than the roughness substrate; then the ratio (δ_j/δ_s) is in the range [0; 1].

Figure 3 gives us the calculated variations of η as a function of the ratio δ_j/δ_s (interface roughness δ_j / substrate roughness δ_s), for two extreme values ($\alpha = 0$ and $\alpha = 1$) of the cross-correlation coefficient. Whatever the number of layers, the case of uncorrelated surfaces ($\alpha = 0$) never leads to reduction of scattering: the smallest value for η is greater than 10 in the case $\alpha = 0$. Such results obviously show the interest of the preceding half-wave multilayers for the study of the scattering parameters: the curves $\alpha = 0$ and $\alpha = 1$ get more different as the number of layers increases.

Let us now interpret the experimental results of Table II by comparing them with the calculated values of figures 2 and 3.

(2H) designs

The conclusions are presented in Table III. The case of uncorrelated surfaces is never possible, whatever the roughness at interfaces. For A23 and A29 samples, the only interpretation is:

$\alpha = 1$ and δ_j/δ_s close to 0.7 ou 0.8

As for the best micropolish (A27), correlation must be perfect ($\alpha = 1$) but the roughness is close to 0.5 or 1.

Sample	A27 ($9\ 10^{-6}$)	A29 ($42\ 10^{-6}$)	A23 ($83\ 10^{-6}$)
η	1.53	0.23	0.23
α ($\delta_j = \delta_s$)	=1.0	No solution	No solution
δ_j/δ_s ($\alpha = 0$)	No solution	No solution	No solution
δ_j/δ_s ($\alpha = 1$)	= .5 or = 1.0	= .7 or = .8	= .7 or = .8

Table III:

Interpretation of the experimental results of Table II for a (2H) stack with the help of figure 2 and figure 3. We give below each sample the scattering before coating (A27 has scattering losses equal to $9\ 10^{-6}$ for instance). η is the ratio of scattering after and before coating: $\eta = D_T/D_N$. The value of $\alpha(\delta_j=\delta_s)$ is deduced from figure 2, while the ratio δ_j/δ_s(α=0 or α=1) is deduced from figure 3.

(2H 2L 2H) and (2H 2L 2H 2L 2H) designs

The conclusions (Tables IV and V) are exactly the same as the preceding of Table III. Experiment can never be interpreted with uncorrelated surfaces. For the samples (A22, A32, A21, A33), we find that $\alpha = 1$ and δ_j/δ_s close to 0.7 or 0.8. As for the best micropolishes (A31 and A36) α is close to unity but δ_j/δ_s can be 0.5 or 1.

So we conclude for these multilayers that interfaces are practically homothetic: our deposition conditions lead to a cross-correlation coefficient near unity. As for the roughness, we find a slight diminution with respect to the substrate roughness; it would be interesting to control such reduction by adapting the ion beam power during the assisted deposition.

Sample	A31 ($10\ 10^{-6}$)	A22 ($40\ 10^{-6}$)	A32 ($81\ 10^{-6}$)
η	1.85	0.25	0.21
α ($\delta_j = \delta_s$)	=1.0	No solution	No solution
δ_j / δ_s ($\alpha = 0$)	No solution	No solution	No solution
δ_j / δ_s ($\alpha = 1$)	= .5 or = 1.0	= .7 or = .8	= .7 or = .8

Table IV:
Interpretation of experimental results of Table II for a (2H 2L 2H) stack, with the help of figures 2 and 3. We give below each sample the scattering before coating. η is the ratio of scattering after and before coating: $\eta = D_T/D_N$. The value of $\alpha(\delta_j=\delta_s)$ is deduced from figure 2, while the ratio $\delta_j/\delta_s(\alpha=0$ or $\alpha=1)$ is deduced from figure 3.

Sample	A36 ($25\ 10^{-6}$)	A21 ($42\ 10^{-6}$)	A33 ($111\ 10^{-6}$)
η	1.58	0.32	0.14
α ($\delta_j = \delta_s$)	=1.0	No solution	No solution
δ_j / δ_s ($\alpha = 0$)	No solution	No solution	No solution
δ_j / δ_s ($\alpha = 1$)	= .5 or = 1.0	= .7 or = .8	= .7 or = .8

Table V:
Interpretation of the experimental results of Table II for a (2H 2L 2H 2L 2H) stack, with the help of figures 2 and 3. We give below each sample the scattering before coating. η is the ratio of scattering after and before coating: $\eta = D_T/D_N$. The value of $\alpha(\delta_j=\delta_s)$ is deduced from figure 2, while the ratio $\delta_j/\delta_s(\alpha=0$ or $\alpha=1)$ is deduced from figure 3.

4. Conclusion

We were interested in an attempt to generalize antiscattering effect to multilayer systems. As far as such effect only occurs in the case of perfectly correlated surfaces, the first difficulty was to determine the key parameters of scattering, in order to possibly control them in a second stage. We demonstrated how the use of specific half-wave multilayers enabled us to determine both cross-correlation coefficients and roughness at interfaces: for the coatings produced by ion assisted deposition in our laboratory, we find a perfect correlation between interfaces and a slight reduction of interface roughness with respect to the substrate roughness.

Now that we have such information at our disposal, we must introduce scattering parameters in the filter design conception to obtain simultaneously well defined spectral properties (a high reflection coefficient for instance) and minimal scattering losses; we have the theoretical tools for this type of study.

From a point of view of experiment, we must not forget that it is *a priori* possible to modify the preparation conditions of the layers obtained by ion assisted deposition. To which extent is it possible to control the roughness at each interface? The ideal would be to produce multilayers with roughnesses that exactly correspond to a criterion of minimal scattering losses. Then, in spite of the unavoidable substrate defects and the grain size of the materials in thin film form, we could appreciably reduce scattering in optical multilayers.

References

1 J.H. Apfel, Optical coating design with reduced electric field intensity, Appl. Opt., 16, 1880-1885, (1977)

2 C.K. Carniglia and J.H. Apfel, Maximum reflectance of multilayer dielectric mirrors in the presence of slight absorption, J.Opt.Soc.Am., 70, 523-534, (1980)

3 P. Roche and E. Pelletier, Characterizations of optical surfaces by measurement of scattering distribution, Appl. Opt., 23, 3561-3566, (1984)

4 P. Bousquet, F. Flory and P. Roche, Scattering from multilayer thin films: theory and experiment, J. Opt.Soc.Am., 71, 1115-1123, (1981)

5 J.M. Elson and J.M. Bennett, Relation between the angular dependence of scattering and the statistical properties of optical surfaces, J.Opt.Soc.Am., 69, 31-47, (1979)

6 C. Amra, G. Albrand and P. Roche, Theory and application of antiscattering single layers: antiscattering antireflection coatings, Appl.Opt., 25, 2695-2702 (1986)

7 P. Roche, E. Pelletier and G. Albrand, Antiscattering transparent monolayers: theory and experiment, J.Opt.Soc.Am., 1, 1032-1033, (1984)

8 P. Roche, C. Amra, E. Pelletier, Measurement of scattering distribution for characterization of the roughness of coated or uncoated substrtes, SPIE Proceedings, Thin Film Technologies II, 652, 256-263, (1986)

9 C. Amra, P. Roche, E. Pelletier, Interface roughness cross-correlation laws deduced from scattering diagram measurements on optical multilayers: effect of the material grain size, J.Opt. Soc.Am. B, 4, 1087-1093, (1987)

10 J.M. Elson, J.P. Rahn and J.M. Bennett, Light scattering from multilayer optics: comparison of theory and experiment, Appl. Opt., 19, 669-679, (1980)

11 C. Amra, Scattering distribution from multilayer mirrors - Theoretical research of a design for minimum losses. To be published in "Laser damage in optical materials", (1986)

12 P.J. Martin, H.A. Macleod, R.P. Netterfield, G.C. Pacey, W.G. Sainty, Ion Beam Assisted Deposition of optical films, Appl. Opt., 22, 178, (1983)

13 F. Flory, G. Albrand, C. Montelymard, E. Pelletier, Optical study of the growth of Ta_2O_5 and SiO_2 layers by Ion Assisted Deposition, SPIE Proceedings, Thin Film Technologies II, 652, 248-253, (1986)

Proc. of the "Int. Symp. on trends and new applications in thin films" Strasbourg, March 1987 - p. 61-64 - Supp. "Le vide, les couches minces" n° 235

38

INFLUENCE OF THE STOICHIOMETRY OF OXIDES DURING DEPOSITION OF MULTILAYER FABRY PEROT FILTERS

B. Schmitt, E. Pelletier

Laboratoire d'Optique des Surfaces et des Couches Minces. Associé au CNRS - U.A. 1120 - Ecole Nationale Supérieure de Physique de Marseille - Domaine Universitaire de St Jérôme - 13397 Marseille Cedex 13 - France.

Résumé: Les performances spectrales des filtres interférentiels à bande étroite sont essentiellement limitées par des défauts de stoechiométrie et de microstructure des matériaux constituant les couches. Des mesures d'indices effectuées sur un large domaine spectral sous vide, puis à l'air, permettent de détecter les effets de l'adsorption d'humidité sur les performances spectrales des filtres. Des calculs de simulation et des résultats expérimentaux sont utilisés conjointement pour étudier la précision du contrôle de la formation des empilements.

I - INTRODUCTION

Narrow bandpass interference filters have been proposed to solve the problems of multiplexing or demultiplexing in optical telecommunications. More precisely, it concerns layer stacks of Fabry Perot type with multiple cavities. The high contrasts required are then obtained by coupling in series three Fabry Perot filters centered on the same wavelength (Triple Half Wave multilayer systems) /1/. The interest of these solutions and their ability to be realized have been demonstrated by using classical materials (ZnS/Cryolite) which are easy to evaporate /2/; but, unfortunately, they have not good mechanical properties. So we have developed the manufacturing of these stacks with more hard materials. These are essentially oxides (TiO_2/SiO_2); and the main difficulties lie in the particular evaporation conditions which have to be used to realize layer stacks with good optical qualities. In particular, the thin film refractive index values change between vacuum and air and these phenomena have to be taken into account in order to realize complex layer stacks with accurately defined spectral performances.

II - TECHNOLOGY USED FOR THE REALIZATION OF TiO_2 AND SiO_2 LAYERS

These materials have a tendency to be decomposed during their evaporation condensation. So we are induced to carry out the evaporation under a residual oxygen pressure, to heat the substrates at a high temperature (300-350°C) and to adjust deposition rates. Consequently, the stoichiometric composition and the microstructure of the layers which condense on the substrates tightly depend on these parameters /3/.

During the first contact with air, the optical properties of the coatings realized under vacuo appreciably change owing to oxido-reduction reactions and moisture adsorption in the layer porosities /4/.

Characterization techniques which are at our disposal in our laboratory help us to overcome these difficulties. A measurement technique, henceforward classical, leads to the refractive indices and absorption coefficients which are those of the layers exposed to air /5/. An *in situ* characterization method gives access to informations which previously passed totally unnoticed since it permits to measure refractive indices during layer formation /6/. So it has been shown that the condensation conditions not only determine the layer indices, but also the increase of refractive indices due to moisture

adsorption /7/. We must also add that absorption coefficients are never totally negligible. Their values also depend on condensation conditions and are difficult to determine with accuracy. We quantify the effects of moisture by means of refractive index relative variation, defined as:

$$\eta(\lambda) = \{ n_a(\lambda) - n_v(\lambda) \} / n_v(\lambda)$$

in this relation, $n_a(\lambda)$ and $n_v(\lambda)$ are, for each material, the refractive indices measured in air and under vacuo for the wavelength λ. This way of quantifying adsoption is convenient because it directly accounts for the relative increases of layer optical thicknesses.

III - APPLICATION TO THE REALIZATION OF COMPLEX LAYER STACKS

The examples given here concern filters with the structure:

glass/(H L H L H H L H L H) L (H L H L H H L H L H) L (H L H L H H L H L H)L

centered, under vacuo, on λ_v = 632.6 nm. With this notation, H and L respectively represent TiO_2 and SiO_2 layers of optical thickness $\lambda_v/4$.

A) Figure 1 concerns a filter realized with condensation conditions which lead to very low absorption losses. We can note that under vacuo the optical properties are reasonably good. The tolerances of realization have been respected. Let us recall that the layers of the stack must have an optical thickness of $\lambda_v/4$ to within some parts of a nanometer. But here, the relative increases $\eta(\lambda_v)$ of the refractive indices of the two materials are not identical $\eta_{(TiO_2)}(\lambda_v)$ = 4.8 % and $\eta_{(SiO_2)}(\lambda_v)$ = 7.1 %. And so, in air, the stack is no more constituted of quarterwave layers and we can observe an important decrease of the spectral performances. In fact, the final result will be good if the stack that was quaterwave under vacuo ($\lambda_v/4$) remains quarterwave in air ($\lambda_a/4$). Then we have to adjust the parameters involved in layer production so as the ratio $\eta_{(TiO_2)}(\lambda_v)/\eta_{(SiO_2)}(\lambda_v)$ would be close enough to unity in order to be compatible with the tolerances of stack realization. Putting the filter in contact with air will only induce a shift of the centering wavelength. Let us emphasize that searching for optimal evaporation conditions has to be made taking account of the values of refractive indices that are finally obtained. Indeed, we can show that the cross talk attenuation of the filters is all the more good as the ratio between TiO_2 and SiO_2 indices n_{TiO_2}/n_{SiO_2} is high.

B) The fabrication conditions of the filter given as a second example (Fig. 2a and 2b) have been adjusted so that $\eta_{(TiO_2)}(\lambda_v)$= 3.8 % and $\eta_{(SiO_2)}(\lambda_v)$= 3.5%. Fig 2a gives the optical properties under vacuo, after that the plant has been brought again at room temperature. We can see that, owing to an uncompleted layer oxidation, absorption losses are no more negligible (Fig. 2a). The measured optical properties are compared with the calculated ones assuming quarter wave layers and using the index values measured for these deposition conditions. Material extinction coefficients have been determined by simulation calculations. The values $k_{(TiO_2)} = 3.\ 10^{-3}$ and $k_{(SiO_2)} = 1.5\ 10^{-3}$ can explain the losses noted in the filter transmission window. Due to the monitoring quality, we can observe a good agreement between calculations and mesurements. Nevertheless, this absorption is too week to perturb the layer deposition monitoring /8/.

Optical properties plotted two days after contact with air are given in Fig. 2b. Absorption losses have almost disappeared. In addition, the expected optical properties are well consistent with the result obtained. In these calculations, it has been supposed that the layer mechanical thicknesses are not affected by moisture adsorption. Refractive index values and extinction coefficients $k_{(TiO_2)} = 1\ .\ 10^{-3}$ and $k_{(SiO_2)} = 0$ result from measures in air on layers deposited in the same conditions on silica substrates.

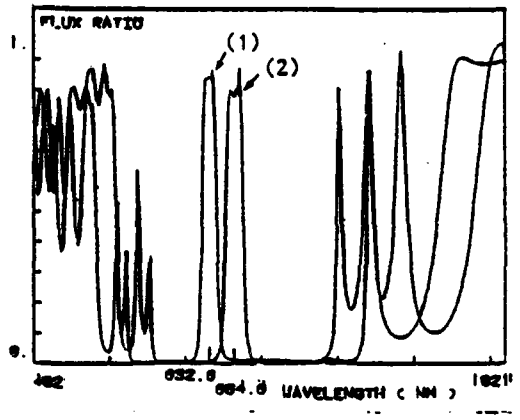

Figure 1

Triple halfwave TiO_2/SiO_2 filter.
("Flux ratio" is the ratio between the flux transmitted by the coated substrate and the flux transmitted by the bare substrate).

Design under vacuo:

glass/(H L H L H H L H L H) L (H L H L H H L H L H) L (H L H L H H L H L H) L
H : TiO_2 layer of optical thickness $\lambda_0/4$;
L : SiO_2 layer of optical thickness $\lambda_0/4$; λ_0 = 632.6 nm

(1) optical properties under vacuo at room temperature;
(2) Optical properties after two days of air exposure.
The shift between vacuum and air of the optical properties is due to moisture adsorption. The related increase of the refractive indices is η = 4.8 % for TiO_2 and η = 7.1 % for SiO_2.

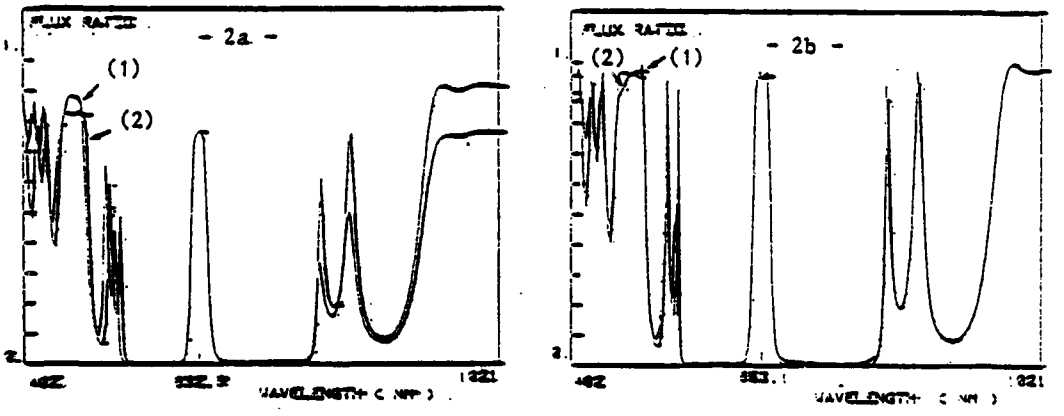

Figure 2

Same design and same notations as in Figure 1.
η = 3.8 % for TiO_2 η = 3.5 % for SiO_2

2a - under vacuo - comparison between optical properties calculated (1) and measured (2).
2b - in air - comparison between optical properties calculated (1) and measured (2).
We can note - the good agreement between experiment and theory;
- the spontaneous decrease of absorption between vacuum and air.

IV - CONCLUSION

With TiO_2 and SiO_2, refractive indices and extinction coefficients depend on layer formation conditions. This difficulty can nevertheless be easily overcome if these optical constants can be measured with well adapted characterization techniques. In fact, the main problems arise when the layer stacks are put in contact with the surrounding atmosphere. The spontaneous moisture adsorption gives rise to index increases which correspond to a shift of transmission curves towards great wavelengths. Important decreases of spectral performances can then be observed. This difficulty can be avoided if the stack which is made of quarterwave layers made under vacuo keeps this property when put in contact with air. This condition is fulfilled by adjusting the formation conditions in such a way that the refractive index relative increase of the two materials remain close from each other. This can lead to work with evaporation conditions which give rise to absorption losses. But they do not perturb the layer deposition monitoring, and fortunately, they spontaneously decrease when the filter is put in contact with air.

REFERENCES

/1/ E. Pelletier, P. Bousquet, Filtres optiques interférentiels pour multiplexeurs et démultiplexeurs destinés aux communications par fibres., Cannes 21-24 sept., European Conf. on Optics Communications, 1982.

/2/ A. Fornier, R. Richier, E. Pelletier, B. Bovard, G. Salvini, Contrôle optique du dépôt de couches multidiélectriques quart d'onde: techniques hybrides de traitement du signal utilisées pour améliorer les performances. A paraître dans "Annales des Télécommunications", Paris.
B. Bovard, A. Fornier, E. Pelletier, R. Richier, Problèmes posés par la réalisation des filtres interférentiels utilisés dans les démultiplexeurs optiques., Rev. Phys. appl. 19, 103-105, (1984)

/3/ H.K. Pulker, G. Paesold, E. Ritter, Refractive indices of TiO_2 films produced by reactive evaporation of various titanium-oxygen phases., Appl. Optics, 15, 2986-2991, (1976)
J.P. Borgogno, P. Bousquet, F. Flory, B. Lazaridès, E. Pelletier, P. Roche Inhomogeneity in films; limitation of the accuracy of optical monitoring of thin films., Applied Optics, 20, 90-94, (1981)

/4/ H.A. Macleod, D. Richmond, Moisture penetration patterns in thin films, Thin Solid Films, 37, 163-169, (1976)

/5/ J.P. Borgogno, B. Lazaridès, E. Pelletier, Automatic determination of the optical constants of inhomogeneous thin films, Applied Optics, 21, 4020-4029, (1982)
J.P. Borgogno, B. Lazaridès, P. Roche, An improved method for the determination of the extinction coefficient of thin film materials., Thin Solid Films, 102, 209-220, (1983)

/6/ F. Flory, B. Schmitt, E. Pelletier, H.A. Macleod, Interpretation of wide band scans of growing optical thin films in terms of layer microstructure. S.P.I.E. (The Society of Photo Instrumentation Engineers) vol 401, Thin Film Technologies, 109-116, (1983)

/7/ B. Schmitt, J.P. Borgogno, G. Albrand, E. Pelletier, In situ and air index Measurements: influence of the deposition parameters on the shift of TiO_2/SiO_2 Fabry Perot filters., Applied Optics, 25, 3909-3915, (1986)

/8/ H.A. Macleod, Absorption in turning value monitoring of narrow band thin-film optical filters., Optica Acta, 20, 493-508, (1973)

END